UNCOVERING REVERSIBLE AMPYLATION OF BIP

MEDIATED BY DFIC DURING ER HOMEOSTASIS

APPROVED BY SUPERVISORY COMMITTEE

Kim Orth, Ph.D.

Benjamin Tu, Ph.D.

Helmut Krämer, Ph.D.

Qinghua Liu, Ph.D.

ACKNOWLEDGEMNTS

It is still surreal to remind myself that my graduate school years have finally come to an end and I'm getting my Ph.D at last. It sure was a long and incredible journey that has taught me countless valuable lessons both in science and in life. I have been extremely lucky to have so many wonderful and talented scientists as colleagues and friends throughout the graduate school years.

First and foremost, my mentor Kim Orth, you are one of the most passionate and enthusiastic scientists I've met and a very caring and compassionate mentor who really has your people's back. Thank you for all your positive energy and encouragement that really pushed me to finish my project. It truly has been an honor to be one of your students.

I would also like to thank all my committee members for all their support and brilliant ideas. Dr. Helmut Krämer, you have been such an integral part of my thesis project and I really appreciate all your guidance and help. It was a lot of fun working with fruit flies. Dr. Benjamin Tu and Dr. Qinghua Liu, thank you so much for your positive inputs and warm encouragements.

To my former and current lab members, my time in graduate school would never have been the same without you guys. I had such an amazing time in and outside of lab thanks to all of you. TJ Calder, or Thomas Calder rather, having you as a bench mate was one of the best things that happened to me in graduate school. I'm truly blessed to have met a best friend for life who has always been there for me even in the most difficult

times. To all my dear friends that I can’t name all here, thanks for being part of my priceless graduate school memories.

I’d also like to say huge thanks my wonderful family. Mom and dad, the reason why I could make it all the way here is because of your endless support and unconditional love. You are hands down the best parents in the world and I hope I make you proud. And to my dear sister Yeilin who is also working on her Ph.D. in Japan, I know you are very close too so stay strong and be positive. I love you and miss you all so much!

Also many thanks to Mike, Gretchen, Michelle, Scott, and the two beautiful angels Sawyer and Willa, you guys are amazing and I’m so happy to be part of such a great family.

Last but not least, my wonderful husband Michael, thank you for believing in me in every way and always being there for me at the end of the hard day at work. This whole journey would not have been possible without you. I love you so much!

UNCOVERING REVERSIBLE AMPYLATION OF BIP MEDIATED BY DFIC DURING ER HOMEOSTASIS

by

HYEILIN HAM

DISSERTATION / THESIS

Presented to the Faculty of the Graduate School of Biomedical Sciences

The University of Texas Southwestern Medical Center at Dallas

In Partial Fulfillment of the Requirements

For the Degree of

DOCTOR OF PHILOSOPHY

The University of Texas Southwestern Medical Center at Dallas

Dallas, Texas

May, 2015

UNCOVERING REVERSIBLE AMPYLATION OF BIP

MEDIATED BY DFIC DURING ER HOMEOSTASIS

HYEILIN HAM, Ph.D.

The University of Texas Southwestern Medical Center at Dallas, 2015

Supervising Professor: KIM ORTH, Ph.D.

AMPylation is a posttranslational modification involving a covalent attachment of an AMP moiety from ATP to hydroxyl side chains of target substrates. Fic domain which mediates AMPylation is highly conserved across species, including higher eukaryotes, implicating an essential role of this modification in cellular function. Despite the recent discoveries and characterization of a number of bacterial AMPylators and their targets during pathogenesis, the knowledge of AMPylation in eukaryotic system is still elusive. Therefore, the goal of my thesis is to determine the eukaryotic function of AMPylation and identifying the endogenous substrates of this novel modification.

In an attempt to understand the physiological function of AMPylation in eukaryotes, we used *Drosophila melanogaster* as our genetic model organism and created mutant flies lacking functional *Drosophila* Fic (dFic). We found that the flies without enzymatic function of dFic exhibit blind phenotype due to impaired synaptic transmission. dFic enzymatic activity is required in glial cells for the normal visual neurotransmission. This suggests that a target of dFic may be a component of the visual signaling pathway. dFic was observed in the cell surface of the glial cells particularly enriched in capitate projections. However, dFic is localized to the ER in a number of fly tissues and also in the S2 cells, indicating that there may be another target of dFic in the ER that plays a more general role in the cellular function.

In this study, we identified an ER molecular chaperone BiP/GRP78 as a novel substrate for dFic-mediated AMPylation. BiP was predominantly labeled with AMP by dFic in S2 cell lysate. AMPylation of BiP decreases during ER stress but increases upon the reduction of unfolded proteins. Both dFic and BiP are transcriptionally activated upon ER stress induction, implicating a role for dFic in the UPR. We identified a conserved threonine residue, Thr366, as the AMPylation site, which is in close proximity to the ATP binding site of BiP's ATPase domain. Our study presents the first substrate of AMPylation by a eukaryotic protein and proposes a new mode of posttranslational regulation of BiP, which is likely to serve a crucial role in maintaining ER protein homeostasis.

TABLE OF CONTENTS

PUBLICATIONS

Ham H, Woolery AR, Tracy C, Stenesen D, Krämer H, and Orth K. (2014) Unfolded protein response-regulated dFic reversibly AMPylates BiP during endoplasmic reticulum homeostasis. *J Biol Chem, pii: jbc.M114.612515.*

Ham H and Orth K. (2012) The role of type III secretion system 2 in Vibrio parahaemolyticus pathogenicity. *J Microbiol*, 50(5): 719-25.

Rahman M, **Ham H**, Liu X, Sugiura Y, Orth K, Krämer H. (2012) Visual neurotransmission in Drosophila requires expression of Fic in glial capitate projections. *Nat Neurosci*, 15(6):871-5.

Krachler AM, **Ham H**, Orth K. (2012) Turnabout is fair play: use of the bacterial Multivalent Adhesion Molecule 7 as an antimicrobial agent. *Virulence*, 3(1):68-71.

Ham H, Orth K. (2011) De-AMPylation unmasked: modulation of host membrane trafficking. *Sci Signal*, 4(194):pe42.

Ham H, Sreelatha A, Orth K. (2011) Manipulation of host membranes by bacterial effectors. *Nat Rev Microbiol*, 9(9):635-46.

Krachler AM, **Ham H**, Orth K. (2011) Outer membrane adhesion factor multivalent adhesion molecule 7 initiates host cell binding during infection by gram-negative pathogens. *Proc Natl Acad Sci U S A*, 108(28):11614-9.

LIST OF FIGURES

LIST OF TABLES

LIST OF ABBREVIATIONS

AMP	Adenosine 5’ monophosphate
Amp	Ampicillin
ATF4	Activating transcription factor 4
ATF6	Activating transcription factor 6
ATP	Adenosine triphosphate
BIK1	Botrytis-induced kinase1
BiP	Binding immunoglobulin protein
CDP	Cytidine diphosphate
CHOP	C/EBP homologous protein
Cm	Chloroamphenicol
Doc	Death on cure
DTT	Dithiothreitol
eIF2α	Eukaryotic translation initiation factor 2α
EDTA	Ethylenediaminetetraacetic acid
EF-Tu	Elongation factor Tu
ERO1L	ER oxidoreductin-1-like
ER	Endoplasmic reticulum
ERG	Electroretinogram
FBS	Fetal Bovine Serum
Fic	Filamentation induced by cAMP
FPLC	Fast protein liquid chromatography
GADD34	Growth arrest and DNA damage-inducible 34

GAP	GTPase activating protein
GDI	Guanine nucleotide dissociation inhibitor
GEF	Guanine nucleotide exchange factor
GFP	Green fluorescent protein
GRP78	Glucose-regulated protein 78kDa
GS	Glutamine synthetase
GS-ATase	Glutamine synthetase adenylyl transferase
GST	Glutathione S-transferase
GTP	Guanine triphosphate
GTPases	Guanosine triphosphatases
HPLC	High pressure liquid chromatography
HRP	Horseradish peroxidase
IPTG	Isopropyl-beta-D-thiogalactopyranoside
IRE1	Inositol requiring enzyme 1
kDa	Kilodaltons
LB	Luria Bertani
LC	Liquid chromatography
MAPK	Mitogen-activated protein kinase
MS	Mass spectrometry
NBD	Nucleotide binding domain
NFκB	Nuclear factor kappa B
Ni-NTA	Nickel-nitriloacetic acid matrix
O.D.	Optical density
PBS	Phosphate buffered saline

PMSF	Phenylmethylsulfonylfluoride
PERK	Protein kinase RNA (PKR)-like ER kinase
PHD	Prevent host death
PPM	Metal-dependent protein phosphatase
RIPK	Receptor-interacting protein kinase
SBD	Substrate binding domain
SDS-PAGE	Sodium dodecyl sulfate-polyacrylamide gel electrophoresis
Ser	Serine
Thr	Threonine
TM	Transmembrane
TPR	Tetratricopeptide repeat
Tyr	Tyrosine
UMP	Uridine monophosphate
UPR	Unfolded protein response
UTP	Uridine triphosphate
Vop	*Vibrio* outer protein
XBP1	X-box binding protein 1
Yop	*Yersinia* outer protein

CHAPTER 1
Introduction and Review of Literature

AMPylation, a conserved posttranslational modification

AMPylation (also referred to as adenylylation) is a posttranslational modification involving a covalent attachment of an adenosine monophosphate (AMP) moiety from ATP to target protein substrates (1,2). This modification is comparable to phosphorylation mediated by kinases as they both use ATP as a substrate and transfer a part of it to hydroxyl side chains of protein substrates **(Figure 1A)**. AMPylation was first discovered in *E.coli* in the 1960s from a study characterizing glutamine synthetase adenylyl transferase (GS-ATase) (3,4). GS-ATase has two adenylyl transferase domains at the N- and C-terminus and uses these domains to catalyze both addition and removal of AMP on glutamine synthetase, respectively. AMPylation occurring on glutamine synthetase inhibits its ability to synthesize glutamine. By reversibly modifying this enzyme, GS-ATase regulates the nitrogen metabolism in *E. coli*, thereby demonstrating an endogenous regulatory function for AMPylation.

However, whether this modification was a general mechanism used by other organisms remained elusive until the recent rediscovery of AMPylation from the study of bacterial protein VopS. This Type III secreted bacterial effector from pathogenic bacteria *Vibrio parahaemolyticus* was observed to cause cell rounding during infection (5). VopS was shown to modify the Rho family GTPases, key regulators of actin cytoskeleton, with AMP on a threonine in the switch I region. Addition of bulky AMP moiety in this region

blocks the binding of Rho GTPases to downstream signaling proteins resulting in actin cytoskeleton disruption and consequent host cell rounding **(Figure 1B)**. In addition, AMPylation of Rho GTPases by VopS inhibits multiple host signaling pathways including NFκB and MAPK pathways and also Reactive Oxygen Signaling (ROS) pathway, that collectively contribute to *Vibrio* pathogenesis (6). For its AMPylation activity, VopS utilizes a Fic (Filamentation induced by cyclic AMP) domain with a conserved HPFX(D/E)GNGR motif that is found in many other bacteria and higher eukaryotes. The conserved histidine within this motif is crucial for the catalytic activity as its mutation abolishes the cell rounding phenotype caused by VopS **(Figure 1B)**.

Shortly after the characterization of VopS, a number of other bacterial AMPylators were identified. A secreted antigen IbpA from respiratory pathogen *Histophilus somni* contains two Fic domains and also targets Rho GTPases, although it modifies a tyrosine instead of threonine (7). Another bacterial AMPylator SidM/DrrA, secreted by *Legionella pneumophila,* modifies Rab1 GTPase to manipulate host membrane trafficking (8). AMPylation occurs on a tyrosine residue in the switch II region of Rab1, which restricts the access of its GTPase activating protein (GAP) and thereby renders Rab1 a constitutively active GTP-bound state. Interestingly, this protein catalyzes the modification using a nucleotidyl transferase domain which, instead of Fic domain, is the active site domain found in the aforementioned *E.coli* GS-ATase. This domain has a $GX_{11}DXD$ with the two aspartate residues playing a critical role in the catalytic reaction. To date, the Fic domain and the nucleotidyl transferase domain are the only two domains known to mediate AMPylation.

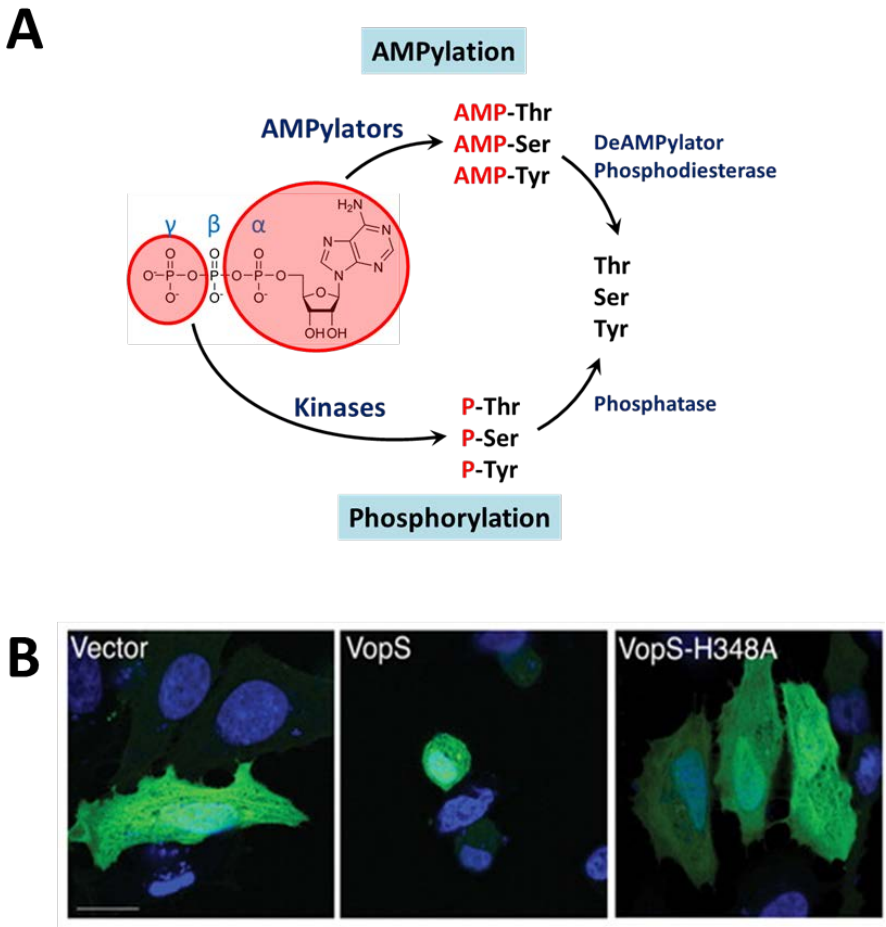

Figure 1. Overview of AMPylation.
(A) AMPylation uses ATP as a substrate and transfers its AMP moiety to modify hydroxyl side chains of protein substrates, whereas kinases use γ-phosphate from ATP to phosphorylate substrates. Both modifications are reversible by the activity of phosphates in case of phosphorylation, and deAMPylators and phosphodiesterases in AMPylation.
(B) A bacterial AMPylator VopS modifies Rho family GTPases in the host cell resulting in cell rounding phenotype. This is dependent on the catalytic Fic domain as mutation of the conserved histidine residue within this motif completely abolishes the cell rounding phenotype. Figure reproduced from (5).

DeAMPylation

AMPylation, similar to most posttranslational modifications, is a reversible process involving counteracting enzymes. The first known AMPylator GS-ATase is a bifunctional enzyme capable of both AMPylation and deAMPylation on its substrate glutamine synthetase (9). These two different catalytic reactions are mediated by adenylyl transferase (AT) domain at the C-terminus and adenylyl removase (AR) domain at the N-terminus of the GS-ATase. AR domain is structurally homologous to the nucleotidyl transferase family proteins and contains the conserved $GX_{11}DXD$ motif. The overlap between AT and AR domains shows the high structural similarity with a root mean square deviation (RMSD) of 24 Å (10). Many years later, and after the rediscovery of AMPylation from bacterial proteins, *Legionella* effector protein SidD was shown to deAMPylate Rab1 modified by DrrA (11). It removes AMP added by SidM/DrrA on Rab GTPases, which occurs in a spatially and temporally regulated manner during infection. No sequence homology was found between SidD and AR domain from GS-ATase or other known proteins. Interestingly, the crystal structure of the catalytic site of SidD shows a phosphatase-like fold with notable resemblance to members of the metal-dependent protein phosphatase (PPM) family (12). This finding demonstrates a complete pathway of reversible AMPylation regulated by specific bacterial enzymes to modulate host membrane trafficking.

Structural features of Fic proteins

Crystal structures of several bacterial Fic proteins mediating AMPylation have been recently determined (13-16). The structures of Fic family proteins have a conserved core topology with various additional secondary structures elements (17). VopS from *V. parahaemolyticus* is mainly alpha-helical with two subdomains (14) **(Figure 2A)**. The N-terminal subdomain comprised of 9 alpha-helices is rather unique with the minimal homology to other known Fic domains. The C-terminal subdomain comprises 8 alpha-helices with a conserved Fic motif located in two internal helices encircled by outer helices. Structural superpositions of VopS with *H. pylori* and *Bartonella henselae* BepA Fic domains demonstrate a conserved positioning of the active loop carrying the consensus HPFX(D/E)GN(G/K)R and the side chains within the motif. The active site formed by these conserved residues creates a shallow pocket which is completed by residues from the proximal hairpin loop **(Figure 2B)**. Different conformations were observed with this hairpin loop element from different Fic proteins and it is speculated that the substrate binding induces such structural changes. The conserved histidine within the Fic motif acts as a general base and deprotonates the attacking hydroxyl side chain of the target substrate. Phenylalanine anchors the catalytic loop to the hydrophobic core of the enzyme. The acidic aspartate/glutamate residue within the consensus sequence coordinates magnesium and the conserved asparagine interacts with pyrophosphate in the active site. The GNG submif forms an “anion hole” that favors the interaction with the oligophosphate moiety of nucleotides.

Crystal structure of IbpA Fic2 in complex with its substrate Cdc42 revealed that Cdc42 adopts a conformation similar to that of the GDP-dissociation inhibitor (GDI)-bound state of Rho family GTPases (15). This suggests that IbpAFic2 is able to induce a conformational change on its substrates into their inactive GDI-bound form. The extensive binding interface between the enzyme and the substrate engages the switch 1 and switch 2 regions of Cdc42, which could ensure tight substrate specificity. As predicted, the conserved beta/hairpin loop coordinates the substrate binding.

Crystal structure of human Fic protein or HYPE has been recently solved, presenting the structure of the first eukaryotic Fic protein (18). The catalytic loop, beta/hairpin loop, and the alpha-inhibitory motif of HYPE were similar to the existing structural elements of bacterial Fic proteins. Notably, three main structural features (TPR motif, Fic domain, and the linker between the two domains) exhibit a compact structure with intramolecular interaction resulting in restricted flexibility. In addition, HYPE formed asymmetric dimers with a binding interface exclusively composed of Fic domain contacts. TPR motifs are not involved in dimerization and positioned at the opposite sides of the dimer surface. Whether this dimer formation is a naturally occurring event in cells remains to be determined, especially considering our findings that near the interface of this dimer is the predicted N-linked glycosylation site (Chapter 3).

Together, these structural studies of various Fic proteins provide insights into the nucleotide and substrate binding mechanism as well as catalytic mechanisms in the active site of the Fic domain.

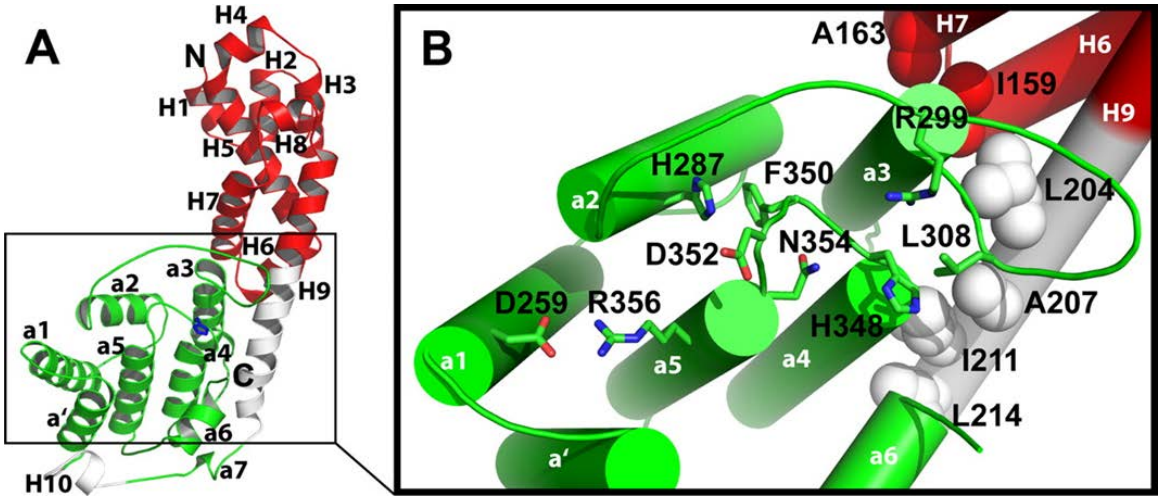

Figure 2. Crystal structure of VopS.
(A) A ribbon diagram of VopS-(75–387). The N-terminal subdomain of VopS contains helices H1-H9 (red) and the C-terminal subdomain contains the later half of H9 and H10 (white) with the structurally conserved Fic domain (green). (B) A detailed view of residues in the catalytic Fic domain. Hydrophobic residues from H6, H7, and H9 depicted in spheres structurally stabilize the C-terminal Fic domain of VopS. Residues in the Fic motif (HPFX(D/E)GN(G/K)R) and His-287 and Asp-259 are displayed as sticks. Leu-308 and Arg-299 are positioned in the hairpin loop which is structurally conserved in all Fic domain proteins. Figure reproduced from (14).

Fic inhibitory motif

Study of VbhT, a Fic protein from the bacterial pathogen *Bartonella schoenbuchensis* and its antitoxin VbhA provided a valuable insight to the common structural feature of Fic proteins (19). VbhT inhibits bacterial growth when expressed in *E. coli*, and this is dependent on the catalytic activity of the Fic motif which exhibits AMPylation activity *in vitro*. VbhA, a protein encoded by a gene immediately upstream of *vbhT*, represses VbhT toxicity by inhibiting its AMPylation activity. A comprehensive analysis of this toxin-antitoxin module involving Fic-domain-encoding genes identified 158 bacterial *vbhA* homologs. These putative antitoxins contain a conserved (S/T)XXXE(G/N) motif which is located in the alpha-helix that tightly embraces VbhT and is positioned in proximity to the putative ATP binding site for VbhT. Serine and glutamate residues within this inhibitory motif form a hydrogen bond and a salt bridge, respectively, with the conserved arginine residue following the Fic catalytic motif. Therefore, this alpha-helical inhibitory motif competes with ATP binding and obstructs the Fic active site **(Figure 3)**. Structural comparison revealed that this inhibitory motif is also found within the other Fic proteins, suggesting the co-evolution of catalytic and inhibitory function in such proteins. When the conserved glutamate residue is mutated, the inhibition is released and the Fic proteins exhibit robust AMPylation activity in vitro. Therefore, this study reveals a general inhibitory mechanism adopted by Fic proteins through intra- or intermolecular active-site obstruction.

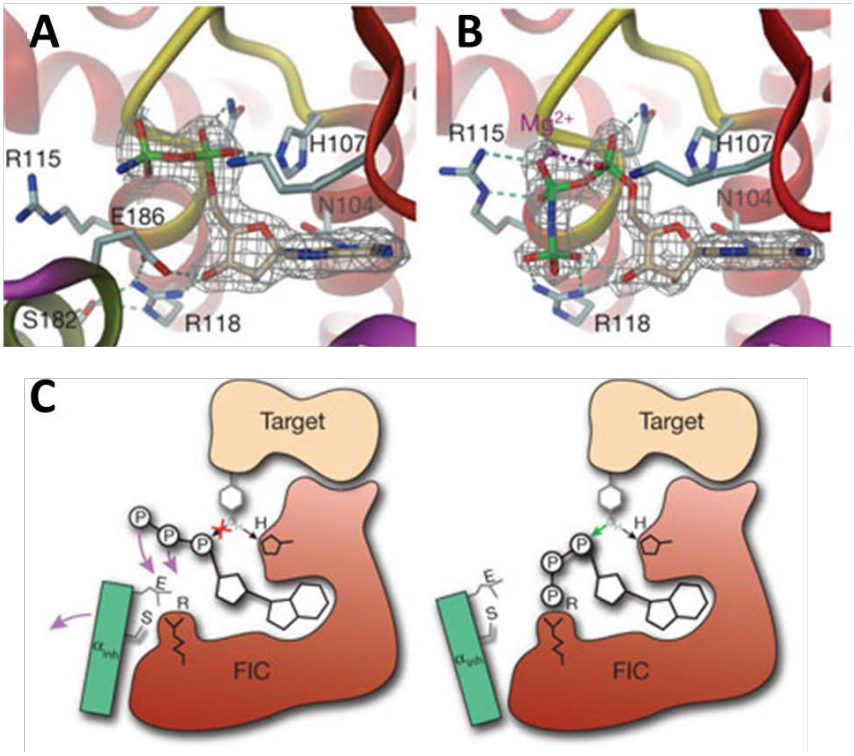

Figure 3. Structural view of the inhibitory mechanism by active-site obstruction.
(A) Active site of Fic domain protein from *Neisseria meningitides* (NmFic) with bound ATP analogue AMPPNP. (B) Active site of NmFic(Δ8) missing the inhibitory alpha-helix with bound AMPPNP and Mg^{2+}. The γ-phosphate occupies the position taken by E186 of the (S/T)XXXE(G/N) motif in the wild-type. (C) Scheme of the general inhibitory mechanism adopted by Fic proteins. The inhibitory alpha-helix (green) with the (S/T)XXXE(G/N) motif prevents the productive binding of ATP in the active site. Upon dissociation with the inhibitory helix, γ-phosphate of ATP is positioned adjacent to the conserved arginine residue (R) in the Fic motif. The α-phosphate is then properly oriented to be attacked by the hydroxyl side chain of the target substrate. Figure reproduced from (19).

Fic domain exhibiting a versatile catalytic mechanism

Phosphocholination

Further studies revealed that Fic domains are capable of mediating more than just AMPylation. AnkX, a *Legionella* effector that contains a Fic domain, was shown to be the phosphocholine transferase that targets Rab1 GTPase (20). From its substrate CDP-choline, AnkX transfers phosphocholine instead of the NMP moiety to the target side chain. Phosphocholination of Rab1 in host cells disrupts the Golgi apparatus and blocks secretion of host alkaline phosphatase. This modification occurs on a serine residue in the switch II region adjacent to the tyrosine residue that is AMPyated by DrrA. Rab35, a Rab1 family member that regulates the sorting of cargo from early endosomes, was also shown to be modified by phosphocholine, thereby demonstrating the specificity of AnkX for Rab1 family members. Investigating a repertoire of Rab proteins for modification revealed that AnkX and DrrA have some overlapping but non-identical Rab specificities. Phosphocholinated Rab35 has a defect in binding to connecdenn, a Rab35-specific eukaryotic GEF, thus inhibiting the activation of Rab35. Therefore, AnkX and DrrA modulate the function of Rab GTPases during *Legionella* infection by employing different modifications and diversifying the proteins that bind to the modified Rab. It is fascinating to note that the two biochemically distinct effector proteins from the same pathogen modulate the host signaling pathway by targeting the same substrate. However, their different *in vivo* specificities for Rab proteins implicate that they also exert functions that do not overlap, which requires further investigation.

The crystal structure of AnkX in complex with CDP-choline provides molecular details on how this enzyme recognizes a different substrate and exerts unique modification despite the conservation of the active site (21). Both ATP and CDP-choline share a nucleotide diphosphate group. However, CDP-choline binds to AnkX in the inverse orientation in comparison to ATP binding with canonical Fic proteins so that the choline moiety rather than cytidine is placed as a leaving group. Furthermore, presence of Phe, Ile, and Asp in the vicinity of the choline moiety excludes the binding of the adenine base through steric hindrance. The recognition of the substrate CDP-choline is achieved by the CMP domain that is unique to AnkX. Despite the transposed nucleotide binding mode, the catalytic groups in the active site and the chemical reactions driven by AnkX are the same as those of the Fic proteins mediating AMPylation.

UMPylation

AvrAC is a type III effector from plant pathogen *Xanthomonas campestris* that suppresses host immune response by targeting two receptor-like cytoplasmic kinases BIK1 and RIPK (22). Fic domain-carrying AvrAC, interestingly, uses UMP to modify these kinases on the conserved serine and threonine residues in the activation loop. These residues are known to undergo phosphorylation which is crucial for plant immune signaling. BIK1 and RIPK modified with UMP exhibited reduced autophosphorylation, demonstrating that UMPylation of these conserved serine and threonine residues prevents their phosphorylation and the activation of the kinases. Interestingly, this competive posttranslational modification is reminiscent of a strategy from YopJ, a bacterial effector

from *Yersinia* species. YopJ inhibits MAPK and NFκB pathways by modifying the critical serine and threonine residues in the activation loop of MAPKK6 with a competitive posttranslational acetyl group, thereby preventing their phosphorylation (23).

Phosphorylation

The bacteriophage P1 toxin Doc belongs to the *doc-phd* toxin-antitoxin (TA) module which serves a critical role in cellular functions including stress response, cell cycle arrest, programmed cell death, and bacterial persistence during antibiotic treatment (24). Interestingly, Doc shares structural similarity and a conserved catalytic core with Fic domain, thus classified as a subfamily of Fic proteins (17). The slight alteration in the catalytic motif of Doc is represented by HXFX(D/N)(A/G)NKR in comparison to canonical Fic motif HXFX(D/E)GNGRXXR. Doc has been reported to cause bacterial growth arrest by inhibiting protein translation, although the precise mechanism or its target had been unknown. Recent studies on Doc shows it is a protein kinase that phosphorylates a conserved threonine residue on the translation elongation factor EF-Tu (25,26). Phosphorylated EF-Tu is unable to bind aminoacylated tRNAs and thereby the ternary tRNA-EF-Tu-GTP complex formation required for translation elongation is inhibited. This distinct enzymatic activity of Doc is likely due to its degenerate form of Fic motif. These studies further illustrate a remarkable divergence of catalytic mechanisms employed by Fic proteins while they maintain the conserved catalytic core **(Figure 4)**.

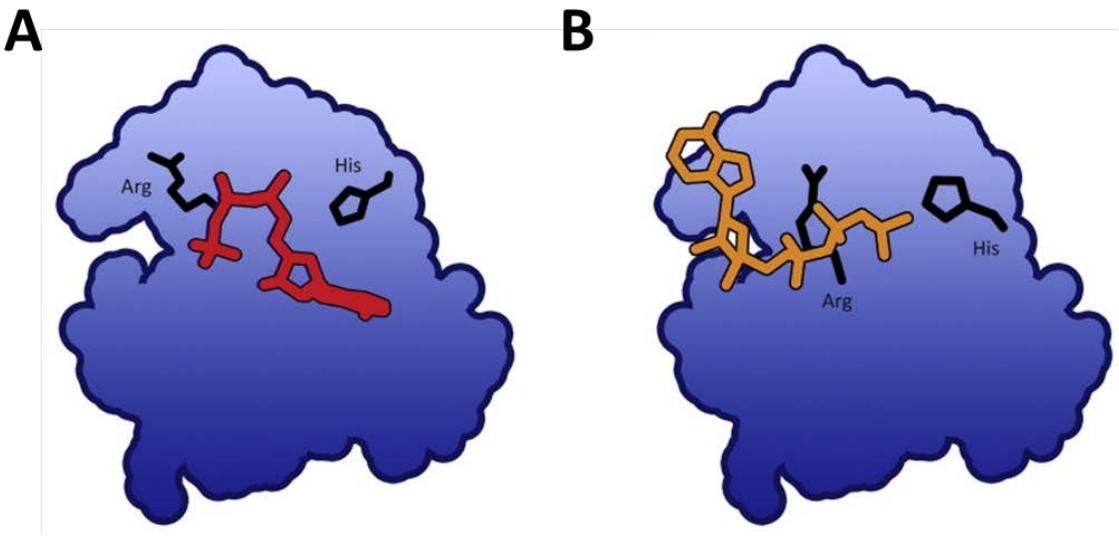

Figure 4. Nucleotide binding site of Fic domains.
(A) Cartoon representation of the typical nucleotide binding mode in Fic NMPylator complex. Enzyme is represented as blue shape. The catalytic His residue shows the N-terminal side of the catalytic loop and the Arg shows the C-terminal side. The nucleotide is shown in red. (B) Cartoon representation of the transposed nucleotide binding mode observed in Fic domains such as Doc and AnkX. Figure reproduced from (27).

ER chaperone BiP

Endoplasmic reticulum (ER) is a major organelle in cells where secretory and membrane proteins undergo proper folding and modifications. Newly synthesized proteins are translocated to the ER and eventually get transported to their target organelles or secreted out of the cell. Therefore, the ER stores an abundant amount of chaperones and folding enzymes to achieve the quality control of these proteins (28-30). Aberrant or misfolded proteins are assisted by the chaperones to be assembled correctly or, if the folding attempts continuously fail, get selectively degraded by the ER-associated degradation (ERAD) pathway (31-36).

BiP (immunoglobulin-binding protein)/GRP78 (glucose-regulated protein 78kDa) is one of the most abundant ER chaperones and a member of a highly conserved heat shock 70 family protein (37,38). It has the C-terminal KDEL sequence which prevents the secretion of BiP and maintains it within the ER lumen. As a molecular chaperone, BiP binds and assists the folding and assembly of newly-synthesized proteins. It also maintains the permeability barrier of the ER membrane by sealing the luminal end of the translocon pore before and early in translocation (39). Studies from Kar2, the yeast homolog of BiP, provided many additional roles of BiP in the ER. It is essential for translocating secretory precursors across the ER membrane (40,41). Furthermore, aberrant or misfolded proteins bind to BiP for assembly or to undergo proteosomal degradation after failed folding attempts (42,43). Thereby, BiP contributes to quality control for protein homeostasis in the ER as a multifunctional chaperone (31,44-47).

BiP at a molecular level

Hsp70 chaperone proteins, including BiP, have two major domains: an N-terminal nucleotide binding domain (NBD) and a C-terminal substrate binding domain (SBD) that are connected by a conserved hydrophobic interdomain linker region (48-50). The N-terminal domain is composed of two lobes of mixed alpha-helices and beta-strands with a deep cleft containing an ATP binding pocket. The SBD is mostly beta strands that recognize the polypeptide substrates enriched in hydrophobic residues. Following SBD is the C-terminal alpha helical lid. These two domains are tightly coupled and undergo allosteric cycle of ATP binding/hydrolysis and substrate binding/release (51-56) **(Figure 5A**). When ATP binds to NBD, the hydrophobic interdomain linker and the alpha-helical lid of the SBD attach to the NBD, which opens the peptide binding pocket in the SBD. Binding of substrate then facilitates ATP hydrolysis in the NBD. ATP hydrolysis triggers the alpha-helical lid to detach from the NBD and close the SBD. This results in the high affinity-binding of substrate to the SBD. When ADP is exchanged with ATP by a nucleotide exchange factor (NEF), the substrate is released allowing folding to proceed. Structural analysis of BiP revealed that when NBD is bound to ADP, the two domains are separated and held loosely by the interdomain linker **(Figure 5B)**. When NBD is bound to ATP, SBD and the linker come in close contact with NBD forming a compact structure **(Figure 5C)**.

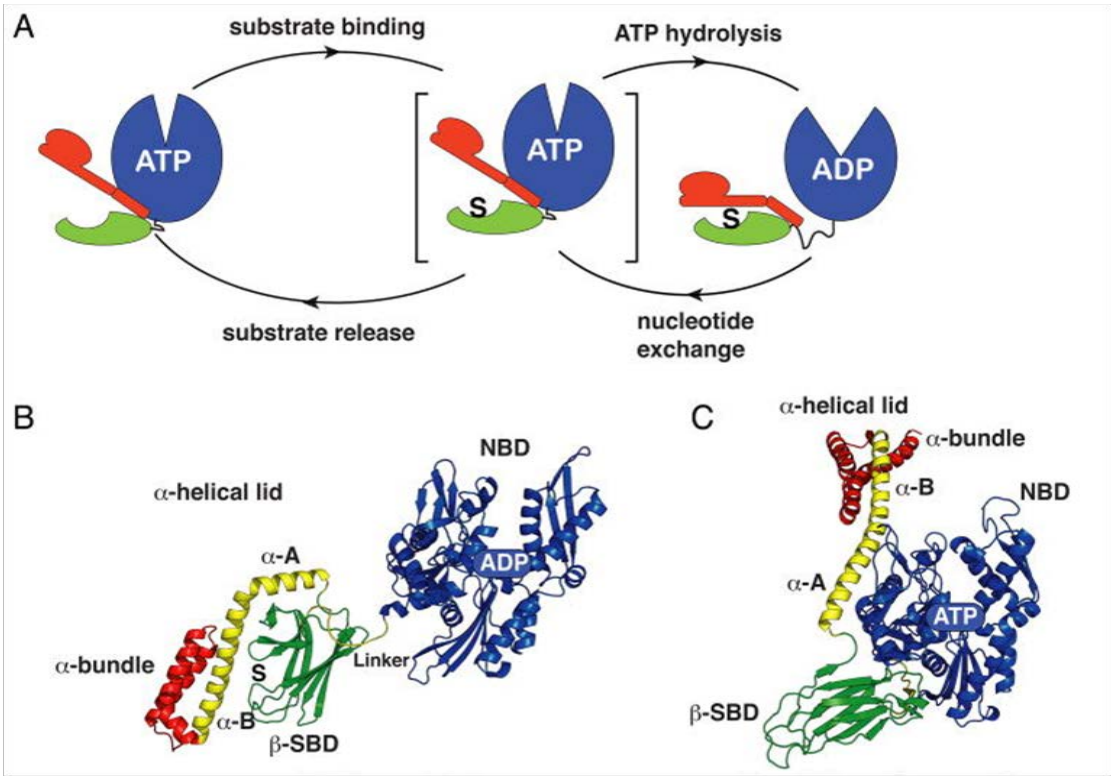

Figure 5. Conformational changes during allosteric cycle of Hsp70.
(A) The allosteric cycle of Hsp70. Blue, nucleotide binding domain (NBD). Green, substrate binding domain (SBD). Red, C-terminal alpha-helical lid. (B) and (C) Two 'end-point' state structures of *E. coli* Hsp70 protein DnaK in the ADP-bound state (B, PDB ID code 2kho) and the Hsp110-based homology model of the ATP-bound state (C). Figure reproduced from (57).

ER stress and the unfolded protein response (UPR)

The accumulation of unfolded or misfolded proteins in the ER lumen is referred to as ER stress, and it triggers multiple adaptive signaling pathways collectively termed the unfolded protein response (UPR). Numerous cellular stress conditions such as disruption of calcium homeostasis, aberrant glycosylation level, and altered redox state of the ER lumen can cause ER stress and activate the UPR. BiP plays a key role as a sensor and regulator of the UPR by activating the ER signal transducers: PERK [protein kinase RNA (PKR)-like ER kinase], IRE1 (inositol requiring enzyme 1), and ATF6 (activating transcription factor 6) (46,47,58). In the resting state, BiP binds to these ER membrane proteins to keep them inactive. Upon ER stress, BiP binds to an increased load of misfolded proteins and is coincidently released from the UPR signal transducers, thereby activating their signaling pathways. These pathways upregulate the production of chaperones and folding enzymes while shutting down the general protein translation to decrease the burden of the ER **(Figure 6)**.

IRE1

IRE1 is a type I transmembrane protein with an N-terminal lumenal domain and C-terminal cytoplasmic kinase and RNase domains. Upon ER stress and disassociation from BiP, IRE1 oligomerizes and triggers *trans*-autophosphorylation of its cytoplasmic domain and activation of its endoribonuclease domain. It then cleaves the mRNA of the UPR transcription factor XBP1 (X-box binding protein 1) in two specific positions excising ~20 bp of its intron. This spliced form of XBP1 mRNA by IRE1 is translated resulting in

an active transcription factor that upregulates multiple genes encoding chaperones and ERAD proteins.

PERK

PERK is a type I transmembrane protein with N-terminal lumenal domain and C-terminal cytoplasmic kinase domain. Similar to IRE1, PERK also undergoes oligomerization when BiP dissociates from its luminal domain resulting in *trans*-autophosphorylation of its cytoplasmic domain. The activated kinase domain then phosphorylates the eukaryotic translation initiation factor eIF2α. This results in decline of general protein synthesis and the reduction of the flux of proteins entering the ER (59). In the meantime, some mRNAs containing short upstream open reading frame in their 5'-untraslated region are preferentially translated (60). This includes an mRNA encoding ATF4, a transcription factor that targets UPR gene expression. Two of the major genes induced by ATF4 are GADD34 (growth arrest and DNA damage-inducible 34) and CHOP (transcription factor C/EBP homologous protein) (61,62). GADD34 encodes a PERK-inducible regulatory subunit of the protein phosphatase PPIC complex that dephosphorylats eIF2α (63), providing a negative feedback loop to reset the translation once the ER stress is resolved. CHOP is a transcription factor upregulating genes involved in apoptosis (64,65). Therefore, PERK can induce the apoptotic pathway via CHOP under prolonged ER stress.

ATF6

Unlike IRE1 and PERK, ATF6 is a type II transmembrane protein with a C-terminal stress sensing domain in the ER lumen and an N-terminal bZip transcription factor domain facing cytoplasm. Upon ER stress, ATF6 is translocated from the ER to the Golgi where it is cleaved by the site-1 and site-2 proteases (S1P and S2P) (66). This releases the N-terminal transcription factor domain which then enters to the nucleus and activates UPR target genes encoding chaperones, folding enzymes, and components of the ERAD pathway (67,68)

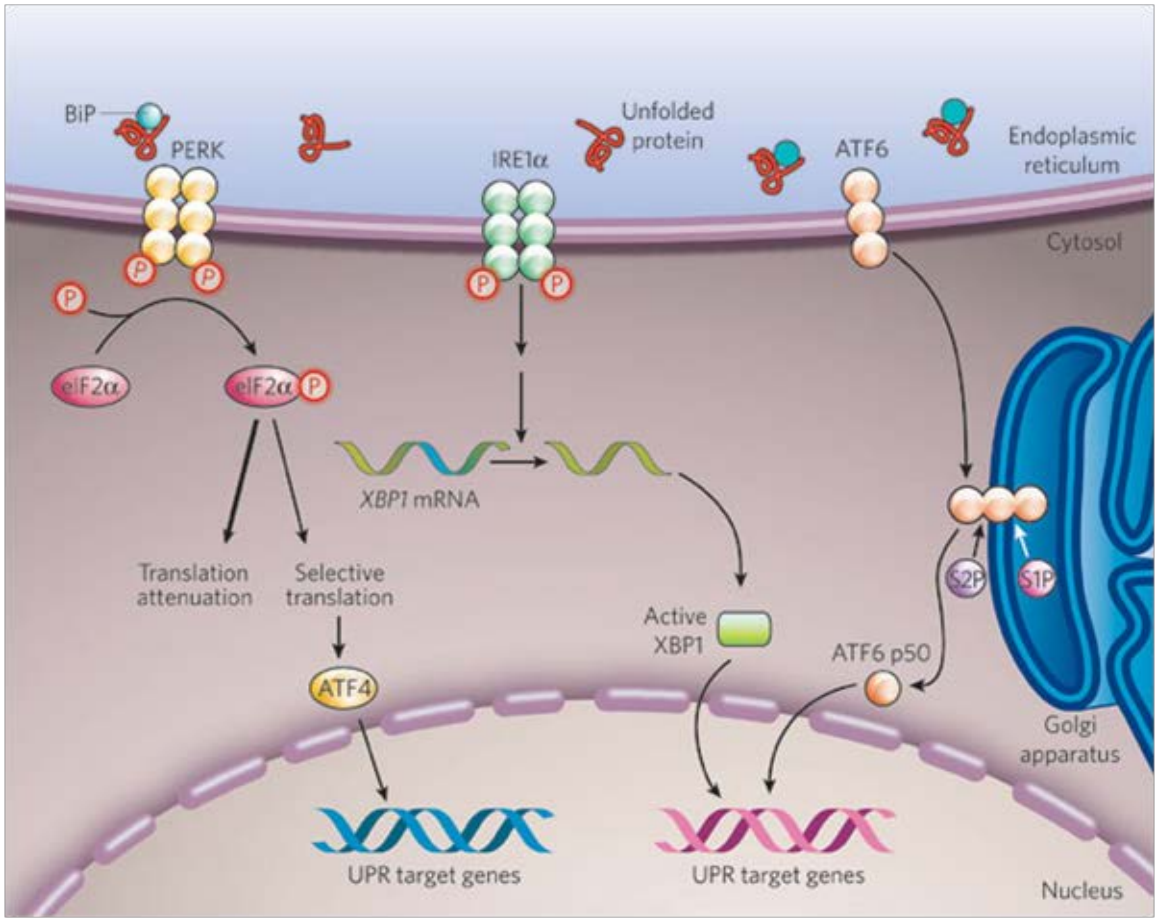

Figure 6. Unfolded protein response (UPR) signaling pathway.
In the resting cells, BiP binds to ER stress sensors PERK, IRE1, and ATF6 to keep them inactive. Upon ER stress, BiP is released from these proteins to bind to misfolded proteins, triggering the UPR signaling cascades. PERK oligomerizes and cross-phosphorylate its cytoplasmic kinase domain, which then phosphorylates eukaryotic translation initiation factor eIF2α. This inactivates eIF2α and attenuates general translation while it selectively translates a set of proteins including a transcription factor ATF4 that induces UPR target genes. IRE1 also oligomerizes and cross-phosphorylate its cytoplasmic domain activating its endoribonuclease activity. It then splices the XBP1 mRNA in an uncanonical manner, which is translated into an active transcription factor and turns on UPR target genes. ATF6 is translocated to the Golgi upon ER stress and selectively cleaved by proteases (S1P and S2P). This renders ATF6 an active transcription factor that can also induce multiple UPR target genes. Figure reproduced by (69).

Posttranslational modifications of BiP

Early studies of BiP revealed that it undergoes different posttranslational modifications: phosphorylation and ADP-ribosylation. It was shown to be autophosphorylated in vitro in a calcium-dependent manner (70). Phosphoamino acid analysis showed that the modification occurs on a threonine residue in vitro whereas both serine and threonine were detected to be phosphorylated in vivo (70,71). Mutational analysis mapped the modification site to Thr229 located in the ATP binding cleft (72). This residue had been predicted to interact with the γ-phosphate of ATP via a polarized water molecule and may serve as an intermediate during ATP hydrolysis. However, phosphorylation of Thr229 was not detected in vivo. Later study showed that the in vivo phosphorylation site maps to the substrate binding domain rather than the ATP binding domain (73). Even though it is speculated that this may alter the substrate binding, how the phosphorylation affects the molecular or biological function on BiP still remains unknown.

In addition to phosphorylation, ADP-ribosylation of BiP was observed from the early studies from in vivo labeling of cells using [^{3}H]-adenosine and two-dimensional gel electrophoresis (74). They observed that heat shock and glucose starvation induced rapid decrease in the modification, which made them speculate that ADP-ribosylation plays an important role for the function of BiP. ADP-ribosylation was also shown to be reversible during nutritional stress (75,76). The detailed molecular mechanism of this modification had not been further investigated until the recent study by Chambers and colleagues (77). They mapped the modification sites to conserved R470 and R492 in the substrate binding

domain and showed that ADP-ribosylation alters the substrate binding and release thereby interfering with the interdomain allosteric coupling. This modification was proposed as a rapid posttranslational mechanism to allow rapid inactivation of BiP.

BiP-related physiological and pathological processes

As a master regulator of UPR which is an essential mechanism of cells to cope with stress, BiP is involved in various physiological and pathological conditions (78-80). For instance, studies have shown that BiP is involved in embryonic and nervous system development. The level of BiP is high at the blastocyst stage of the developing mouse embryo (81), and is highly expressed in the heart, neural tube, gut endoderm, somites, and surface ectoderm of mouse embryo during early organogenesis (82). Knockout of BiP in mice displays lethality, further confirming the essential role of BiP in embryogenesis (83). Another recent study showed that ER stress is involved in the development of central nervous system as higher levels of ER chaperones including BiP and the major UPR indicators such as phosphorylated eIF2α, spliced XBP1 mRNA were predominantly detected in the embryonic brain (84). This is likely due to ER stress induced apoptosis, which is a key event that occurs during development of the central nervous system. The underlying mechanism and the specific role of BiP in embryonic and neuronal development are yet to be determined.

BiP is also implicated in the aging process. IRE1, one of the major UPR signal transducer, is required for the longevity in *Caenorhabditis elegans* (85). This suggests the

crucial role of maintaining ER homeostasis in alleviating deleterious effects of aging. In addition, protein expression and the activity of several ER chaperones including BiP significantly decline during aging process (86-90). Compared to young mice, old mice exhibit considerably lower level of BiP and increased susceptibility to ER stress. Therefore, a cell's growing inability to resolve ER stress and properly maintain ER homeostasis is likely to be associated with many age-related pathologies.

Accumulation of misfolded proteins and protein aggregates in neurons results in detrimental neurological diseases such as Alzheimer's disease, Parkinson's disease, and amyotrophic lateral sclerosis (91-95). A mouse with a conditional knockout of BiP in Purkinje cells (PCs) exhibited accelerated PC degeneration and cerebellar atrophy in addition to several defects in motor coordination (96). In addition, a mouse model bearing a disruptive mutation in the Sil1 gene, which encodes a nucleotide exchange factor for BiP, displays numerous neurodegenerative defects (97,98). Aberrant expression levels of BiP are also associated with various neurological disorders, emphasizing the neuroprotective role of BiP.

The role of BiP in cancer

Tumor microenvironments often mimic the physiological ER stress condition due to glucose deprivation and hypoxic environment, which activates the UPR in cancer cells. Therefore, BiP is observed to be highly expressed in a variety of cancer cell lines, solid

tumors, and human cancer cells, including lung cancer, prostate cancer, gastric carcinoma, hepatocellular carcinoma and breast cancer (99-103). The elevated level of BiP also correlates with malignancy, invasion, and metastasis (100-103). In addition, recent studies with overexpression and siRNA of BiP showed that BiP contributes to tumor growth and confers drug resistance as well as chemoresistance (104,105). Therefore, BiP could potentially be a useful diagnostic and prognostic marker for different types of tumors.

Interestingly, recent studies have shown that BiP can exist outside the ER and is found on the cell surface in a wide variety of cancer cells but not in normal cells (106-108). Cell surface BiP has been shown to act as a receptor and regulator of cell signaling by forming complexes with a variety of extracellular ligands and cell surface anchored proteins in tumor, promoting pro-survival and pro-apoptotic pathways (108-111). The presence of BiP in the plasma membrane of malignant cancer cells makes it an appealing target for cancer therapy, and various antibodies and peptides are being developed to selectively target the cell surface BiP (105).

Aims of this study

The alignment of Fic domain from different organisms revealed that this domain is highly conserved across species, including higher eukaryotes (5) **(Figure 7)**. This implicates that AMPylation mediated by Fic domain serves a critical role in cellular function. There have been extensive studies and characterization of Fic domain proteins in the past years, but the majority of these studies have focused on bacterial proteins

acting on a host signaling system during infection. Bacterial effectors and toxins harboring Fic domain have evolved to utilize various forms of phosphoryltransferase reaction (AMPylation, phosphocholination, UMPylation, phosphorylation) to posttranslationally modify host proteins and subvert their signaling pathways. The fact that Fic domain is found in higher eukaryotes, including mammals, suggests that it may have a regulatory role in an essential signaling pathway. Precedent stems from the observation that *E. coli* GS-ATase regulates nitrogen metabolism in cells by reversibly AMPylating glutamine synthetase (3,4).

Therefore, the goal of this study is to examine the physiological and biological function of a Fic protein from a higher eukaryote and identify its endogenous substrate and biological activity. We are using *Drosophila melanogaster* as a genetic model system to explore the physiological function of *Drosophila* Fic (dFic). We also use *Drosophila* S2 cells for biochemical assays to characterize eukaryotic Fic and identify the endogenous AMPylated substrate. Deciphering the role of AMPylation will not only provide basic principles of a new conserved mechanism employed by eukaryotic cells but also will further our understanding of the various posttranslational modifications in cell signaling network.

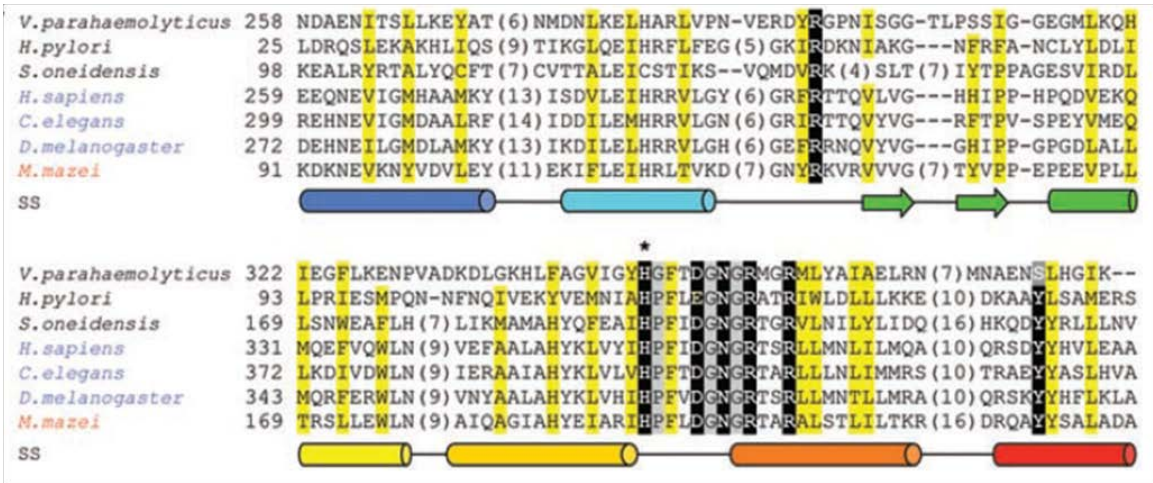

Figure 7. Multiple sequence alignment of representative Fic domains from different organisms. Fic motif represented by HPFX(D/E)GNGR is highly conserved among the homologs. An asterisk marks the conserved histidine residues within the Fic motif. Figure reproduced by (5).

CHAPTER 2
Materials and Methods

S2 cell culture condition

Drosophila melanogaster Schneider 2 (S2) cells were grown according to standard protocols (112). Cells were maintained at 27°C, 5% CO_2 in Schneider's medium supplemented with PSG [1mM sodium pyruvate, 100U/ml penicillin, 100µg/ml streptomycin, 2mM L-glutamine (Invitrogen)] and 10% heat-inactivated fetal bovine serum (Sigma).

S2 cell transfection

Cells were seeded at 3.0 x 10^6 cells/ml per well in 6-well plates. For transfection, 2µg total DNA was added to 180µl of serum free media. Next, 5µl of X-tremeGENE HP DNA transfection reagent (Roche) was added and mixed thoroughly. After 30min, samples were added drop-wise to cells. Cells were then grown for 3 days before harvesting.

Cloning of genes

The genotypes of all the bacterial strains used in this study are listed in **Table** 1. Genes for constructs **(Table 2)** were PCR amplified with Vent DNA polymerase (NEB) and designed primers (Sigma) **(Table 3)**. PCR product was purified and digested, along with the target vector, with digestion enzymes (NEB or Thermo Scientific Fermentas).

DNA was run on an agarose gel and extracted using Gel-extraction kit (BioBasic Inc). Digestion products were then ligated to the vector with T4 DNA Ligase (NEB) and then transformed into the *E. coli* DH5α strain. DH5α bacteria were grown on Luria Bertani (LB) media agar (1% tryptone, 0.5% yeast extract, 1% NaCl, and 1.5% agar) or in 2xYT liquid broth (1.6% tryptone, 1% yeast extract, 0.5% NaCl) with selective antibiotics at 37°C. The cloned plasmid was purified using a mini-prep kit (Invitrogen or BioBasic Inc) and the gene insertion was confirmed by colony PCR and sequencing.

Cell lysate harvest and Western blotting

S2 cells were scraped from the plates and spun down at 6000 rpm for 3 min to pellet the cells. Cells were then washed once with PBS and lysed with ConA RIPA buffer (50mM Tris pH 7.5, 150mM NaCl, 1% NP-40, 0.5% deoxycholate, 5mM MgCl2, 5mM MnCl2, 5mM CaCl2, 1mM PMSF, protease inhibitor cocktail (Roche)) and the soluble fraction was collected after 1000xg centrifugation for 10 min at 4°C. Total amount of proteins were measured by Bradford assay (Thermo Scientific) and 5X SDS sample buffer was added to the lysate. The samples were boiled for 5 min and run on SDS-PAGE gel, transferred to a membrane, and analyzed by western blot analysis. Primary antibodies include: mouse anti-M2-FLAG (Sigma), rat anti-BiP (Troponin H, Abcam), mouse anti-tubulin (Abcam), rabbit anti-AMP-Thr (homemade), rabbit anti-dFic (homemade), anti-phospho-eIF2α (Ser51, Cell Signaling).

Protein purification

GST-tagged protein constructs were transformed into *Escherichia coli* Rosetta (DE3) cells and single colonies were grown to an OD600 of 0.6-0.8 and expressed with 0.4mM isopropyl β-D-thiogalactopyranoside for 20 h at 22°C. Cells were then resuspended in PBST (PBS with 0.1% Triton-X, 14.2mM 2-Mercaptoethanol) and lysed by a cell disrupter (EmulsiFlex-C3, Avestin Inc.) and the protein was purified using a standard protocol for GST affinity chromatography (Pierce). Proteins were bound to glutathione beads, washed 3X with PBST, and eluted with GST elution buffer (50mM Tris pH 7.5, 150mM NaCl, 16.5mM reduced L-glutathione, 14.2mM 2-Mercaptoethanol). His-tagged protein constructs were expressed as described above and purified using a standard nickel-affinity purification protocol (Thermo). Proteins were bound to Ni^{2+} beads, washed 3X with His wash buffer (20mM NaH_2PO_4, 150mM NaCl, 20mM imidazole), and eluted with His elution buffer (20mM NaH2PO4, 150mM NaCl, 250mM imidazole). Protein was changed into buffer (50mM Tris pH 7.5, 50mM NaCl, 10% glycerol) using concentrator column (Amicon). After nickel purification, His-hBiPΔ19 and His-SUMO-hFicΔ47 were further purified on HiLoad 16/60 Superdex 75 (GE) attached to AKTA FPLC.

Concanavalin A pulldown

S2 cells were harvested and lysed with ConA RIPA buffer (50mM Tris pH 7.5, 150mM NaCl, 1% NP-40, 0.5% deoxycholate, 5mM $MgCl_2$, 5mM $MnCl_2$, 5mM $CaCl_2$, 1mM PMSF, protease inhibitor cocktail (Roche)) and the soluble fraction was collected

after 1000xg centrifugation for 10min at 4°C. The fraction was then loaded onto the equilibrated concanavalin A beads (Sigma) and incubated overnight at 4°C. The beads were washed three times with equilibration buffer (200mM Tris pH 7.5, 500mM NaCl, 5mM $MgCl_2$, 5mM $MnCl_2$, 5mM $CaCl_2$). The fraction bound to the beads was directly used for *in vitro* AMPylation assays or eluted with SDS sample buffer for SDS-PAGE and western blot analysis.

Immunoprecipitation

S2 cells transfected with FLAG-tagged BiP constructs were lysed as described above. The lysate was incubated with anti-FLAG M2 agarose (Sigma) overnight at 4°C and the beads were washed three times with TBS (50mM Tris pH 7.5, 150mM NaCl). Proteins bound to beads were eluted with SDS sample buffer for SDS-PAGE and western blot analysis.

***In vitro* AMPylation assay**

In vitro AMPylation assays were performed using GST-dFicΔ70 as an enzyme and either recombinant His-BiP protein or S2 cell lysate as substrate. Each reaction contained 0.2µM GST-dFicΔ70, 250µM cold ATP, 0.1-0.2 µCi [α-^{32}P] ATP, and 2µM His-BiP in 30µl AMPylation buffer (20mM Tris pH 7.5, 100mM NaCl, 10mM $MgCl_2$, 5mM $MnCl_2$, 5mM $CaCl_2$, except where exclusion of $CaCl_2$ is indicated). When S2 cell lysate was used as substrate, 20µg cell lysate was added to the reaction with 1mg/ml RNaseA. The reactions were incubated for 45min at 30°C and stopped by the addition of

SDS sample buffer. Samples were analyzed by autoradiography following SDS-PAGE. For the assays where AMPylation was detected by the anti-AMP-Thr antibody (113), the experiment was performed as described above but excluding radiolabeled ATP.

In vitro phosphocholination assay

100ng of GST-AnkX (1-484) or 1µg of GST-dFicΔ70 was incubated in buffer (20mM HEPES pH 7.5, 100mM NaCl, 1mM MgCl2, 1mM ATP) and incubated for 1 hr at 30°C in the presence of 1mM CDP-choline. Samples were boiled in SDS sample buffer were analyzed by western blot analysis using an antibody specific for phosphocholine (TEPC-15, Sigma).

In vitro UMPylation assay

100ng or 1µg of GST-dFicΔ70 E247G, GST-AnkX (1-484), or GST-DrrA was incubated in 20 µl reaction buffer containing 25 mM Tris pH 7.5, 25 mM $MgCl_2$, 500 µM UTP, 1 mM DTT, α-^{32}P UTP (5 µCi) for 30 min at 30 °C. Samples were analyzed by autoradiography following SDS-PAGE.

ATPase assay

ATPase assay using His-BiP constructs were performed on Ni-NTA beads (Pierce). 500nM of BiP was bound to the beads for 1h at 4°C and 100µM ATP was added to the bound proteins in ATPase assay buffer (20mM Hepes pH 7.0, 2mM $MgCl_2$, 25mM KCl). After 3 h of ATP hydrolysis reaction at 30°C, supernatant was collected and the

remaining ATP was measured using the ATP bioluminescent assay kit (Sigma) according to manufacturer's protocol. Luminescence was measured by FLUOstar OPTIMA (BMG Labtech).

Immunohistochemistry

Cover slips were sterilized and pretreated with 100 µl of FBS for 2 hrs at 37°C and washed once with PBS. 100µl of transfected cells were plated in a droplet on the cover slips and left to adhere for 1-2 hrs. Cells were rinsed once with PBS and fixed with 4% formaldehyde in PBS for 10 min. Cells were then washed 3X with PBST for permeabilization for total of 5 min. Cells were then blocked for 1 hr at room temperature (RT) with 5% BSA in PBS. Primary antibody in 1% BSA were added to the cells and incubated for 1 hr. After 3X PBST wash, cells were incubated wit secondary antibody in PBST for 1 hr. Cells were then washed 3X with PBST and 150 µl dyes diluted in PBS were added directly to the coverslip. After staining for 10 min, cells were washed 2X with PBS. The cover slips were then mounted on slides and analyzed by a Zeiss LSM 510 scanning confocal microscope.

Quantitative real-time PCR

Total RNA was extracted from treated and untreated S2 cells using Trizol reagent (Ambion). 2µg RNA was reverse transcribed into cDNA using High-Capacity cDNA Reverse Transcription (Applied Biosystems) utilizing random hexamers. RT-PCR was performed using Fast SYBR Green master mix (Applied Biosystems) on a 7500 Fast

Real-Time PCR System (Applied Biosystems). Amplification was carried out in 20µl reaction mixtures containing 100ng cDNA (in 5µl), 7.5pmol each primer (in 5µL) and 10µl of 2X SYBR Green master mix. Rp49 (ribosomal protein) was used as an internal control and all reactions were performed in triplicate. Quantification of relative gene expression was analyzed using the ΔΔCt method. The primers used for amplification were dFic (F: 5' – CAGAACAACCGAGTCCACCT – 3'; R: 5' – CGCAGTTTCCAGACCAGATT – 3'), BiP (F: 5' – GCTATTGCCTACGGTCTGGA – 3'; R: 5' – CATCACACGCTGATCGAAGT – 3'), Ero1L (F: 5' – ATGAGGCGGAAGAGGACTTT – 3'; R: 5' – TGTTAGCCGTCTCGTTGTTG – 3'), and Rp49 (F: 5' – ATCGGTTACGGATCAAACAA – 3'; R: 5' – GACAATCTCCTTGCGCTTC – 3'). For hFic/HYPE and CHOP mRNA analysis, total RNA was extracted from HEK293T cells instead of S2 cells and GAPDH was used as an internal control. The primers used were hFic/HYPE (F: 5' – ATTGACCATCTCACCCTACCA – 3'; R: 5' – ATGTGCCTGATTTCCGAGAGG – 3'), CHOP (F: 5' – GCACCTCCCAGAGCCCTCACTCTCC – 3'; R: 5' – GTCTACTCCAAGCCTTCCCCCTGCG – 3'), and GAPDH (F: 5' – CCATGAGAAGTATGACAACAGCC – 3'; R: 5' – GGGTGCTAAGCAGTTGGTG – 3').

LC-MS/MS

Proteins contained in SDS-PAGE gel bands were reduced with DTT and alkylated with iodoacetamide (Sigma-Aldrich, St Louis MO), followed by digestion overnight with

trypsin (Promega, Madison WI). After concentration and de-salting on an HLB µ-elution plate (Waters Corporation, Milford MA), LC-MS/MS analysis was performed using an Ultimate3000 RSLCnano liquid chromatography system (Dionex, Sunnyvale CA) coupled to a Q Exactive mass spectrometer (Thermo, Bremen). Samples were loaded onto a 50µm ID, 15cm length ES801 PepMap RSLC C18 EASY-Spray column (Thermo). A 60 minute linear analytical gradient of 2-28% acetonitrile in water with 0.1% formic acid was used to elute peptides into the MS. The Q Exactive was operated using a data dependent acquisition method. MS spectra were acquired at 70k resolution. Up to 10 MS/MS fragment spectra were acquired per cycle, at 17.5K resolution, using higher-energy collision induced dissociation (HCD).

Raw data were converted to peak lists with ProteoWizard msconvert (version 3.0.3535) using vendor centroiding of MS2 spectra and the MS2Denoise filter. Peptide and Protein ID was performed using the Central Proteomics Facilities Pipeline (CPFP) version 2.0.3, in which database searches using X!Tandem (v 2008.12.01.1) and OMSSA (v 2.1.8) were combined with iProphet and ProteinProphet (from the Trans-Proteomic Pipeline v4.5.2). Searches were performed against release 2012_07 of the UniProtKB D. melanogaster whole proteome sequence database, with common contaminants from cRAP (http://www.thegpm.org/cRAP) and reversed decoy sequences appended. Tryptic enzyme specificity was used with up to 3 missed cleavages permitted per peptide. Precursor and fragment tolerances were 20ppm and 0.1Da respectively. Carbamidomethylation of Cys was selected as a fixed modification, and oxidation of Met plus AMPylation of Thr were specified as a variable modifications (Unimod definition

Phosphoadenosine (T)). Protein identifications were grouped by ProteinProphet to resolve sequence ambiguity, and filtered to a 1% false discovery rate (FDR) at the protein level using decoy identifications. Further, 2 unique peptide sequences were required per protein.

Fly work

Flies were maintained using standard conditions. The Fic dsRNA line KK105634 was obtained from the Vienna Drosophila RNAi Center. The Bloomington stock center provided repo-Gal4, da-Gal4, GMR-Gal4 and elav-Gal4 driver lines, Df(2L)BSC296, and the P element insertions k11101 and k07502b. Both of these insertions lines were listed as lethal in Flybase. We found, however, that they were viable over each other or over a deficiency of the area (Df(2L)BSC296). Thus, P element k11101 was mobilized using delta 2/3 transposase. Candidate deletions were identified by altered eye color and chromosomes with deletions in the Fic gene were mapped by PCR. All three deletions identified were homozygous viable. For genomic rescue, Pacman vector CmR-BW CH321-69B6 containing the Fic gene was inserted at chromosomal position 65B2 (Best Gene). The same landing site was used for insertion of the transgene encoding genomic Fic-HRP. ERGs were recorded as described previously (114), with at least 20 flies per genotype and five traces per fly. Phototaxis was measured in a T maze with one arm exposed to ultraviolet light and another in the dark. Flies were placed in the center chamber of the T maze and had the choice between ultraviolet light and the dark. After 30 s, the percentage of flies that had moved toward the light was determined. At least 300

flies of each genotype were tested. In each set of experiment, around 45 flies were placed in the center of the chamber and tested three times each. To test nutritional supplements, we placed a yeast paste including histamine (25%, wt/wt) or carcinine (12%, wt/wt) on top of normal food in vials and newly enclosed wild-type adults were allowed to feed for 5 d on this histamine- or carcinine-enriched food.

Subcellular fractionation

S2 cells were harvested and hypotonically lysed in HNMEK lysis buffer (20 mM HEPES (pH 7.6), 150 mM NaCl, 2 mM MgCl2, 2 mM EDTA, 10 mM KCl, 0.5 mM EGTA, 1 mM DTT and protease inhibitor cocktail tablet from Roche) on ice for 20 min. The cells were homogenized using a glass douncer and the total lysate was centrifuged at 500g for 10 min to pellet nuclei (P1). The supernatant was recovered and centrifuged at 10,000g for 10 min to pellet the particulate fraction enriched in organelles such as endoplasmic reticulum and Golgi (P2). The supernatant was then centrifuged at 100,000g for 1 h to separate membrane (P3) and cytosolic fraction (S3). Samples were analyzed by SDS-PAGE and western blotting.

***In vitro* translation with microsomes**

Full-length Fic protein was generated in vitro using TNT Quick Coupled Transcription/Translation Systems (Promega) following the manufacturer's instructions. To analyze glycosylation, we added canine pancreatic microsomal membranes (Promega) to the reaction. Briefly, 0.25 μg of pET23a-Fic (wild type or N288Q) was mixed with

TNT Quick mastermix, [^{35}S]methionine (10 mCi ml–1), microsomal membranes and nuclease-free water to a final volume of 25 µl and incubated at 30 °C for 1 h. The protease protection assay was modified from a previously described protocol (115). Briefly, 9 µl of in vitro–translated reaction was mixed with either 1 µl of proteinase K (10 mg ml–1) or buffer (100 mM potassium acetate, 2 mM magnesium acetate, 50 mM HEPES, pH 7.4) and incubated on ice for 60 min. Proteolysis was terminated by treatment with 0.2 µl of 0.25 M PMSF followed by the addition of 50 µl of preheated PK-kill buffer (1% SDS (wt/vol), 0.1 M Tris, pH 8.0). All reactions samples were boiled for 1 to 2 min at 100 °C and analyzed by SDS-PAGE and autoradiography.

Endo H treatment

Recombinant Fic purified from Sf21 cells and the endogenous Fic from S2 cells were treated with EndoH (New England Biolabs), as described by the manufacturers. N-terminal His/Flag-tagged Fic was expressed in Sf21 cells using a baculovirus expression system (Clontech) according to the manufacturer's instructions and affinity purified using nickel beads (Sigma). For EndoH treatment, 5 µg of recombinant Fic or 50 µg of S2 subcellular fraction enriched in endogenous Fic was denatured at 100 °C for 10 min with denaturing buffer. 2 µl of EndoH and G5 reaction buffer were added to the reaction and incubated at 37°C for 1 h. Following SDS-PAGE, recombinant Fic was analyzed by Coomassie Blue staining and endogenous Fic was detected by western blotting.

Histology

Histamine immunohistochemistry was performed as described previously25. In short, fly heads were fixed for 4 h in ice-cold solution of 4% 1-ethyl-3-(-3-dimethylaminopropyl) carbodiimide (wt/vol, Sigma) in 0.1 M phosphate buffer, washed overnight in 25% sucrose in phosphate buffer (wt/vol), embedded in optimal cutting temperature compound, frozen in liquid nitrogen and sectioned at 20-μm thickness on a cryostat microtome (Hacker-Bright, England). Sections were incubated overnight with antibodies to histamine (1:500, Immunostar, cat# 22939). Secondary antibodies were labeled with Alexa488 (1:500, Molecular Probes, cat# A-11008). Images were captured using Zeiss LSM510 confocal microscope with a 20× NA 0.75 or a 63× NA 1.4 lens on an inverted confocal microscope (LSM510 Meta; Carl Zeiss) at 21–23 °C.

Electron micrographs of 3 d-old fly heads and detection of Fic-HRP by HRP activity was carried out as described previously (116). Size and frequency of capitate projections were determined from images of cross sections of photoreceptor synaptic endings. At least 100 synapses were scored in three lamina each for mutant and wild type. All digital images were imported into Photoshop (Adobe) and adjusted for gain, contrast and gamma settings.

Statistics

One-way ANOVA was used to determine statistical significance of differences in ERGs recordings or phototaxis assays, followed by Tukey’s multiple comparison test. For all ANOVA tests, F values were larger than 150. For these measurements, the

Kolmogorov-Smirnov test indicated a normal distribution (alpha = 0.05). All bar graphs resulting from these comparisons show means ± s.d. Numbers of ERG measurements on individual flies and the number of phototaxis tests (each using 45 to 50 flies per genotype) are indicated in bar graphs for each genotype or supplemental condition. Sample sizes were chosen to be close to previously published examples (117). Average diameters and frequency of capitate projections in wild type and *Fic55* were compared by two-tailed Student's t test. Statistical significance was determined using the Prism software.

Table 1. Bacterial strains used in this study.

Strain	Description	Source
E. coli DH5a	F- endA1 glnV44 thi-1 recA1 relA1 gyrA96 deoR nupG Φ80dlacZΔM15 Δ(lacZYA-argF)U169, hsdR17(rK-mK+), λ–	Invitrogen
E. coli BL21 (DE3)	F- ompT gal dcm lon hsdSB(rB- mB-) λ(DE3 [lacI lacUV5-T7 gene 1 ind1 sam7 nin5])	Novagen
E. coli Rosetta (DE3)	F- ompT hsdSB(RB- mB-) gal dcm λ(DE3 [lacI lacUV5-T7 gene 1 ind1 sam7 nin5])	Novagen

Table 2. Plasmids used in this study.

Plasmid	Description	Source
pET28a	N-terminal His-tag expression vector; Kan^R	Novagen
pGexTev	N-terminal GST-tag expression vector (pGex4T3) with Tev protease cleavage site between GST and MCS; AMP^R	Provided by Yuh Min Chook, UTSW
pAc5.1/V5-His b	C-terminal V5-His tag *Drosophila* expression vector; AMP^R	Provided by Jonathan Terman, UTSW
pET23a	C-terminal His-tag expression vector; Amp^R	
pAc5.1/GFP	C-terminal GFP tag *Drosophila* expression vector; GFP inserted in XhoI and SacII; AMP^R	This study
pBacPAK8-His/FLAG	Baculovirus vector for expression in insect cells with N-terminal His/FLAG tag inserted; AMP^R	Provided by Bing Li, UTSW
pGexTev-dFicΔ70	dFicΔ70 cloned into BamHI and NotI	This study
pGexTev-dFicΔ70 H375A	pGexTev-dFicΔ70 with H375A mutation	This study
pGexTev-dFicΔ70 E247G	pGexTev-dFicΔ70 with E247G mutation	This study
pGexTev-dFicΔ109	dFicΔ109 cloned into BamHI and NotI	This study
pGexTev-dFicΔ223	dFicΔ223 cloned into BamHI and NotI	This study
pGexTev-dFicΔ109 E247G	pGexTev-dFicΔ109 with E247G mutation	This study
pGexTev-dFicΔ223 E247G	pGexTev-dFicΔ223 with E247G mutation	This study
pET23a-dFic	dFic cloned into BamHI and NotI	This study
pET23a-dFic N288Q	pET23a-dFic with N288Q mutation	This study
pBacPAK8-His/FLAG-dFicΔ70	dFicΔ70 cloned into BamHI and NotI	This study
pET28a-BiP	BiP cloned into BamHI and NotI	This study
pET28a-BiPΔ26	BiPΔ26 cloned into BamHI and NotI	This study

pET28a-BiP 27-407	BiP 27-407 cloned into BamHI and NotI	This study
pET28a-BiP 27-417	BiP 27-417cloned into BamHI and NotI	This study
pET28a-BiP SBD	BiP SBD cloned into BamHI and NotI	This study
pAc5.1/V5-His-dFic	dFic cloned into KpnI and NotI	This study
pAc5.1/GFP-dFic	dFic cloned into KpnI and NotI	This study
pAc5.1/GFP-dFicΔ70	dFicΔ70 cloned into KpnI and NotI	This study
pAc5.1/V5-His-BiP-flag+KDEL	BiP cloned into EcoRI and NotI with c-terminal FLAG tag+KDEL+stop codon	This study
pAc5.1/V5-His-BiP-flag+KDEL, T166A	pAc5.1/V5-His-BiP-flag+KDEL with T166A mutation	This study
pAc5.1/V5-His-BiP-flag+KDEL, T366A	pAc5.1/V5-His-BiP-flag+KDEL with T366A mutation	This study
pAc5.1/V5-His-BiP-flag+KDEL, T166A/T366A	pAc5.1/V5-His-BiP-flag+KDEL with T166A/T366A mutations	This study
pAc5.1/V5-His-BiP-flag+KDEL, R470K	pAc5.1/V5-His-BiP-flag+KDEL with R470K mutation	This study
pAc5.1/V5-His-BiP ATPase-flag+KDEL	BiP ATPase (27-407) cloned into EcoRI and NotI with c-terminal FLAG tag	This study
pET28a-SortaseΔ59	SortaseΔ59 cloned into BamHI and NotI	This study
pET28a-BiP 27-402+LPETGG	BiP 27-402+LPETGG cloned into BamHI and NotI	This study
pET28a-BiP 27-407+LPETGG	BiP 27-407+LPETGG cloned into BamHI and NotI	This study
pET28a-DnaJ	DnaJ cloned into EcoRI and NotI	This study
pET28a-CG14476	CG14476 cloned into EcoRI and NotI	This study

Table 3. List of primers.

Primer	Sequence
dFic 5'BamHI	5'-CTG AGG ATC CAT GGG CAC GGA AGC AGA-3'
dFic 3'NotI	5'-CTG AGC GGC CGC TCA CGG TAG ATC TCC AGA-3'
dFicΔ70 5'BamHI	5'-TAC GGG ATC CGC CCA CTA CTT GCA GAC G-3'
dFic H375A F	5'-CAC TAC AAG TTG GTC CAT ATT GCC CCA TTC GTC GAT GGA AAT GGA-3'
dFic H375A R	5'- TCC ATT TCC ATC GAC GAA TGG GGC AAT ATG GAC CAA CTT GTA GTG-3'
dFic N288Q F	5'-GAT CTG GCT ATG AAG TAC ATA CAG GCT AGT CTG GTG CAA AAA ATC-3'
dFic N288Q R	5'-GAT TTT TTG CAC CAG ACT AGC CTG TAT GTA CTT CAT AGC CAG ATC-3'
dFic 110 (Δ109) 5'BamHI	5'-TGA CGG ATC CGC GGA GCA GAC GAA CAT C-3'
dFic 224 (Δ223) 5'BamHI	5'-TGA CGG ATC CTC CAA CGG AGC CCT GCG-3'
dFic 269 (Δ268) 5'BamHI	5'-TGA CGG ATC CGG CAA ATC CAT TGA CGA GC-3'
dFic E247G F	5'-ATT TAC CAC TCA GTA GGC ATT GAG GGC AAC ACC ATG ACG CTG GCA-3'
dFic E247G R	5'- TGC CAG CGT CAT GGT GTT GCC CTC AAT GCC TAC TGA GTG GTA AAT-3'
dFic T7 5'	5'-TAA TAC GAC TCA CTA TAG GGA GCC CAC TAC TTG CAG ACG-3'
dFic T7 3'	5'-TAA TAC GAC TCA CTA TAG GGA CAA CAG CGT GTT CAT CAG C-3'
T7 GFP 5'	5'-TAA TAC GAC TCA CTA TAG GGA CAC TGG AGT TGT CCC AAT TC-3'
T7 GFP 3'	5'-TAA TAC GAC TCA CTA TAG GGA CCA TGT GTA ATC CCA GCA GC-3'
dFic seq 5'	5'-CGC CAT TCA CGA GTC CAA C-3'
dFic seq 3'	5'-GTT TAT GTA CTT CAT AGC CAG-3'
dFic T7_2 5'	5'-TAA TAC GAC TCA CTA TAG GGA GGC ACG GAA GCA GAA CAA C-3'
dFic T7_2 3'	5'-TAA TAC GAC TCA CTA TAG GGA GAG AGG GCG TCT CGT TTG-3'

dFic T7_3 5’	5’-TAA TAC GAC TCA CTA TAG GGA CAC GAG TCC AAC GGA GCC-3’
dFic T7_3 3’	5’-TAA TAC GAC TCA CTA TAG GGA CCG TCT GGA TGA GCA TAG GG-3’
BiP 5’BamHI	5’-TAG CGG ATC CAT GAA GTT ATG CAT ATT ACT GGC-3’
BiP 5’EcoRI	5’- TAG CGA ATT CAT GAA GTT ATG CAT ATT ACT GGC-3’
BiP 3’NotI	5’-TAC GGC GGC CGC TTA CAG CTC GTC CTT GAG ATC-3’
BiP c-flag+KDEL 3’NotI	5’- TAG CGG CCG CTT ACA GCT CGT CCT TCT TGT CGT CGT CGT CCT TGT AGT CCA GCT CGT CCT TGA GAT CG-3’
BiPΔ26 5’BamHI	5’- TAG CGG ATC CGA GCT GGG CAC AGT GAT C-3’
BiP 407 3’NotI	5’-TAC GGC GGC CGC GCC AGA GAG CAC GCC AGC-3’
BiP 417 3’NotI	5’- TAG CGC GGC CGC GAG CAG GAC AAT AGC ATC GG-3’
BiP ATPase+c-flag 3’NotI	5’-TAC GGC GGC CGC GCC AGA GAG CAC GCC AGC-3’
BiP SBD 5’BamHI	5’-TAG CGG ATC CGA ACA AGA TAC CGA TGC-3’
BiP T166A F	5’-GCT TAT CTG GGC AAG AAG GTC GCA CAT GCC GTC GTT ACC GTG CCA-3’
BiP T166AR	5’- TGG CAC GGT AAC GAC GGC ATG TGC GAC CTT CTT GCC CAG ATA AGC-3’
BiP T366A F	5’- ATT GTG CTG GTC GGT GGC TCC GCA CGT ATC CCC AAG GTG CAG CAG -3’
BiP T366A R	5’- CTG CTG CAC CTT GGG GAT ACG TGC GGA GCC ACC GAC CAG CAC AAT -3’
BiP R470K F	5’- ATC CAG GTG TAC GAG GGC GAG AAG CCC ATG ACC AAG GAC AAC CAT -3’
BiP R470K R	5’- ATG GTT GTC CTT GGT CAT GGG CTT CTC GCC CTC GTA CAC CTG GAT -3’
BiP N402 LPETGG 3’NotI	5’- TAG CGC GGC CGC TTA TCC TCC GGT CTC AGG TAG AGC CTG CAC AGC AGC ACC GT-3’
BiP N407 LPETGG 3’NotI	5’- TAG CGC GGC CGC TTA TCC TCC GGT CTC AGG TAG GCC AGA GAG CAC GCC AGC- 3’
Sortase Δ59 5’BamHI	5’- TAG CGG ATC C CA AGC TAA ACC TCA AAT TCC G -3’
Sortase 3’NotI	5’- TAG CGC GGC CGC TTA TTT GAC TTC TGT AGC TAC A-3’

CG14476 5’EcoRI	5’- TAG CGA ATT CAT GCG ATT CGC TCT GGC CAC-3’
CG14476 3’NotI	5’- TAG CGC GGC CGC CTA CGC AAA GTT GAG TTT AAT G-3’
CG14476 Δ32 5’EcoRI	5’- TAG CGA ATT CAG TTT TTG TCG ACG CTC CCG -3’
CG14476 c-flag 3’NotI	5’- TAG CGC GGC CGC TTA CTT GTC GTC GTC GTC CTT GTA GTC CGC AAA GTT GAG TTT AAT GGC -3’
DnaJ 5’EcoRI	5’-TAG CGA ATT CAT GGG CAA AGA CTT CTA CAA G-3’
DnaJ 3’NotI	5’-TAG CGC GGC CGC CTA GTT GGG CAG CAG CTC G-3’

CHAPTER 3
Biochemical and genetic analysis of dFic

INTRODUCTION

AMPylation, a posttranslational modification involving a covalent attachment of adenosine monophosphate (AMP) to a hydroxyl side chain of protein substrates, is mediated by either Fic domain or nucleotidyl transferase domain (1). This modification is implicated to serve a universal role in cellular function as these two domains catalyzing AMPylation are well conserved across species. Specifically, Fic domain is found in human Huntingtin-interacting protein E (HYPE) and the *Drosophila* Fic protein (dFic, Flybase: CG9523). Despite the recent discoveries and characterization of a number of bacterial AMPylators and their targets during pathogenesis, the physiological relevance of AMPylation in eukaryotes still remains unknown. Therefore, we aim to determine the eukaryotic function of AMPylation by biochemical characterization of dFic and genetic analysis using *Drosophila* as a model system.

Herein, we show that dFic is an ER-localized protein that undergoes N-linked glycosylation. dFic has an AMPylation activity in vitro which is dependent on a catalytic histidine residue in the essential Fic motif. We also access the membrane topology of the dFic as an ER transmembrane protein using a protease protection assay. For genetic analysis, we generated *dfic* null mutant flies and analyzed its phenotype. We found that the flies without enzymatic function of dFic exhibit blind phenotype due to impaired synaptic transmission. dFic enzymatic activity is required in glial cells for the normal

visual neurotransmission. In addition, dFic was enriched in the surface of glial cells when analyzed by electron microsopy. Together, these studies reveal the physiological function for dFic in flies and establish a previously unknown regulatory mechanism in visual neurotransmission.

RESULTS

In vitro AMPylation activity of recombinant dFic

First, we explored the enzymatic activity of dFic in a biochemical assay using recombinant proteins. dFic is composed of an N-terminal transmembrane domain, TPR (tetratricopeptide repeat) domain involved in protein interactions, and a C-terminal catalytic Fic domain **(Figure 8)**. For bacterial purification, the transmembrane domain was deleted (Δ70) and dFic was fused to N-terminal GST tag. The recombinant dFic purified from *E. coli* was then used in the *in vitro* AMPylation assay with ^{32}P-α-labeled ATP. dFic exhibited an autoAMPylation, which was abolished when the catalytic histidine was mutated into an alanine (H375A) **(Figure 9A)**. Fic proteins have a conserved alpha-helical inhibitory motif that obstructs the ATP binding site (19). When a glutamate residue within this inhibitory motif was mutated (E247G), the enzymatic activity of dFic was significantly increased compared to the wild-type enzyme **(Figure 9B)**. For the future assays using S2 cell lysates to search for AMPyalted substrates, this constitutively active dFic (E247G) was used instead of the wild-type.

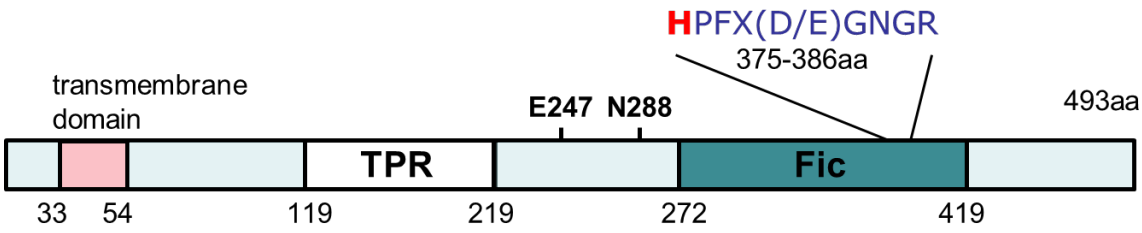

Figure 8. Domain structure of dFic. It has N-terminal transmembrane domain, TPR domain, and C-terminal catalytic Fic domain containing conserved histidine residue (in red). E247 is the conserved glutamate in the inhibitory helix and N288 is the glycosylation site.

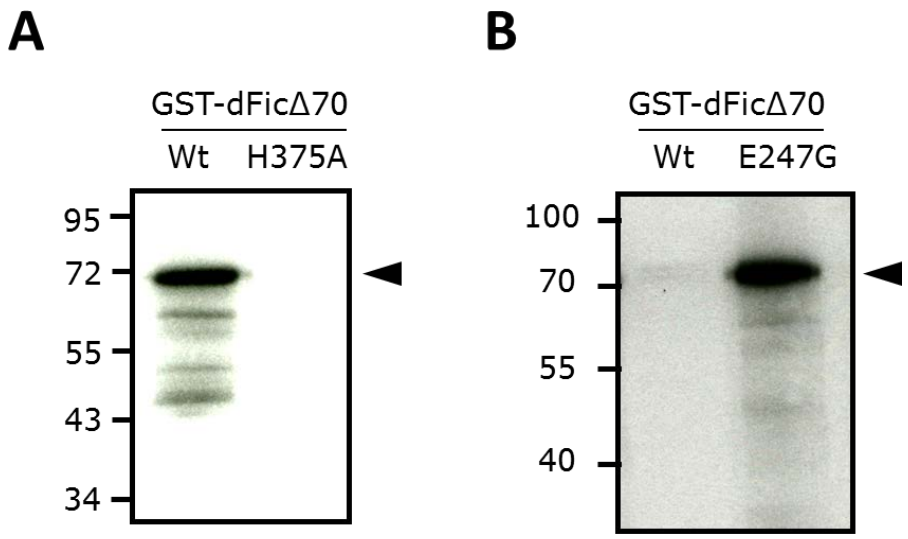

Figure 9. *In vitro* AMPylation activity of recombinant dFic. (A) Wild-type GST-dFicΔ70, but not the catalytically inactive H375A, has autoAMPylation activity. (B) Mutation of conserved glutamate residue in the inhibitory motif of dFic (E247G) shows significantly higher autoAMPylation activity compared to wild-type.

Nucleotide substrate specificity of dFic

Fic domains have been shown to catalyze diverse phosphotrasferase reactions. AnkX from *Legionella pneumophila* uses CDP-choline as a substrate to modify Rab1 GTPase with phosphocholine moiety (20). AvrAC from *Xanthomonas campestris* uses UTP to catalyze UMPylation on BIK1 and RIPK (22). We already observed that dFic acts as an AMPylator but we also wanted to see whether it can catalyze other modifications as well. We first performed *in vitro* phosphocholination assay using CDP-choline as a substrate with wild-type and catalytically inactive H/A mutant of AnkX and dFicΔ70 **(Figure 10)**. AnkX wild-type displayed robust auto-phosphocholination whereas dFic wild-type had a minimal activity indistinguishable from that of the H/A mutant. We also examined the UMPylation activity of dFic E247G using ^{32}P-α-UTP as a substrate. Compared to a strong auto-AMPylation observed with 100ng of dFic, auto-UMPylation of 1μg dFic was significantly low **(Figure 11)**. Altogether, these data suggest that, of the three substrates tested, ATP is the prefered substrate for dFic and that AMPylation is likely to be the primary catalytic mechanism employed by dFic.

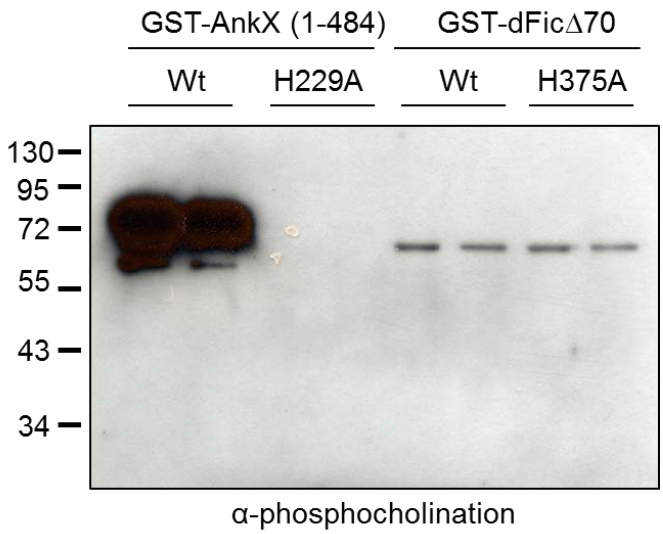

Figure 10. ***In vitro*** **phosphocholination of recombinant AnkX and dFic**. Phosphocholine transferase activity of GST-AnkX (1-484) and GST-dFicΔ70 were analyzed by anti-phosphocholination antibody. Wild-type but not the catalyticially inactive H299A AnkX has robust auto-phosphocholination activity whereas wild-type dFic has weak activity comparable to the catalytically inactive mutant for dFic (H375A).

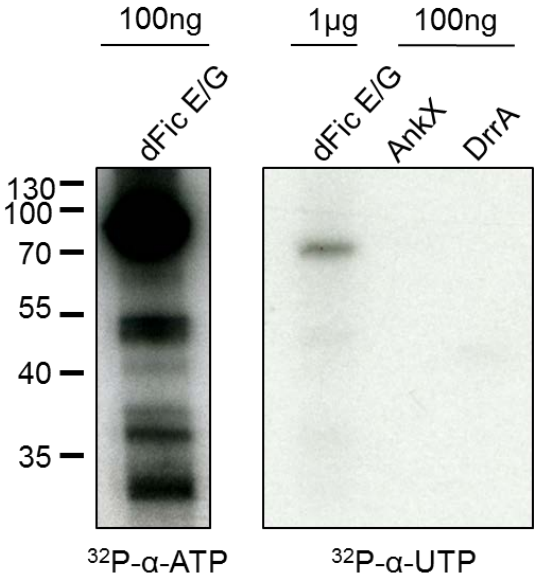

Figure 11. *In vitro* AMPylation versus UMPylation activity of recombinant dFic. GST-dFic Δ70 E247G (E/G) was incubated with either ^{32}P-α-ATP or ^{32}P-α-UTP and its automodification was analyzed by autoradiography. DrrA and AnkX are the bacterial effectors from *Legionella pneumophila* that catalyze AMPylation and phosphocholination, respectively. Only 100ng was used for these bacterial effectors as they are more potent enzymes.

Subcellular localization and membrane topology of dFic

We then explored the subcellular localization of dFic, which could help narrow the pool of relevant substrates of AMPylation. Subcellular fraction of S2 cells using differential centrifugation revealed that dFic was enriched in a fraction containing ER, indicated by an ER marker BiP **(Figure 12)**. To confirm that dFic is localized in the ER, we used endoglycosidase H (endo H), which is an enzyme that cleaves the N-mannose rich oligosaccharides but not the highly complex oligosaccharides. ER proteins are heavily glycosylated with N-mannose which makes them susceptible to endoH, whereas proteins translocated from the ER and processed with complex sugar and resistant to endo H. When dFic was purified from insect cells that allow the posttranslational modification to occur in the expressed protein, a molecular weight shift was observed upon treatment with endoH **(Figure 13)**. The endogenous dFic protein from S2 cells was also cleaved by endoH, suggesting that dFic is an ER-localized protein. Most ER proteins undergo N-linked glycosylation in the ER lumen, and a conserved N-linked glycosylation site (N-X-S) was found in dFic (N288, **Figure 8**), further confirming the ER localization of dFic . When dFic was fused to GFP at the C-terminus and expressed in S2 cells, we observed a perinuclear localization of GFP signal which is indicative of ER distribution **(Figure 14)**. GFP signal also co-localized with that of the ER tracker. When the first 70 amino acids including the translocation signal were deleted (Δ70), dFic lost the co-localization with the ER.

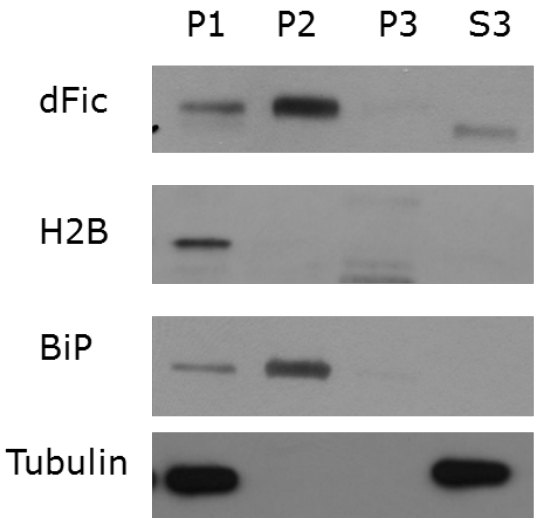

Figure 12. Subcellular fractionation of dFic. Differential centrifugation of S2 cell homogenates at 500g (P1), 10,000g (P2) and 100,000g (P3). Fic co-fractionated with endoplasmic reticulum marker BiP, but not nuclear histone 2B (H2B), or cytosolic tubulin (Tub) and actin (Act).

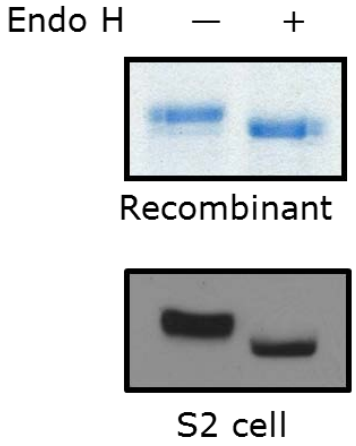

Figure 13. EndoH-mediated deglycosylation of dFic. Endo H treatment of recombinant dFic purified from Sf21 cells or endogenous dFic from S2 cells caused a mobility shift indicating the presence of high mannose N-glycans.

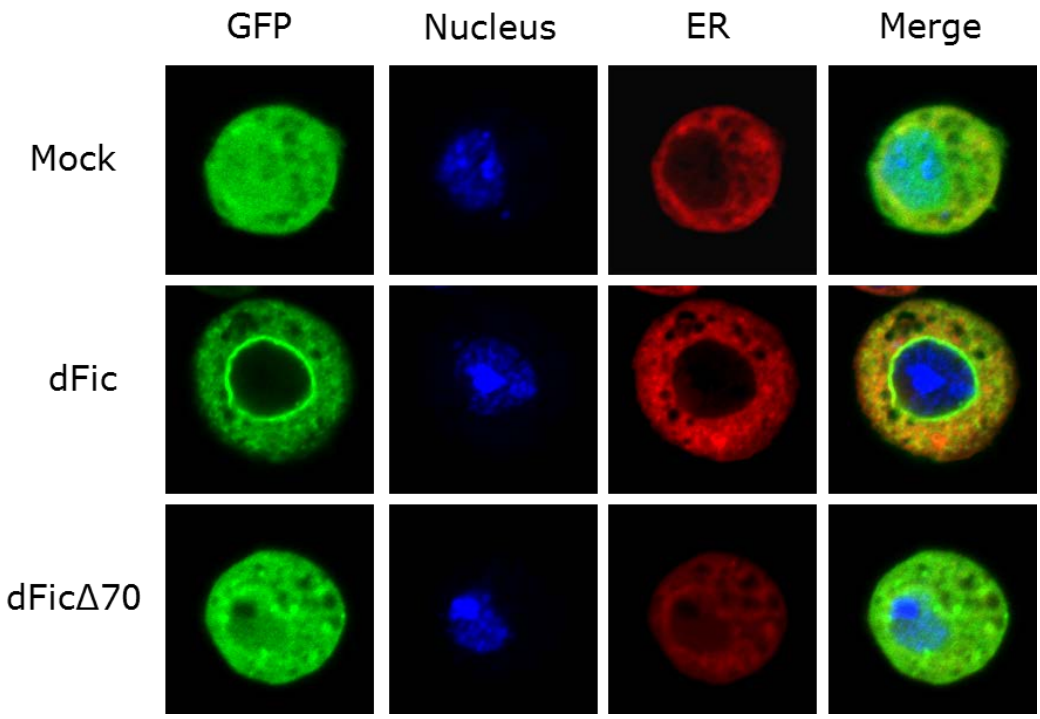

Figure 14. Subcellular localization of dFic in S2 cells. dFic wild-type or dFicΔ70 fused to GFP were expressed in S2 cells and analyzed by confocal microscopy. dFic colocalizes with ER tracker with marked perinuclear distribution. This localization is lost upon the deletion of 70 amino acids which contains the signal peptide.

To further analyze the membrane topology of dFic, we performed a protease protection assay using microsomal membranes. Microsomal membranes are biochemically purified ER fractions that are widely used to analyze the cotranslational and posttranslational processing of the in vitro translated proteins. When dFic was in vitro translated in the presence or absence of microsomal membranes, we observed a higher molecular weight band when dFic was incubated with the membranes **(Figure 15)**. This band collapsed when dFic was treated with endoH or the putative N-linked glycosylation site was mutated (N288Q), confirming that it represents the glycosylated form of dFic. When in vitro translated dFic was treated with proteinase K in the absence of the membranes, it was effectively degraded. However, when dFic was translated in the presence of the membranes, we observed a band with slightly lower molecular weight. This suggests that dFic was translocated to the ER lumen and was protected from the protease, although the N-terminal portion of dFic upstream of the transmembrane domain was facing outside the membrane and degraded. These data suggest that dFic is a type II transmembrane protein with its single N-terminal hydrophobic stretch functioning as a transmembrane domain and its N-glycosylation site and catalytic domain in the lumen of the secretory pathway.

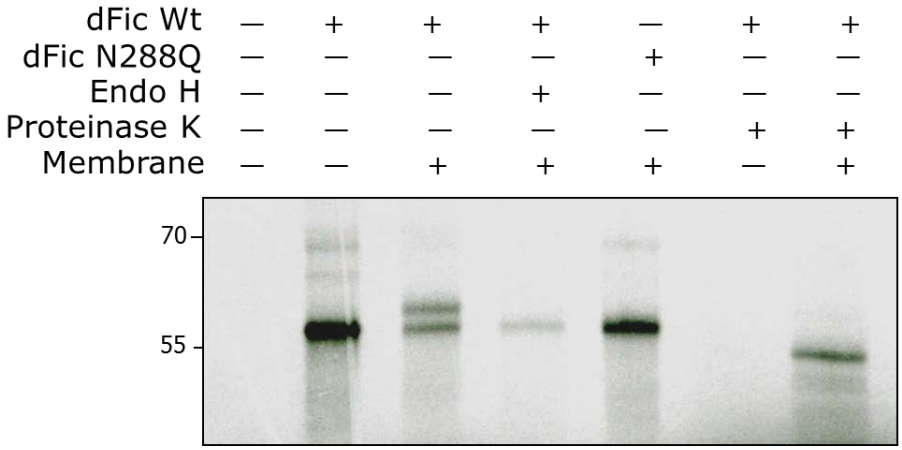

Figure 15. Membrane topology analysis of dFic. dFic wild-type or N288Q were in vitro translated in the presence or absence of microsomal membranes. EndoH and dFic N288Q were used to confirm the glycosylation of dFic. In vitro translated dFic were also treated with proteinase K for protease protection assay.

dFic is required for visual neurotransmission in flies

We sought to examine the regulatory role of dFic by genetically manipulating its expression in flies. Notably, high-level overexpression of UAS-Fic by the da-Gal4 driver was lethal. This lethality depended on the enzymatic activity of dFic, as no phenotypes were detected following expression of the catalytically inactive dFic H375A mutant. Flies expressing wild-type dFic or mutant UAS-Fic transgenes at low levels under arm-Gal4 control did not exhibit externally visible phenotypes or lethality. These data suggest that AMPylation may regulate important cellular processes.

Next, we generated dFic loss-of-function deletion mutations by excision of a nearby P element **(Figure 16A)**. One of the resulting alleles, *Fic55*, lacked the 5′ UTR and the first 260 of 493 amino acids, including the TPR domain. We confirmed the loss of dFic protein by western blot **(Figure 16B)**. Flies homozygous for *Fic55* were viable and fertile, but their behavior seemed sluggish compared with wild-type flies. This deficit was quantified in a fast-phototaxis assay (118,119), which showed that the *Fic55* mutants were not attracted to a light source; in other words, they were blind **(Figure 17)**. This phenotype was specific for *Fic55* flies, as it was also observed in flies expressing a UAS-Fic dsRNA transgene under da-Gal4 control, and wild-type behavior was restored by a genomic dFic transgene.

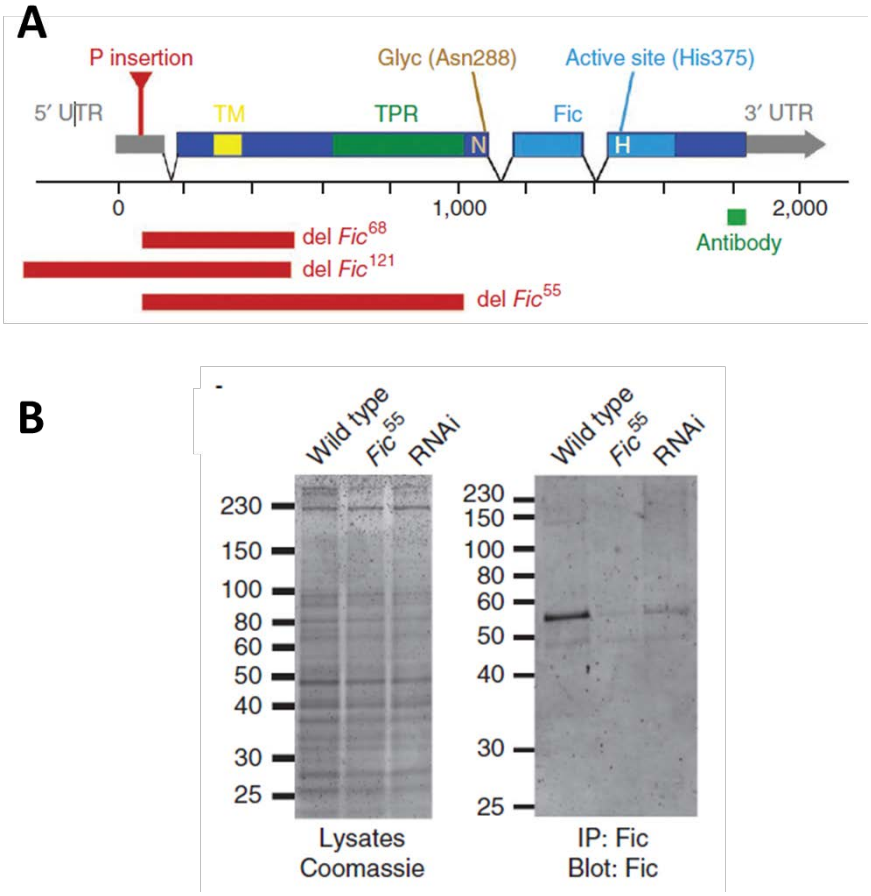

Figure 16. Generation of *dfic* null mutant flies, *Fic55*. (A) Map of *dFic* gene and protein, including transmembrane domain (TM), N-glycosylation site Asn288, TPR domain and Fic domain with active site at His375. *Fic*68, *Fic*121 and *Fic*55 lack the 5′ UTR and N-terminal 125, 150 or 260 amino acids, respectively. (B) Coomassie blue-stained gel with lysates from wild-type, *Fic*55 and *Fic* RNAi flies and western blot detecting dFic protein after enrichment by immunoprecipitation with antibody to dFic (wild type: Ore-R; *w*1118; *Fic*55: *Fic*55*; w*1118; RNAi: *UAS-Fic* dsRNA; *da-Gal4*).

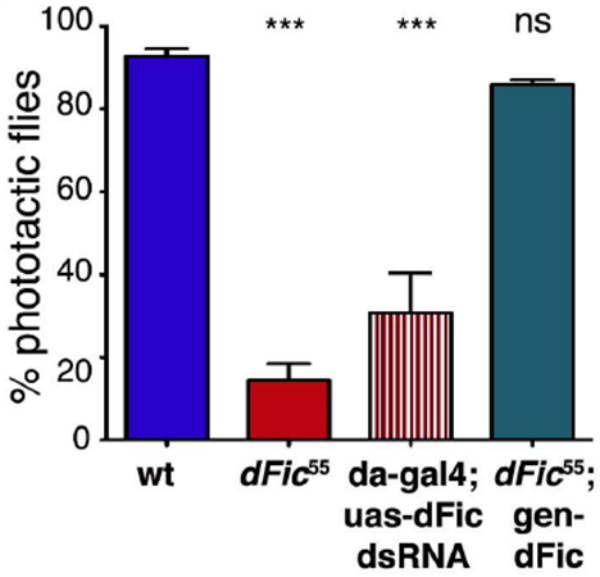

Figure 17. Phototactic behavior of wild-type and mutant flies. Fast-phototaxis assays revealed a difference in behavior between wild-type and *Fic*55 or Fic knockdown flies. A genomic *Fic* transgene restored the normal behavior.

To determine whether this deficit was due to impaired visual signaling, we measured the electrical response to a light pulse using electro-retinograms (ERGs). We found that the ERGs of *Fic55* flies missed the characteristic ON transient of the response to light **(Figure 18A)**. ON transients in ERGs are a reflection of synaptic activation of the postsynaptic laminar neurons (120,121). This defect was specific for the loss of dFic function, as it was also observed in *Fic55*/Df(2L)BSC296 hemizygotes and after dFic knockdown (*UAS-Fic* dsRNA; *da-Gal4*). Furthermore, ON transients were restored by a genomic dFic transgene or by expression of a dFic cDNA under the control of the low-level arm-Gal4 driver **(Figure 18B)**. Notably, expression of the catalytically inactive dFic H375A mutant was not able to restore ON transients, indicating that dFic enzymatic activity is necessary for the normal activity of photoreceptor synapses required for vision.

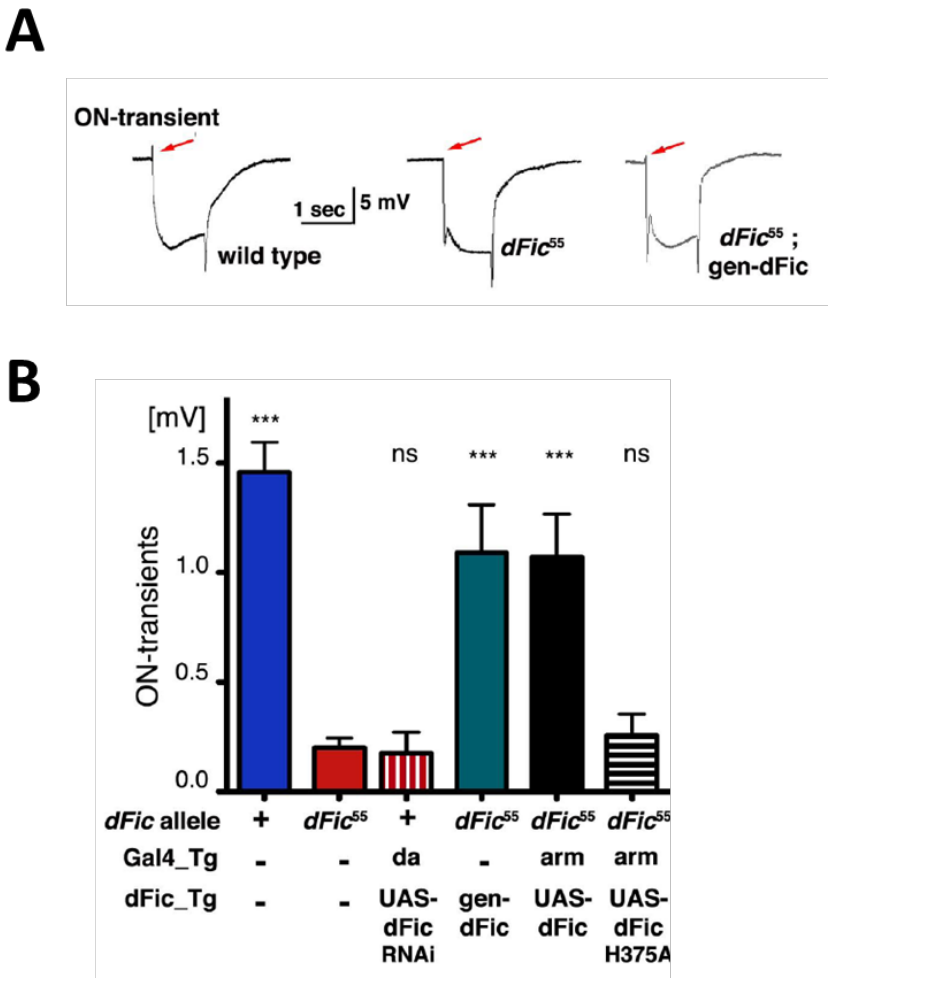

Figure 18. dFic is required for visual neurotransmission. (A) ERG recordings of wild-type, *Fic*55 and *Fic*55*; Fic* rescued flies showed photoreceptor depolarization in response to light. Only *Fic*55 flies missed the ON transient, indicated by the red arrows. (B) Quantification of ON transients from ERG recordings of indicated genotypes with respect to *Fic* allele, *Fic* transgenes (*Fic*-Tg) and *Gal4* drivers (*Gal4*-Tg).

Visual neurotransmission requires dFic enzymatic activity in glia cells

To further narrow the focus of dFic activity, we explored which cells require its expression for normal visual neurotransmission. To test the requirement in photoreceptor cells, we generated chimeric flies with whole-eye clones homozygous for *Fic55* (*ey3.5-Flp; FRT Fic55*). These flies still exhibited ON transients, as did flies with photoreceptor-specific knockdown of dFic (*GMR-Gal4/UAS-Fic* dsRNA) **(Figure 19A)**. Furthermore, expression of dFic in both photoreceptors and their lamina target neurons under control of the elav-Gal4 neuronal driver did not restore ON transients in *Fic55* mutants. In contrast, glia-specific expression of dFic under the control of the repo-Gal4 driver was sufficient to restore ON transient. Moreover, glia-specific knockdown of dFic *(UAS-Fic* dsRNAi; *repo-Gal4*) indicated that dFic is necessary for normal ON transients in glia cells. To test the relevance of these electrophysiological responses to behavior, we evaluated flies in the fast-phototaxis assay **(Figure 19B)**. Consistent with the ERG recordings, loss of dFic function in whole-eye clones or its photoreceptor-specific knockdown (*GMR-Gal4*/*UAS-Fic* dsRNA) did not eliminate fast phototaxis. Furthermore, neuronal Fic expression (*elav-Gal4*; *UAS-Fic*) did not restore normal behavior in *Fic55* mutants. In contrast, repo-Gal4–driven knockdown of dFic indicated its requirement in glia cells for fast-phototaxis. Moreover, glia-specific expression of dFic (*repo-Gal4; UAS-Fic*) significantly improved fast phototaxis of *Fic55* mutants, although it did not fully restore normal behavior, indicating a requirement in additional cells of the phototaxis circuits (122). Notably, expression of the catalytically inactive H375A mutant in glia cells did not rescue the characteristic ON transient of the response to light or

improve the fast-phototaxis behavior of *Fic55* flies. Together, these data indicate that dFic enzymatic activity in glia cells is necessary and sufficient for normal synaptic transmission in the visual system.

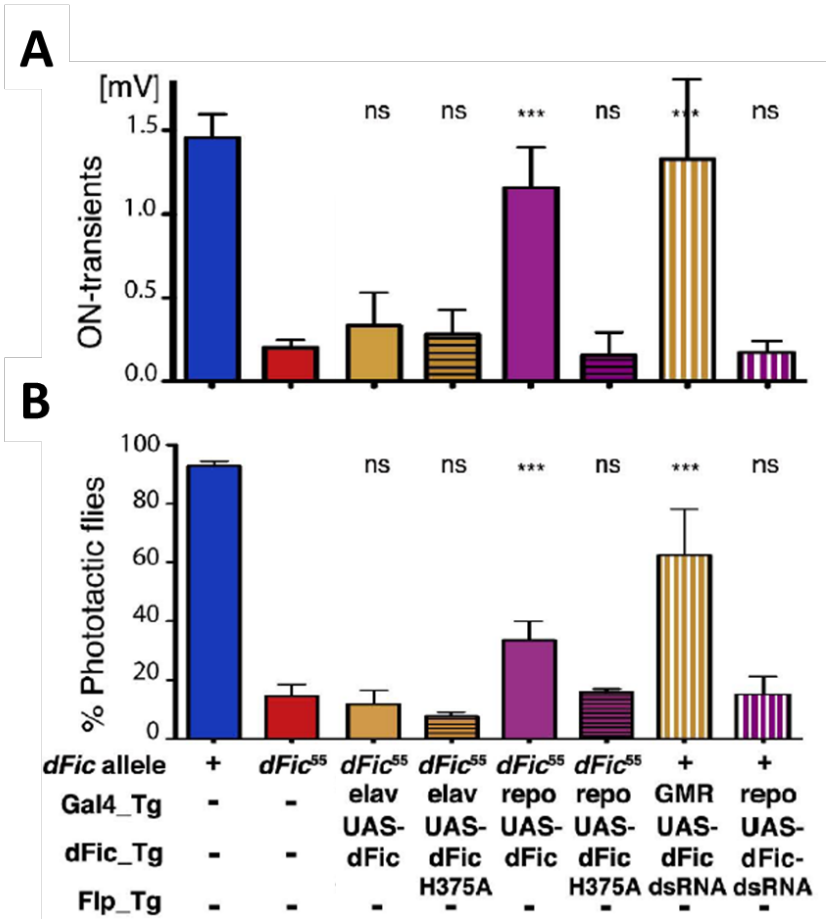

Figure 19. Visual neurotransmission requires dFic enzymatic activity in glia cells. Quantification of ON transients from ERG recordings (A) and fast phototaxis response (B) of flies with the indicated genotypes with respect to Fic allele, Gal4 drivers (Gal4-Tg) and Fic transgenes (Fic-Tg), and Flipase transgene (Flp-Tg).

dFic is required for recycling of the histamine neurotransmitter

One important role of glia cells in the *Drosophila* lamina is the recycling of histamine, the neurotransmitter released by photoreceptors (123-125). Histamine is synthesized in photoreceptors by histidine decarboxylase (Hdc) (126). However, Hdc activity covers only a fraction of the histamine requirement for their normal synaptic activity; the balance of histamine is provided by recycling (127). After release by photoreceptor synapses, histamine is removed from the synaptic cleft by active uptake into glia cells. There, a β-alanyl-histamine synthetase encoded by ebony catalyzes the condensation of histamine with β-alanine (128,129). The resulting product, carcinine, is extruded from glia cells and taken up by photoreceptor cells in a poorly understood process (123,130,131). In photoreceptors, histamine is recovered from carcinine by a β-alanyl-histamine hydrolase encoded by tan (125). Interruption of this cycle results in the loss of visual transmission, as indicated by behavioral deficits and the loss of ON transients in ERG recordings (121,123,124,126).

Notably, phenotypes caused by mutants interfering with histamine metabolism can be partially rescued by dietary histamine or carcinine, which as a result of the recycling pathway, can be taken up into photoreceptor cells (123,124). When *Fic55* flies were fed a diet enriched with histamine or carcinine, we observed partial restoration of ON transients **(Figure 20A)**, although the level of rescue was not sufficient to restore normal behavioral in the fast-phototaxis assay **(Figure 20B)**. To test whether histamine distribution is altered, we stained sections of wild-type and *Fic55* heads with antibodies

to histamine (130). Wild-type flies exhibited some variable staining in photoreceptor cell bodies and strong staining in the layer of epithelial glia cells just proximal to photoreceptors and in photoreceptor axon terminals **(Figure 20C)**. In contrast, histamine immunoreactivity in epithelial glia was strongly reduced in *Fic55* flies **(Figure 20D)**, although staining was still observed in photoreceptor cell bodies. Staining in epithelial glia cells was partially restored by glia-specific expression of dFic **(Figure 20E)**. Specificity of staining for histamine was indicated by its absence in Hdc^{P218} heads (126) **(Figure 20F)**. Loss of histamine staining in *Fic55* lamina is reminiscent of the changes in histamine distribution in other mutants that disrupt histamine recycling in photoreceptor synapses, including *tan*, *ebony* and *Vmat* (125,128,130,132). Together, these data are consistent with the notion that histamine metabolism is one of the physiological processes regulated by the enzymatic activity of dFic in glia cells.

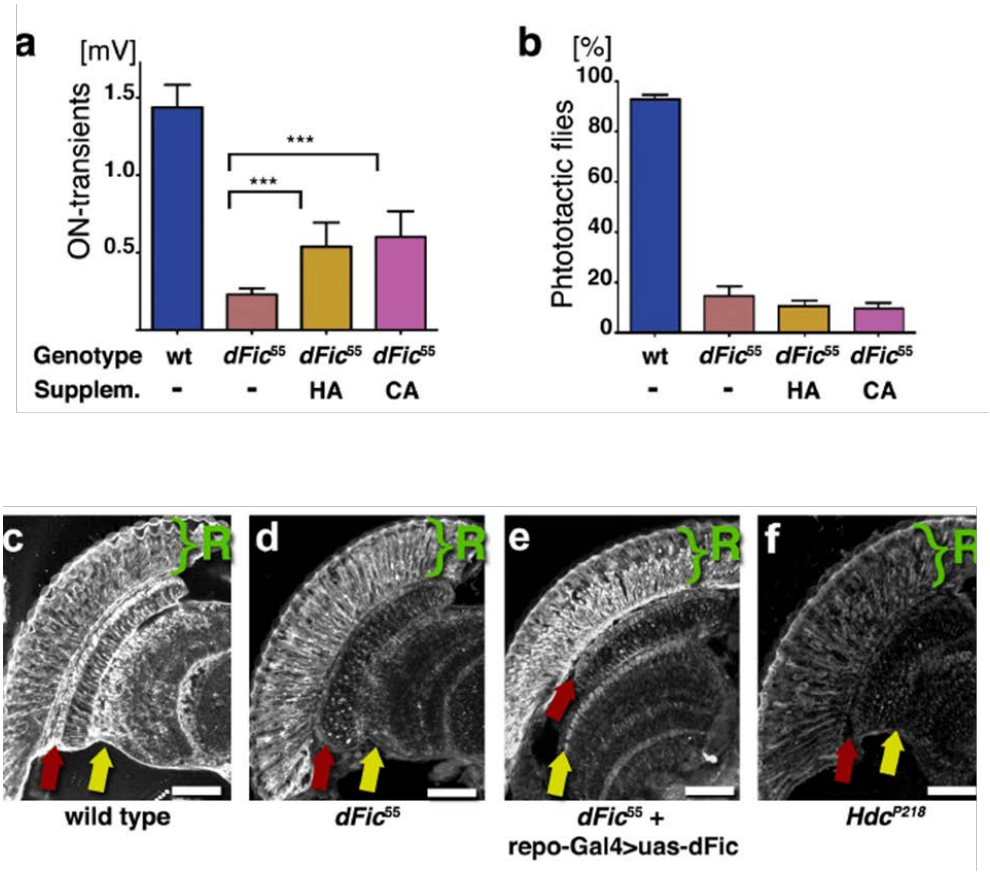

Figure 20. dFic is required for recycling of the histamine neurotransmitter. (a,b) Quantification of ON transients from ERG recordings (a) and fast phototaxis response (b) of wild-type or Fic55 flies fed food supplemented with histamine (HA) or carcinine (CA) or without supplement (−).(c–f) Frozen sections of fly heads stained for histamine. Histamine is synthesized in photoreceptor cells (P), which show variable levels of staining in wild-type (c) and Fic55 (d), but not HdcP218 (f) flies. In wild-type (c), but not in Fic55 (d) or HdcP218 (f), heads21, histamine was enriched in glia cells (red arrows) just proximal to the photoreceptor cells and in synapses of the lamina and medulla (yellow arrows). This staining was partially restored in Fic mutants following expression of Fic in glia cells (e).

dFic localizes to capitate projections in the glial cells

To determine the localization of dFic in glia cells **(Figure 21)**, where it is required for normal visual neurotransmission, we expressed a functionally active dFic-HRP fusion protein either under the control of the endogenous Fic promoter and enhancer elements **(Figure 21d,f)** or under control of the repo-Gal4 driver **(Figure 21h,j,l–o)**. HRP activity of the chimeric protein was used to detect dFic-HRP by electron microscopy (116). dFic-HRP was expressed on the surface of glia cells and prominently enriched in capitate projections that epithelial glia cells insert into synaptic endings of photoreceptors **(Figure 21d,f,h,j,l–o)**. HRP activity was strongest in the head of capitate projections, as revealed by the electron-dense DAB precipitate in the extracellular space between glia cell and neuron **(Figure 21d,f,h,j,l–o)**. Control sections of flies lacking dFic-HRP expression showed no such DAB accumulation **(Figure 21e,g,i)** instead revealing the slightly expanded extracellular space typical for capitate projections **(Figure 21k,p–r)** (117,133). Prompted by this localization of Fic, we quantified the appearance of capitate projections. In *Fic55* mutant heads, the frequency of capitate projections was slightly reduced; we observed 4.3 ± 0.3 capitate projections per synaptic cross-section in wild type compared with 2.8 ± 0.2 in Fic55 (mean ± s.d., n = 3 heads each, P = 0.012, t = 4.32, F = 3.0). However, the shape and average diameter of capitate projections were not altered in *Fic55* mutants (wild type, 184 ± 5.8 nm; Fic55, 190 ± 4.0 nm (mean ± s.d.); n = 3 heads each, P = 0.4, t = 0.846, F = 2.079), indicating that dFic activity is not necessary for their formation. Notably, capitate projections have been speculated to be the site of neurotransmitter recycling into photoreceptor cells (117), although no transporter or other

transmembrane protein, besides dFic, is known to specifically localize to these specialized synaptic organelles.

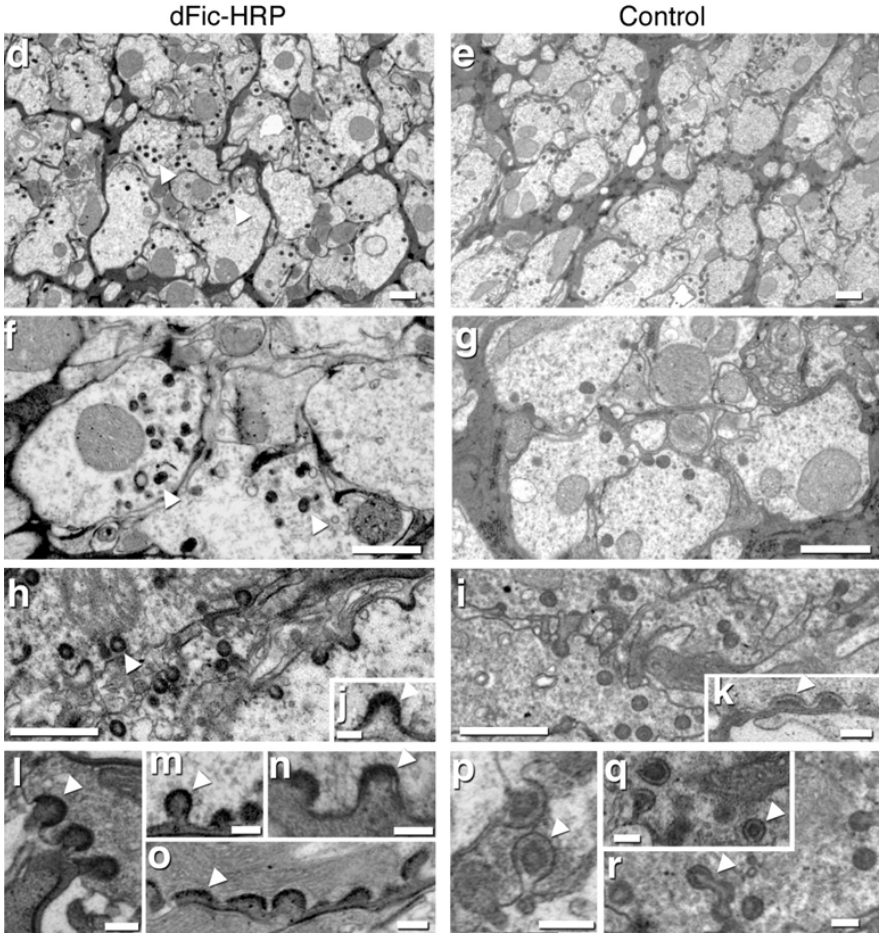

Figure 21. dFic localizes to capitate projections in the glial cells. (d–r) Electron micrographs of lamina cartridges from flies expressing genomic Fic-HRP (d,f) or under repo-Gal4 control (h,i,l–o) revealed the presence of Fic-HRP on glial cells surrounding laminar cartridges and at capitate projections. HRP activity was enriched in the extracellular space between glia and photoreceptor terminals at the head of capitate projections (for example, arrowheads in l–o), regardless of whether they assumed flat (o) or deeply invaginated shapes (h,l,m). Electron micrographs of wild-type flies lacking Fic-HRP expression (e,g,j,k,p–r) confirmed the specificity of the DAB precipitate and revealed the slightly extended extracellular space typical of capitate projections (arrowheads in p–r). Scale bars represent 1 μm (d–h,j) and 200 nm (i,k–r).

DISCUSSION

We show that dFic appears to employ AMPylation as a primary catalytic mechanism and that it is an ER-localized transmembrane protein. This suggests that the substrate of dFic is also likely to localize to the ER or undergo secretory pathway. While attempting to identify substrates being AMPylated in the ER, we analyzed the phenotypes of *dfic* mutant flies to understand the physiological role of dFic. We found that dFic enzymatic activity is required for the visual neurotransmission in glial cells and it is likely that this enzymatic activity is involved in the regulation of histamine, a visual neurotransmitter critical for the function of photoreceptor synapses and vision. Therefore, proteins involved in the histamine metabolism, its uptake or transport in the secretion pathway might be a potential target for dFic.

It is interesting to note that dFic is observed in the surface of glial cells, whereas it is localized to the ER in other fly tissues including fat bodies, eye discs, and salivary glands. dFic also displays ER localization in S2 cells. This suggests that dFic may have another target in the ER that might play an essential to the cellular function. The discrepancy between the ER-localization and cell surface-localization of dFic can be explained by the possibility that there may be cell-type specific factors that can induce the secretion of dFic from the ER to cell surface in glial cells. This could be a posttranslational modification or specific binding partners that facilitate the translocation of dFic to the cell surface.

Capitate projections, the invaginations of glia cells into the synaptic endings of photoreceptor cells, are dynamic organelles that can occur as shallow indentations or with extended necks with one or multiple heads. They have long been speculated to be sites of neurotransmitter recycling due to the changes in their number in mutant flies with impaired histamine recycling, and the close association with sites of active endocytosis (117,131). The localization of dFic to these organelles provides functional data to support this speculation. The localization of dFic in glia cells may reflect a direct interaction with transporters that are targeted to capitate projections and serve as targets of dFic. The identity of these target proteins and the molecular mechanism behind the regulation of visual neurotransmission by dFic-mediated AMPylation remains to be determined.

CHAPTER 4
Reversible AMPylation of BiP during ER homeostasis

INTRODUCTION

AMPylation is a posttranslational modification involving a covalent attachment of an AMP moiety from ATP to hydroxyl side chains of target substrates (1). Fic domain which mediates AMPylation is highly conserved across species, including higher eukaryotes (albeit, only in a few fungi (5,17)), raising the possibility that AMPylation serves a critical role in cellular function. However, all AMPylators characterized thus far have been bacterial proteins, most of which are involved in pathogenesis. In an attempt to understand the physiological function of AMPylation in eukaryotes, we knocked out the gene encoding the *Drosophila* FicD protein (*dfic*). We found that dFic enzymatic activity is required in glial cells for visual neurotransmission in flies (134). In addition, this study demonstrated that the catalytic domain of dFic resides in the lumen of the ER in a number of fly tissues (fat bodies, eye discs, and salivary glands) and in the S2 cells.

Another protein that resides in the ER is the molecular chaperone BiP/GRP78, a highly conserved heat shock 70 family protein and a crucial molecular chaperone in the ER (37,38,135). BiP binds and assists the folding and assembly of newly-synthesized proteins. It is also essential for translocation of secretory precursors across the ER membrane (40,41). Aberrant or misfolded proteins bind to BiP for assembly or to be directed to the ER-associated degradation pathway (ERAD) when the folding attempts continuously fail (31-35). Thereby, BiP contributes to quality control for protein homeostasis in the ER (46,47,136). BiP has been shown to be phosphorylated on

theronine residues *in vitro* and *in vivo* (70,72,73), although how this modification affects the molecular or biological function on BiP is unclear. In addition, BiP undergoes ADP-ribosylation, which is thought to affect substrate binding and release (74-77). Misregulation of BiP is implicated in numerous diseases including neurodegenerative disorders and many types of cancers (78-80,95,105,137).

Here, we report that BiP is a novel substrate for dFic-mediated AMPylation. BiP was predominantly labeled with AMP by dFic in S2 cell lysate. AMPylation of BiP decreases during ER stress but increases upon the reduction of unfolded proteins. Both dFic and BiP are transcriptionally activated upon ER stress induction, implicating a role for dFic in the UPR. We identified a conserved threonine residue, Thr366, as the AMPylation site, which is in close proximity to the ATP binding site of BiP's ATPase domain. Our study presents the first substrate of AMPylation by a eukaryotic protein and proposes a new mode of posttranslational regulation of BiP, which is likely to serve a crucial role in maintaining ER protein homeostasis.

RESULTS

BiP is identified as a substrate for dFic

Our previous finding that *dfic* deletion in *Drosophila* results in blindness suggests that the molecular target of dFic could be a component of a visual signaling pathway. Although dFic was enriched in the capitate projections in the glial cell surface, we also observed that dFic is localized to the ER in a number of fly tissues including fat bodies, eye discs, and salivary glands, and in S2 cells (134). Therefore, we postulated that there

might be more common and ubiquitous substrates for dFic, and used S2 cells to identify substrates using a biochemical approach. In an attempt to enrich the substrates that are located in the ER, we performed a pull down with S2 cell lysate using the lectin concanavalin A (ConA), a procedure commonly used to enrich for glycoproteins or glycolipids. We observed a protein of approximately 72kDa in glycoprotein-enriched lysate that could be AMPylated by recombinant dFic carrying a constitutive activating mutation, E247G, in an in vitro labeling assay with 32P-α-ATP **(Figure 22A)**. The E247G mutation releases the intramolecular autoinhibition within the catalytic Fic motif, resulting in a protein with significantly enhanced enzymatic activity including robust auto-AMPylation (19).

We also observed the labeling of a ~72 kDa band in raw whole cell lysates, which had not been previously observed. It is possible that using the ConA buffer, which contains high concentrations of cation ($Mg2^{+}$, $Mn2^{+}$, and $Ca2^{+}$), to the lysate increases the dFic catalytic activity by better mimicking the ER environment. Indeed, the AMPylation of ~72kDa protein from the whole cell lysate was observed only with ConA buffer but was not observed with standard RIPA buffer **(Figure 22B)**. In order to identify this protein, glycoprotein-enriched S2 lysate was visualized by silver stain SDS-PAGE, and a single band was observed around 72kDa **(Figure 23A)**. MS analysis revealed this protein as heat shock protein 70 cognate 3, also known as BiP/GPR78. We confirmed that BiP was indeed highly enriched during ConA purification **(Figure 23B)**. Since BiP is not a glycoprotein itself, the detection of BiP

from ConA beads is likely due to its indirect binding to other ER localized glycosylated proteins.

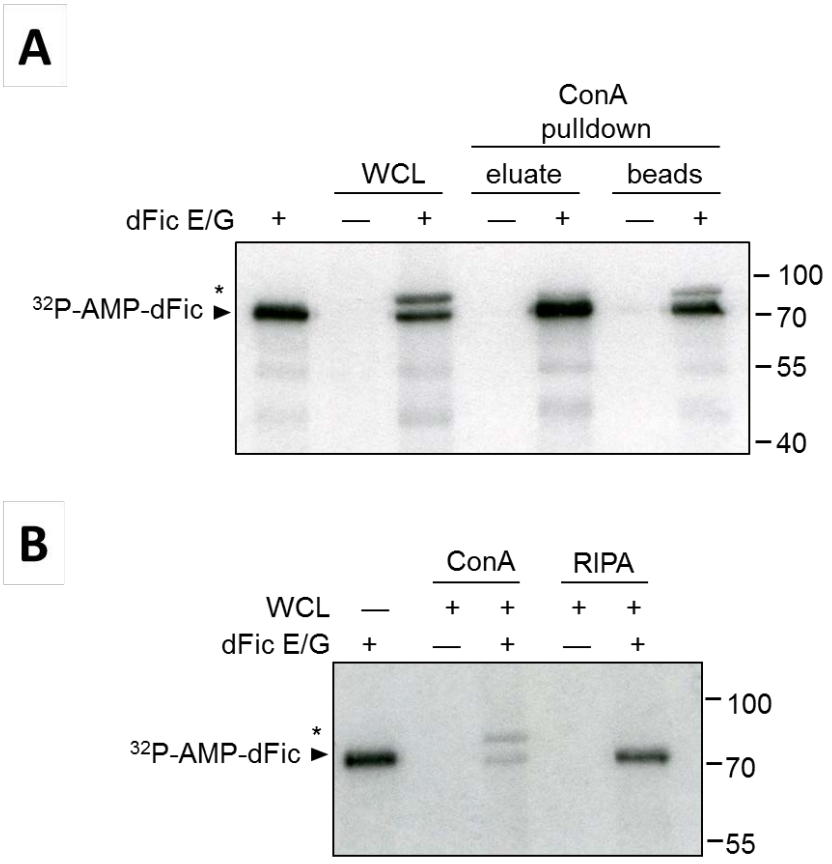

Figure 22. *In vitro* AMPylation activity of recombinant dFic. (A) Recombinant GST-dFicΔ70 E247G (dFic E/G) was incubated with S2 whole cell lysate and the ConA-bound fraction of lysate in the presence of 32P-α-labeled ATP. The arrowhead indicates the autoAMPylated dFic and the asterisk marks the putative substrate of ~72kDa from the lysate labeled with dFic. WCL, whole cell lysate. (B) dFic E/G was incubated with S2 whole cell lysate prepared with either standard RIPA buffer or ConA buffer with 5mM of Mg2+, Mn2+, and Ca2+, which is required for ConA binding.

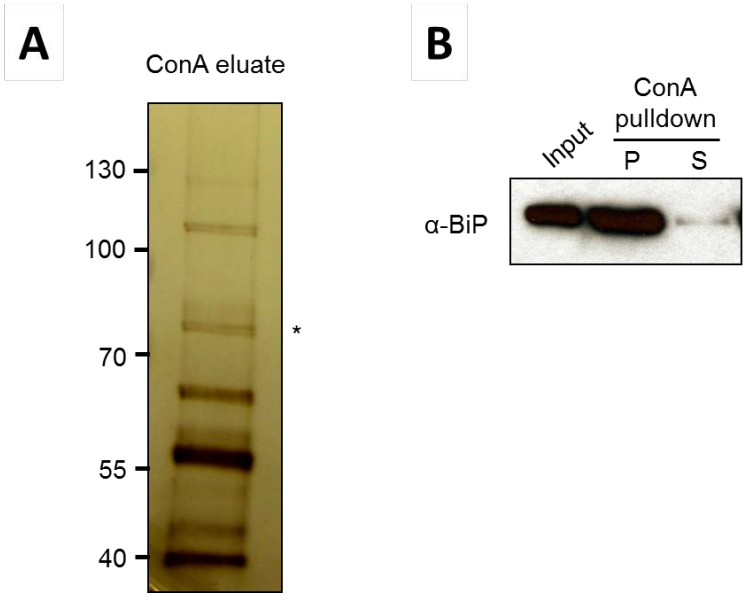

Figure 23. Identification of BiP as a substrate of dFic. (A) ConA-bound proteins were eluted from the beads, concentrated and analyzed by silver stain following SDS-PAGE. The asterisk indicates a single band with the size corresponding to the putative substrate of dFic observed from previous AMPylation assays. (B) S2 cell lysate was incubated with ConA)-agarose and the bound (P) and unbound (S) proteins were analyzed by anti-BiP.

Recombinant BiP is AMPylated by dFic in vitro

Due to their shared ER localization, BiP appeared to be a possible substrate candidate for dFic. To test whether BiP can be AMPylated by dFic, recombinant BiP with 6xHis tag at the N-terminus was purified from E. coli and used as a substrate in the in vitro AMPylation assay. We observed significant radiolabeling of both BiP and dFic E247G **(Figure 24A)**. The catalytic reaction was enhanced in the presence of calcium ions, which was consistent with the previous finding that BiP undergoes in vitro phosphorylation in a calcium-dependent manner (29). BiP was also AMPylated when wild-type dFic was used, albeit with significantly weaker activity **(Figure 24B)**. This suggests that the labeling mediated by dFic is not likely to be caused by an artifact due to the E247G mutation. Mutating the conserved histidine residue in the Fic motif to an alanine (H375A) abolished the catalytic activity of dFic. Furthermore, human Fic (FicD or HYPE) E234G was also able to efficiently modify human BiP **(Figure 25)**.

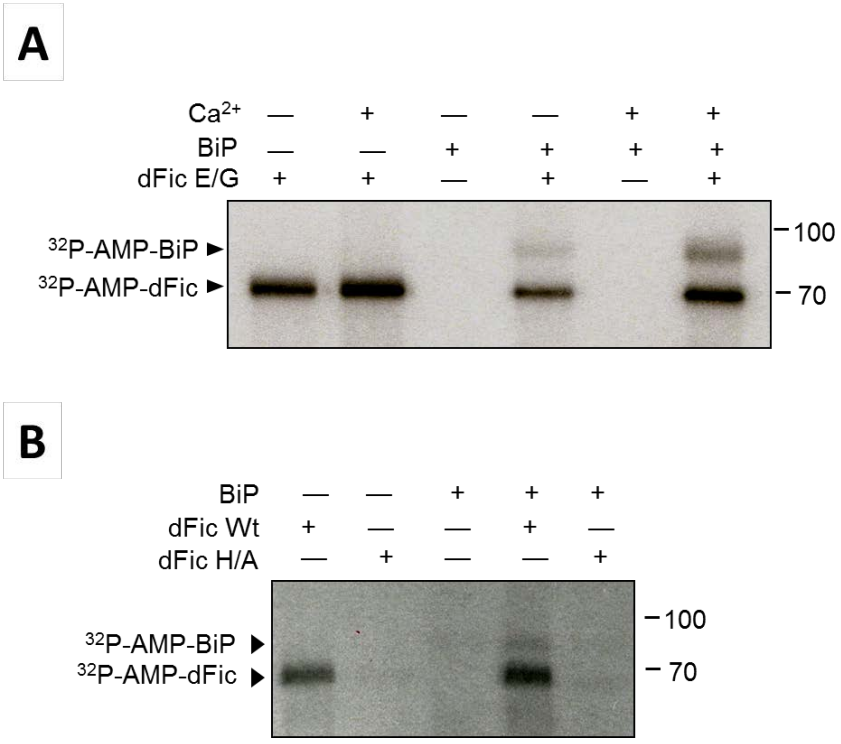

Figure 24. Recombinant BiP is AMPylated by dFic in vitro. (A) Recombinant His-BiP was used as a substrate for dFic in the AMPylation assay in the presence or absence of 5mM Ca2+. Arrowheads indicate the AMPylated proteins. (B) BiP is AMPylated by wild-type dFic. GST-dFicΔ70 (dFic Wt) and GST-dFicΔ70 H375A (dFic H/A) were incubated with His-BiP in the presence of 32P-α-labeled ATP. Arrowheads indicate the AMPylated proteins.

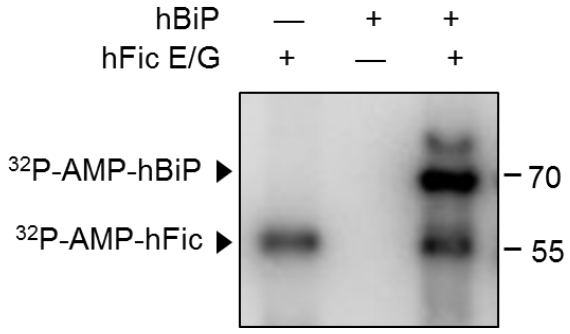

Figure 25. Human BiP is AMPylated by human Fic in vitro. Human version of His-SUMO-FicDΔ47 E234G (hFic) and His-BiPΔ19 (hBiP) were used for the AMPylation assay.

AMPylation of BiP is modulated by ER stress

As BiP is an important sensor and regulator for the UPR, we analyzed whether the AMPylation status of BiP is differentially regulated when cells are undergoing ER stress. We treated S2 cells with tunicamycin, a pharmacological inducer of ER stress, for different times and blotted the whole cell lysate with anti-AMP-Thr antibody (42). A protein with the size of BiP was AMPylated in S2 cells but AMPylation started to decrease within 30 minutes of tunicamycin treatment and was completely absent after 24 hours **(Figure 26A)**. The same trend was observed when DTT was used to trigger ER stress **(Figure 26B)**, supporting the hypothesis that the level of AMPylated protein recognized by anti-AMP-Thr antibody decreases as more misfolded proteins accumulate in the ER. We then treated the cells with cycloheximide, which reduces the load of unfolded proteins in the ER by decreasing the amount of newly synthesized proteins. The signal of the ~72kDa band detected by anti-AMP-Thr antibody was increased upon

cycloheximide treatment, in contrast to the effect observed with the ER stress inducers **(Figure 27A)**. To confirm that the protein being regulated by AMPylation was BiP, we treated cells transfected with Flag-tagged BiP with DTT or cycloheximide, immunoprecipiated BiP and analyzed using the anti-AMP-Thr antibody. As predicted, BiP was AMPylated in untreated cells, whereas lower and higher levels of AMPylation were observed in DTT-treated and cycloheximide-treated cells, respectively **(Figure 27B)**. The results followed the same pattern of modification shown in Figure 3C for the S2 whole cell lysate, confirming BiP as the relevant band observed. The level of AMPylated BiP was low when cells were treated with both DTT and cycloheximide **(Figure 28)**. Blocking protein degradation with MG132 did not affect the level of AMPylated BiP, which indicates that the decrease of BiP AMPylation upon ER stress is not due to protein degradation. BiP needs to be acutely activated upon accumulation of misfolded proteins caused by ER stress, while it needs to stay inactive in the absence of unfolded protein loads. Our results show that the AMPylation status of BiP inversely correlates with its active state during ER homeostasis suggesting the potential inhibitory mechanism of AMPylation on BiP.

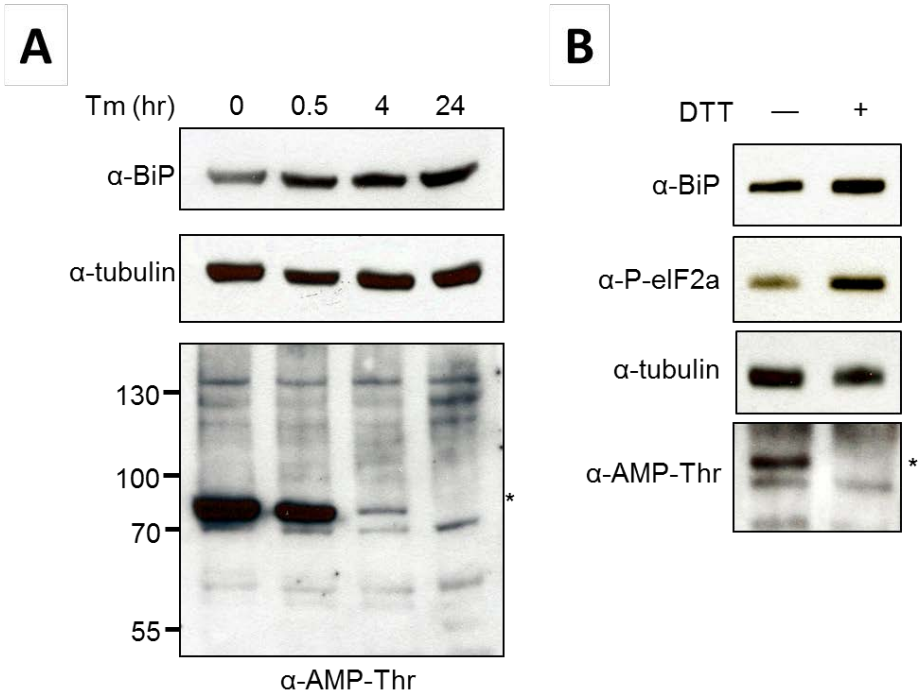

Figure 26. AMPylation of BiP declines upon ER stress. (A) Pharmacological ER stress inducer tunicamycin (Tm) was treated to S2 cells for the indicated time at 2μg/ml. Whole cell lysates from different time points were analyzed by anti-BiP and anti-Thr-AMP. Anti-tubulin was used as a loading control. The asterisk marks the AMPylated protein from cell lysate with ~72kDa. (B) 5mM DTT was used to trigger ER stress in S2 cells for 1 hour and the whole cell lysates were analyzed with indicated antibodies. Anti-phospho-eIF2α was used as a marker for ER stress.

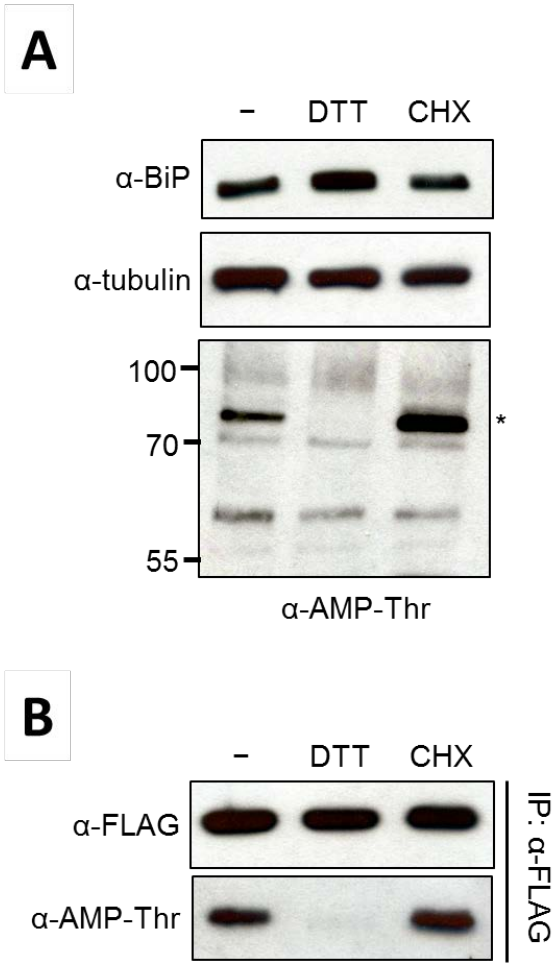

Figure 27. AMPylation of BiP is modulated by ER stress. (A) 5mM DTT and 100μg/ml cycloheximide (CHX), a potent inhibitor of protein synthesis, was added to S2 cells for 4 hours. Whole cell lysates were analyzed with indicated antibodies. (B) Cells were transfected with BiP containing a C-terminal FLAG tag followed by DTT and CHX treatment for 4 hours. BiP was then immunoprecipitated with anti-FLAG agarose and analyzed with anti-BiP and anti-Thr-AMP. Immunoprecipitation was confirmed by anti-FLAG.

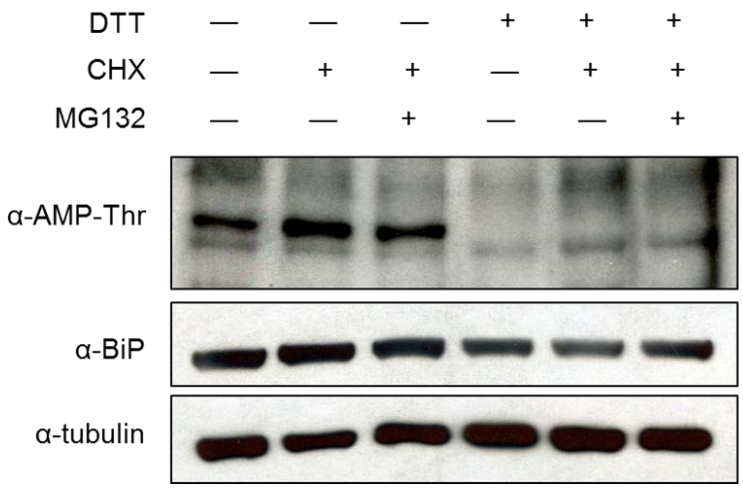

Figure 28. Reduction of BiP AMPylation is not due to degradation. Cells were treated with 5mM DTT and/or 100μg/ml CHX in the presence or absence of 20μM MG132 for 4 hours.

AMPylation of BiP is a reversible event

Our data support the hypothesis that AMPylation occurs upon the reduction of unfolded protein load. In order to explore the reversibility of AMPylation upon different cellular states, we induced ER stress in cells, removed the stress inducer, and monitored the AMPylation state of BiP over time as the cells recovered from stress. After 1 hour of DTT treatment the cells were washed and replated with fresh media to eliminate DTT. As cells slowly recovered from the potent induction of ER stress, we observed that the AMPylation of BiP became visible again after 8 hours **(Figure 29A)**. When cycloheximide was added to the media so that only the existing BiP could be monitored,

we still observed a recovery of AMPylated BiP at 8 hours **(Figure 29B)**. This shows that AMPylation is a reversible modification that readily adapts to the fluctuation of unfolded proteins in the ER.

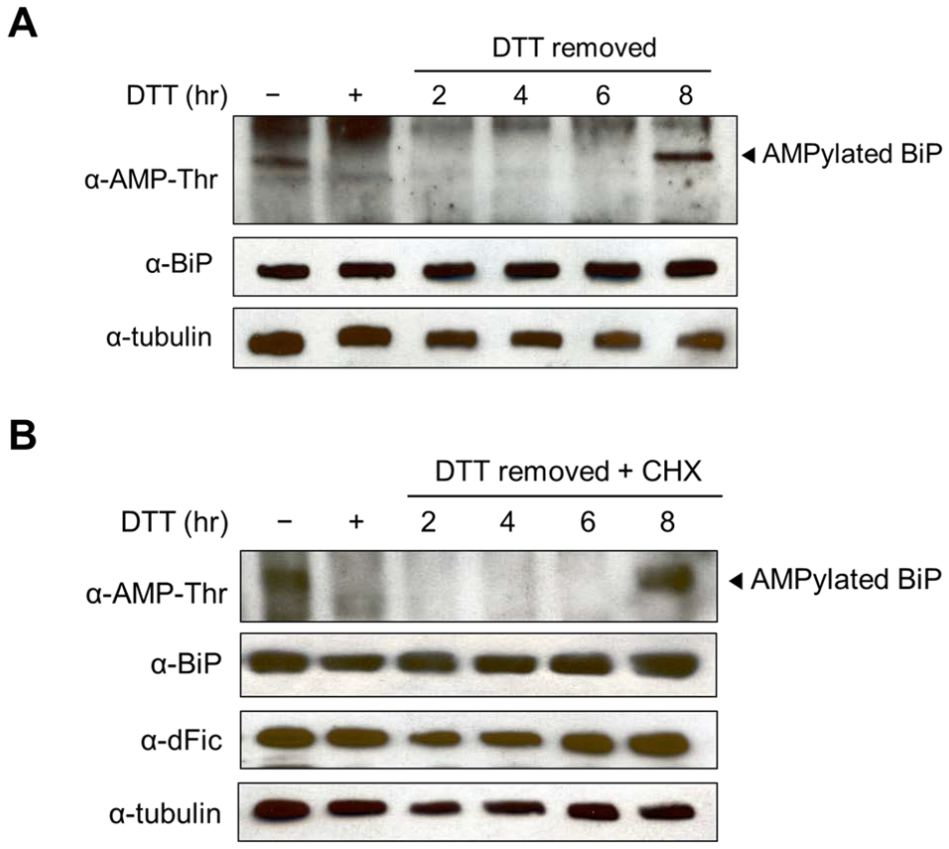

Figure 29. AMPylation of BiP is a reversible event. S2 cells were treated with 5mM DTT for 1 hour for ER stress induction. The cells were then washed and replated with fresh media to remove DTT, and left untreated (A) or treated with 100μg/ml CHX (B). AMPylation of BiP, indicated by an arrowhead, was then monitored over time from the whole cell lysate using anti-AMP-Thr antibody.

dFic is transcriptionally upregulated by ER stress

Upon ER stress, general translation is attenuated in order to reduce the synthesis of new proteins while a number of chaperones and ERAD-associated genes are upregulated to cope with the accumulation of misfolded proteins. BiP is also transcriptionally activated along with many other chaperone genes during ER stress. By modifying this important regulator of UPR, dFic is likely to be involved in the same pathway. To test this, we measured the mRNA level of dFic and BiP in S2 cells upon ER stress induction using DTT, tunicamycin, or thapsigargin. Both dFic and BiP mRNAs were significantly increased by ER stress **(Figure 30A)**. ER oxidoreductin-1-like (ERO1L), which encodes a protein that maintains the oxidative environment of the ER, was also induced consistent with previous studies (44). Human Fic from HEK293T cells was also induced by ER stress along with CHOP **(Figure 30B)**, a UPR gene which induces apoptotic signaling under prolonged cellular stress (45). These results further support the proposal that AMPylation mediated by dFic plays a conserved role in the UPR pathway.

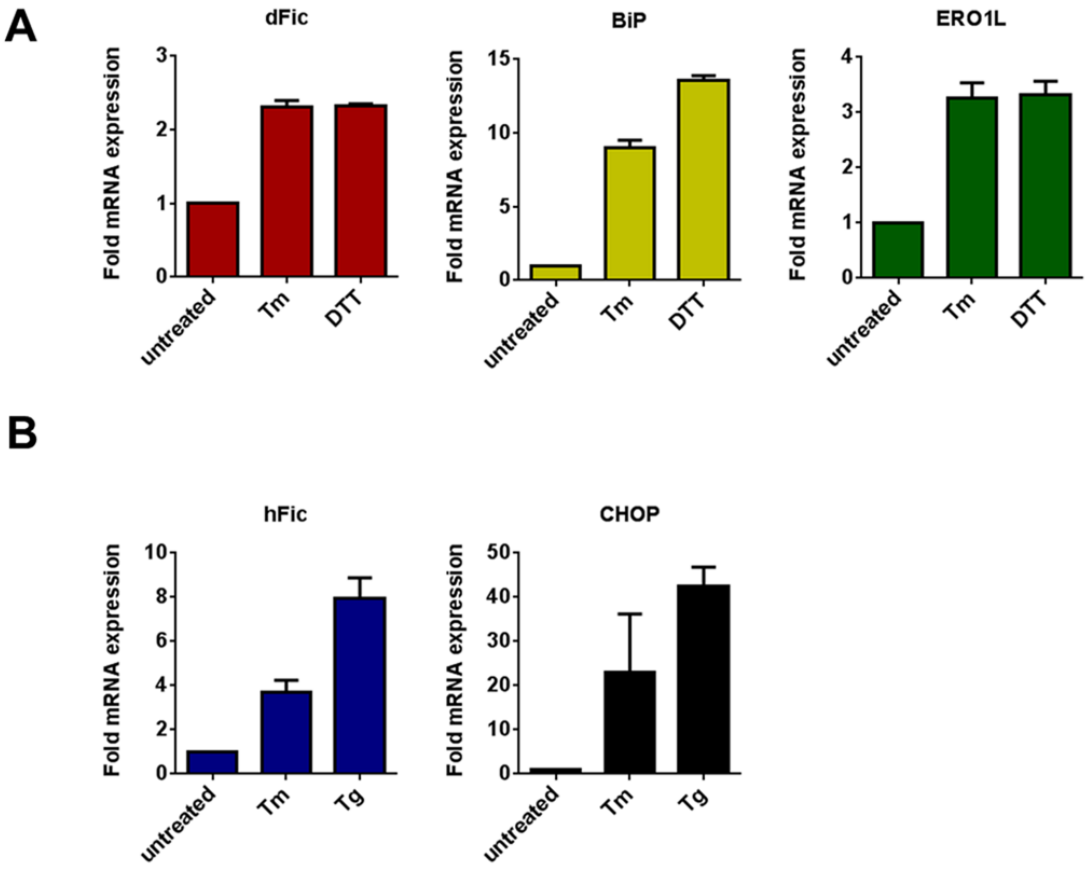

Figure 30. dFic is transcriptionally upregulated by ER stress. (A) S2 cells were treated with 2μg/ml tunicamycin (Tm) or 5mM DTT for 4 hours and mRNA levels of dFic, BiP, and ERO1L were measured by quantitative real-time PCR. (B) HEK293T cells were treated with 2μg/ml tunicamycin (Tm) or 1μM of thapsigargin (Tg) for 6 hours and the mRNA levels of human Fic (hFic) and CHOP were measured by quantitative real-time PCR.

The AMPylation site on BiP maps to Thr366 in the ATPase domain

To elucidate where BiP is modified with AMP, three different truncation mutants of BiP were generated. Constructs containing an N-terminal signal sequence-deleted (Δ26) BiP, which mimics the processed form of BiP in the ER (46), the BiP ATPase domain (ATPase), or the BiP substrate binding domain (SBD) were expressed and purified from E. coli. We found that the ATPase domain could be AMPylated more efficiently than BiPΔ26 whereas no AMPylation was observed with the substrate binding domain **(Figure 31)**. In addition to the radiolabeling assay, the anti-AMP-Thr antibody was used to confirm the AMPylation of the BiP ATPase domain **(Figure 32A)**. To identify the AMPylated residue in BiP, we conducted LC-MS/MS analysis on recombinantly AMPylated BiP. Threonine 166 and 366 appeared to be the most probable candidates based on the preliminary MS analysis.

To establish the in vivo site of AMPylation on BiP, we transfected S2 cells with C-terminally Flag-tagged BiP containing threonine mutations and used the anti-AMP-Thr antibody to monitor the AMPylation of immunoprecipitated BiP. Mutation of Thr366 to alanine completely abolished the AMPylation of BiP, suggesting it is the sole in vivo site of modification **(Figure 32B)**. BiP was previously reported to undergo ADP-ribosylation, so to rule out the possibility that the anti-AMP-Thr antibody was detecting ADP-ribosylation we made an ADP-ribosylation defective R470K mutant (35). The anti-AMP-Thr still recognized the transfected R470K mutant of BiP, confirming the specificity of the antibody for AMPylation **(Figure 33)**. In support of T366 being a legitimate AMPylation site rather than a cause of structural perturbation, BiP T366A was shown to

be a functional ATPase **(Figure 34)**. Thr366 was also found to be highly conserved in all heat shock protein 70 homologs of other species **(Figure 35A)**. The published structure of BiP reveals that Thr366 is in close proximity to the ATP binding pocket, raising the possibility that AMPylation, a bulky post-translational modification, might hinder ATP hydrolysis **(Figure 35B)**. This mechanism would be similar to that observed for gluatamine synthetase, the first protein observed to be regulated by AMPylation (2).

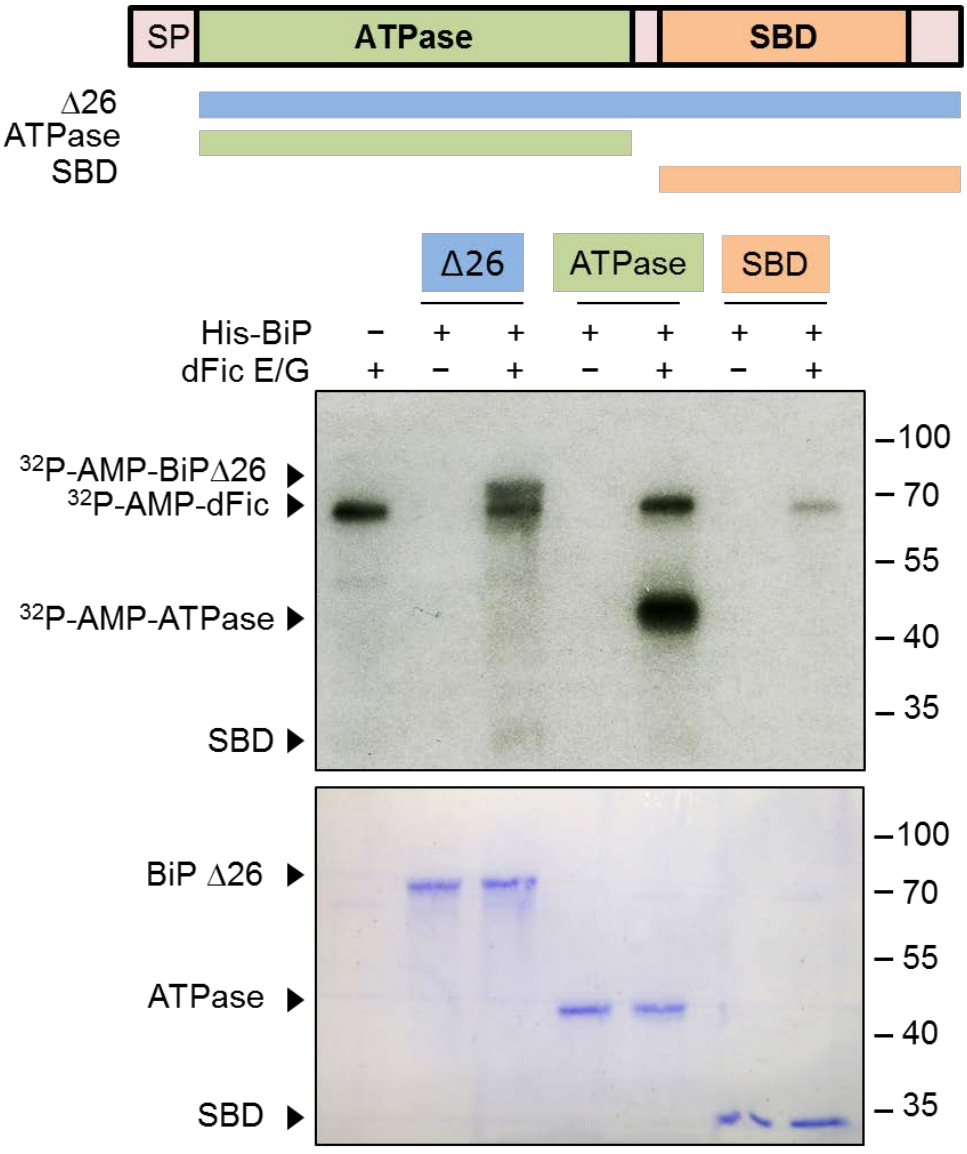

Figure 31. AMPylation occurs on the ATPase domain of BiP. Domain structure of BiP and different protein constructs generated are shown. These constructs were purified from *E.coli* with N-terminal 6xHis tag and used as substrates for GST-dFicΔ70 E247G (dFic E/G) in the AMPylation assay. SP, signal peptide. SBD, substrate binding domain.

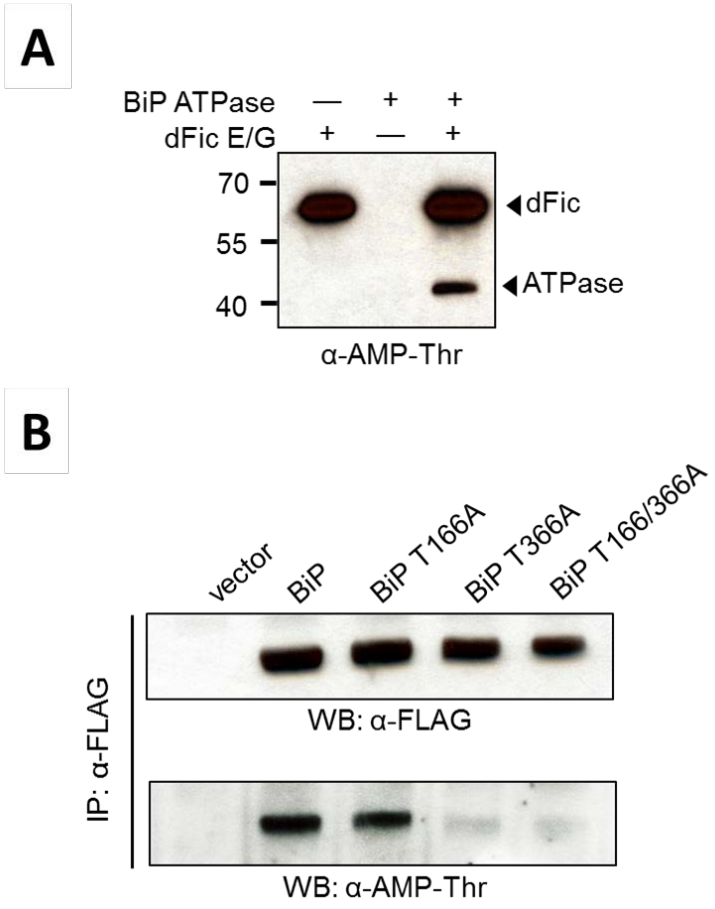

Figure 32. AMPylation site maps to Thr366 in the ATPase domain of BiP. (A) His-BiP ATPase was incubated with GST-dFicΔ70 E247G (dFic E/G) and cold ATP and analyzed by anti-AMP-Thr. Arrowheads mark the AMPylated proteins. (B) Various constructs of BiP with a C-terminal FLAG tag followed by ER retention signal KDEL were transfected to S2 cells and immunoprecipitated using anti-FLAG agarose. Purified BiP was analyzed by anti-Thr-AMP. Immunoprecipitation was confirmed by anti-FLAG.

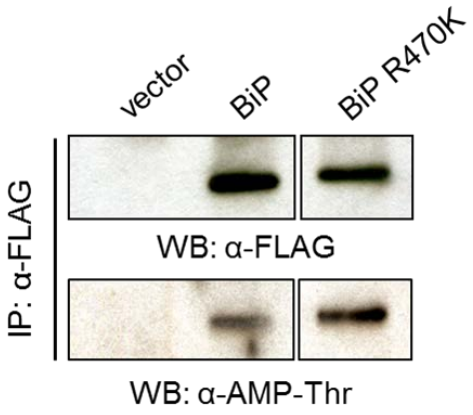

Figure 33. Anti-AMP-Thr is specific for AMPylated proteins. BiP wild-type and ADP-ribosylation mutant R470K were expressed and immunoprecipitated from S2 cells and analyzed by anti-AMP-Thr antibody.

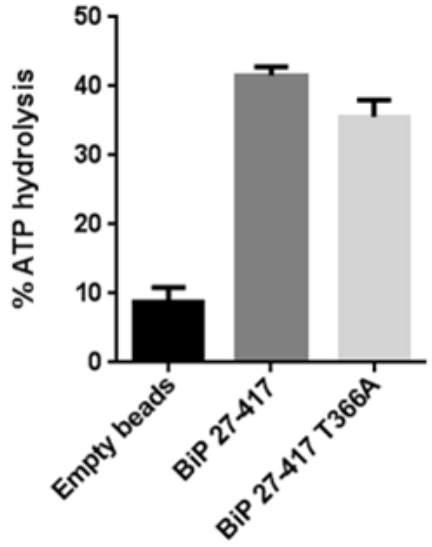

Figure 34. T366A mutation does not disrupt the activity of BiP ATPase. ATPase activity of the recombinant BiP ATPase domain (27-417) wild-type and Thr366A was measured.BiP wild-type and ADP-ribosylation mutant R470K were expressed and immunoprecipitated from S2 cells and analyzed by anti-AMP-Thr antibody.

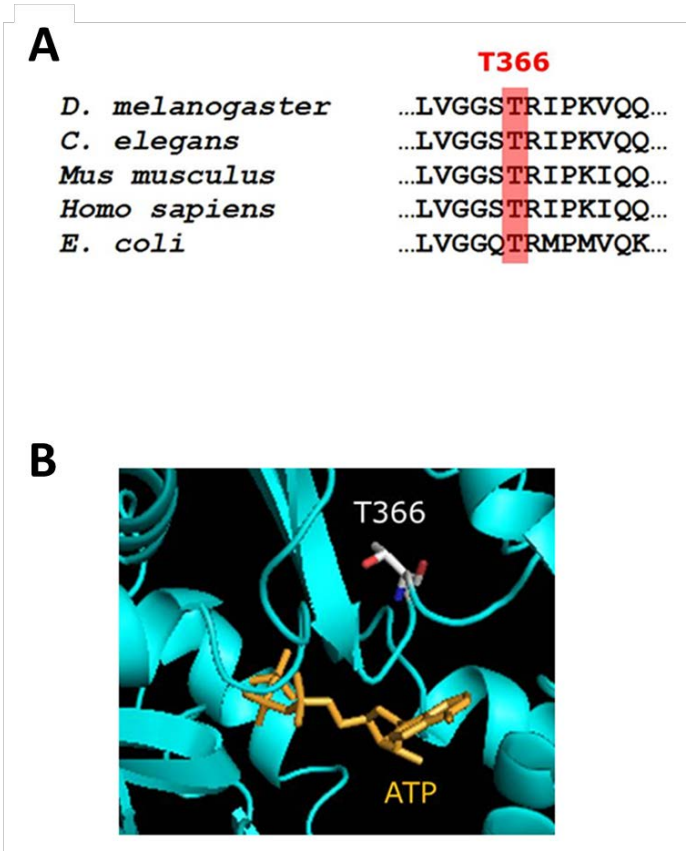

Figure 35. T366A located near ATP binding site. (A) Multiple sequence alignment of BiP homologs from different species. Thr366 identified as a putative AMPylation site is highly conserved in all homologs. (B) Structural view of the ATPase domain of human BiP reveals that Thr366 is located nearby the ATP binding site (PDB: 3LDL).

AMPylation of BiP by dFic correlates with the inactive state of BiP

We next assessed the relationship between AMPylation and the molecular activity of BiP. Due to the complexity of protein folding assays and the fact that both enzymes use ATP as a substrate, definitively proving that BiP is inhibited by dFic AMPylation is beyond the scope of this study. Previous investigators demonstrated that the ATPase domain alone exhibits poor ATPase activity, whereas the addition of a short hydrophobic interdomain linker to the ATPase domain results in robust ATPase activity (47). The ATPase domain of BiP undergoes cycles of ATP binding, hydrolysis, and nucleotide exchange that are tightly coupled to substrate binding and release (28). The linker binding mimics this allosteric coupling of the two domains of BiP. Without the linker, BiP loses the intradomain interaction crucial for its functional cycle and remains inactive. Because the ATPase domain we previously used for the AMPylation assay did not include the linker region (BiP 27-407), we created another construct that carries the linker by adding ten additional amino acids (BiP 27-417). These proteins were tagged with N-terminal 6xHis and purified from E.coli. In line with the previous finding, BiP 27-417 showed significantly increased ATPase activity compared to BiP 27-407 **(Figure 36A)**. We then used these recombinant proteins as substrates for the AMPylation assay. The inactive ATPase domain, BiP 27-407, was efficiently modified by dFic, whereas the active BiP 27-417 was a very poor substrate for dFic **(Figure 36B)**. The observation that Fic AMPylation occurs efficiently on the inactive form of the ATPase domain and inefficiently with the active state of BiP correlates to our finding in cells that the level of

AMPylation was high in normal cells and low upon the increased load of unfolded proteins.

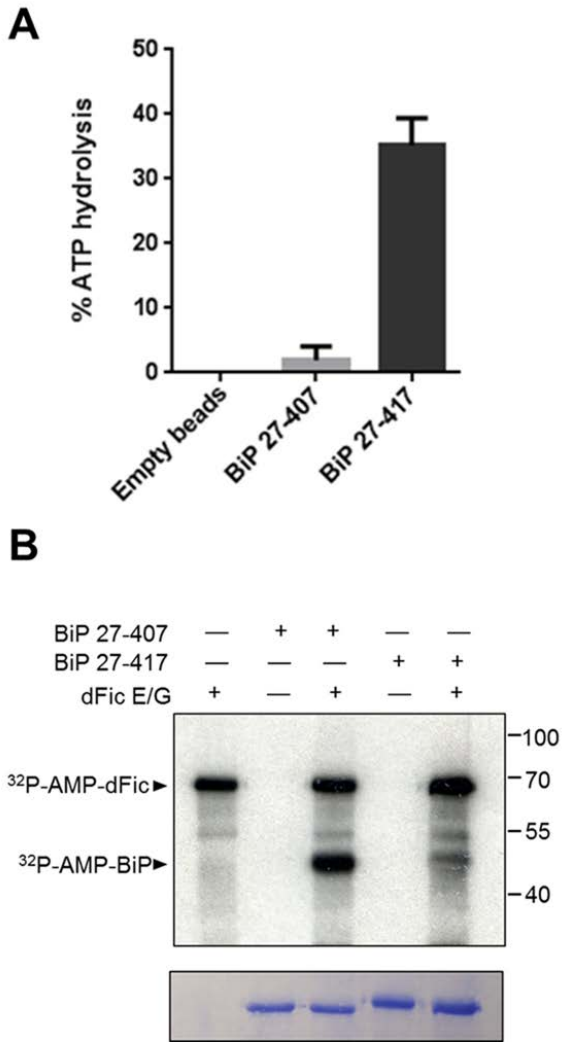

Figure 36. AMPylation of BiP by dFic correlates with the inactive state of BiP. (A) ATPase activity of the recombinant BiP 27-407 and BiP 27-417. His-BiP 27-407 and His-BiP 27-417 (carrying an interdomain linker) proteins were bound to Ni-NTA beads and assessed for the ATPase activity. Empty beads were used as a negative control. (B) His-BiP 27-407 and His-BiP 27-417 were used as substrates for dFic-mediated AMPylation. Arrowheads mark the AMPylated proteins by dFic.

AMPylation of BiP is reversibly regulated during ER homeostasis

To gain insight into the amount of modified BiP in cells, we used lysates from unstressed cells and cells stressed with DTT as substrates for the AMPylation assay. As shown above, the level of in vivo AMPylated BiP declines in the presence of ER stress as detected by the anti-AMP-Thr antibody **(Figure 37A)**. We used the same amount of lysate form unstressed and stressed cells as was used for immunoblotting in an AMPylation assay **(Figure 37B)**. Consistent with the high degree of in vivo AMPylation in unstressed cells, only minimal additional in vitro labeling was observed for BiP. By contrast, considerable in vitro labeling was observed for BiP in lysates from stressed cells **(Figure 37B)**, consistent with our observations that BiP is deAMPylated in DTT-treated cells **(Figure 37A)**. Altogether, we show that when cells are undergoing ER stress, misfolded proteins accumulate and BiP is rapidly deAMPylated; however, in the absence of newly synthesized proteins or upon low unfolded protein load, BiP is AMPylated. Hence, AMPylation is likely to regulate the activity of BiP depending on the state of newly synthesized/misfolded protein loads in the ER **(Figure 38)**.

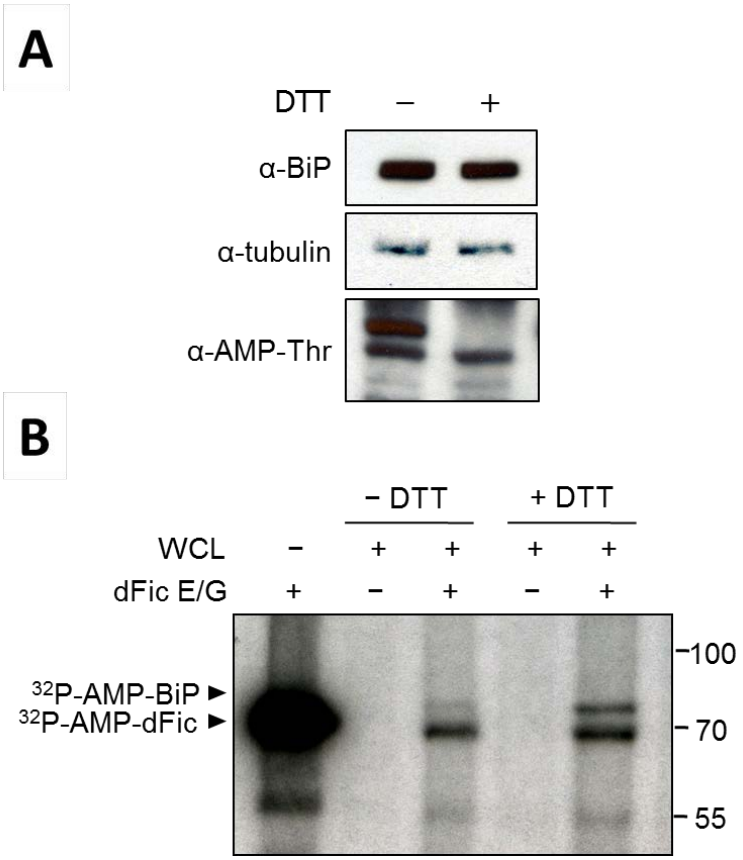

Figure 37. AMPylation of BiP is reversibly regulated during ER homeostasis. (A) *In vivo* AMPylation of BiP was measured in unstressed cells and cells stressed with 5mM DTT for 1hr using anti-AMP-Thr antibody. (B) Equal amount of lysates used for immunoblotting in (A) were used as substrates for the AMPylation assay with GST-dFicΔ70 E247G (dFic E/G). Arrowheads mark the AMPylated proteins.

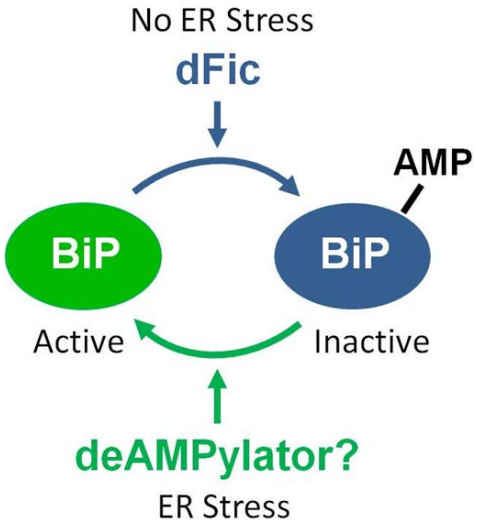

Figure 38. Working model of AMPylation of BiP modulated by ER stress. When cells undergo ER stress and accumulate misfolded proteins, BiP gets deAMPylated and becomes active as unmodified form. In the absence of ER stress and upon the reduction of unfolded protein load, BiP undergoes AMPylation by dFic which renders it inactive. This reversible event of AMPylation ensures a rapid on/off regulation of BiP to maintain protein homeostasis in the ER.

DISCUSSION

AMPylation appears to be a promising posttranslational regulatory mechanism adopted by organisms of varying complexity due to the high conservation of Fic domains and its use of ATP as a substrate. Bacterial AMPylators have already been shown to play an essential role in hijacking host signaling pathways during pathogenesis but the endogenous function of AMPylation in eukaryotes remained elusive. Our study presents BiP, a well-known ER chaperone and a major regulator of UPR, as the first substrate of AMPylation by a eukaryotic protein. BiP from the whole S2 cell lysate was predominantly labeled by dFic enzyme in the presence of divalent cations (Mg^{2+}, Mn^{2+}, and Ca^{2+}). Calcium appears to promote this catalytic reaction as shown by Figure 2A. Indeed, ER is a major organelle for calcium storage with the concentration of calcium ions in the lumen in the millimolar range (138). Therefore, having calcium ions in the reaction may better mimic the chemical environment in the ER. It was also reported that Hsp70 chaperones bind to calcium ions, which may stabilize the protein structure (139). The stable conformation of BiP achieved by calcium binding may render it a better substrate for dFic.

The essential role of BiP in ER stress response and many cellular and pathological processes supports the notion that there may be multiple mechanisms for its regulation. Upon ER stress, BiP is transcriptionally activated to assist in the folding of high levels of unfolded proteins. However, the dynamic fluctuation of unfolded protein loads in the ER due to stress response or alternating rates of protein synthesis may require a more rapid regulation of BiP. This is also supported by the discrepancy between the long half-life of

BiP, which is up to 48 hours, and its excess activity being detrimental to cells as maturation and secretion of critical proteins can be significantly delayed (140,141). A post-translational modification provides an ideal mechanism to readily activate and deactivate BiP upon changes in unfolded protein loads in the ER. Previously, ADP-ribosylation has been suggested to inactivate BiP by attenuating substrate binding and interfering with the allosteric coupling between domains (77). The enzyme catalyzing ADP-ribosylation has not been identified. In contrast to AMPylation, which we observed in the ATPase domain, ADP-ribosylation occurs in the substrate binding domain on arginine residues (Arg470 and Arg492). Therefore, we speculate that BiP undergoes different modifications on both domains, ensuring its tight regulation at multiple levels. The exact molecular event triggering such modifications or the order in which they occur remains to be explored. Furthermore, identifying the enzyme that catalyzes the rapid deAMPylation of BiP during ER stress and understanding its functional consequence will be of great interest.

AMPylation occurs on a conserved threonine residue located near the ATP binding pocket, which suggests that AMPylation may affect the ATPase activity of BiP by either blocking nucleotide binding or inhibiting efficient ATP hydrolysis. Unfortunately, the inverse relationship of BiP's suitability for AMPylation and its ATPase activity makes the measurement of activity differences caused by AMPylation technically challenging.

Another possible inhibitory mechanism of AMPylation on BiP is uncoupling of two-domain allostery, similar to the effect of ADP-ribosylation (77). Upon ATP binding,

Hsp70 proteins undergo a structural change wherein the two domains come in close contact and form a compact structure (57). The addition of the bulky AMP moiety can potentially hinder the contact between the domains and thereby disrupt the functional cycle of BiP. From an intermolecular perspective, AMPylation of BiP may also alter its interaction with binding partners such as DnaJ co-chaperone (142-144) or nucleotide exchange factors (145-147).

Induction of ER stress upregulates not only BiP but also dFic, which was a surprising result considering that AMPylation of BiP decreases during ER stress. Nevertheless, it suggests that dFic is among many UPR genes that cells use to cope with the stress response. It is possible that dFic is induced along with other chaperones but its activity or translocation is blocked until the unfolded protein load decreases and BiP has to be promptly inactivated. dFic could then be released from repression and subsequently inactivate BiP. Otherwise, excess level of active BiP may prolong protein maturation and secretion which would be deleterious to cells. How dFic is regulated upon ER stress is another interesting avenue to be explored. There might be another layer of posttranslational modification governing the function of dFic.

Previous studies have shown that flies without functional dFic in glial cells have impaired visual neurotransmission (134). This suggests that dFic substrate could be a component of visual signaling or a transporter of neurotransmitters. Alternatively, the blind phenotype could result from a loss of regulation on BiP. We can speculate that the protein responsible for the visual signaling is not properly matured or secreted in the absence of tight regulation of BiP in *dfic* null flies, which thereby results in visual defect.

Indeed, imbalance of protein homeostasis is a cause of many pathological processes due to accumulation of aberrant protein or impaired protein secretion (148).

Interestingly, dFic is mainly localized to the cell surface on glial cells where it is particularly enriched in capitate projections. In contrast, dFic appears to localize to the ER in other fly tissues (fat bodies, eye discs, and salivary glands) and in S2 cells. Therefore, dFic may target a different molecule on the cell surface that could directly impact neurotransmission. It is possible that in glial cells, there might be cell-type specific factors that can induce the secretion of dFic from the ER to cell surface.

We show that human Fic also AMPylates BiP *in vitro* and that it is transcriptionally activated by ER stress. This suggests that AMPylation is a conserved regulatory mechanism in multiple species possibly involved in UPR. As both Fic and BiP are highly conserved in many organisms, it will be worth investigating the role of AMPylation in other species.

Understanding the regulatory mechanism of BiP is of utmost importance as misregulation of BiP is associated with numerous diseases including neurological disorders and various cancers (78-80,95,137). Increased level of BiP is a critical factor for tumor progression and has been shown to confer chemoresistance to a variety of cancer cell lines (79,104,137,149). Accordingly, inhibition of BiP activity is emerging as an important cancer target. The discovery of BiP AMPylation and deAMPylation presents a new targetable avenue for drug development.

CHAPTER 5
Preliminary Results and Future Directions

Molecular mechanism of AMPylation on BiP

Most AMPylators characterized thus far have shown to inhibit the function of the modified proteins via steric hindrance. Our observation that the AMPylation site maps to a conserved threonine residue close to the ATP binding site of BiP suggests the hypothesis that AMPylation may hinder the ATPase activity of BiP. However, challenges lie in measuring the effect of AMPylation on BiP ATPase activity. First, both proteins use ATP as a substrate for different catalytic mechanism. Second, the efficiency of AMPylation in vitro is rather weak as shown by the previous AMPylation assay results. Third, BiP ATPase domain without the linker (27-407) which is efficiently AMPylated by dFic has a poor activity whereas the ATPase domain containing the linker (27-417) and therefore an active ATPase is a poor substrate of AMPylation. To overcome these issues, we are trying to ligate the linker to the AMPylated ATPase domain of BiP using a bacterial enzyme sortase A from *Straphylococcus aureus*. Sortase A is a transpeptidase enzyme that has been developed as a tool for site-specific protein labeling (150). It recognizes a LPXTG sequence of the substrate and cleaves the peptide bond between the threonine and glycine resulting in a thioacyl intermediate. Then a probe designed to carry oligoglycine reacts with the thioacyl intermediate and is ligated to the target protein via amide linkage to yield the transpeptidation product. Our strategy is to AMPylate the BiP ATPase domain (27-407) as efficiently as possible and add the 10 amino acid linker using

sortase to obtain the active ATPase that is efficiently AMPylated **(Figure 39)**. We would still need to optimize the efficiency of sortase-mediated transpeptidation and confirm that this additional step does not interfere with the final readout. We will then be able to measure the ATPase activity of the unmodified and AMPylated BiP ATPase domain. To remove the residual ATP used as substrates for AMPylation, BiP will be affinity-purified before measuring the ATPase assay. These experiments may potentially unravel the inhibitory mechanism of AMPylation.

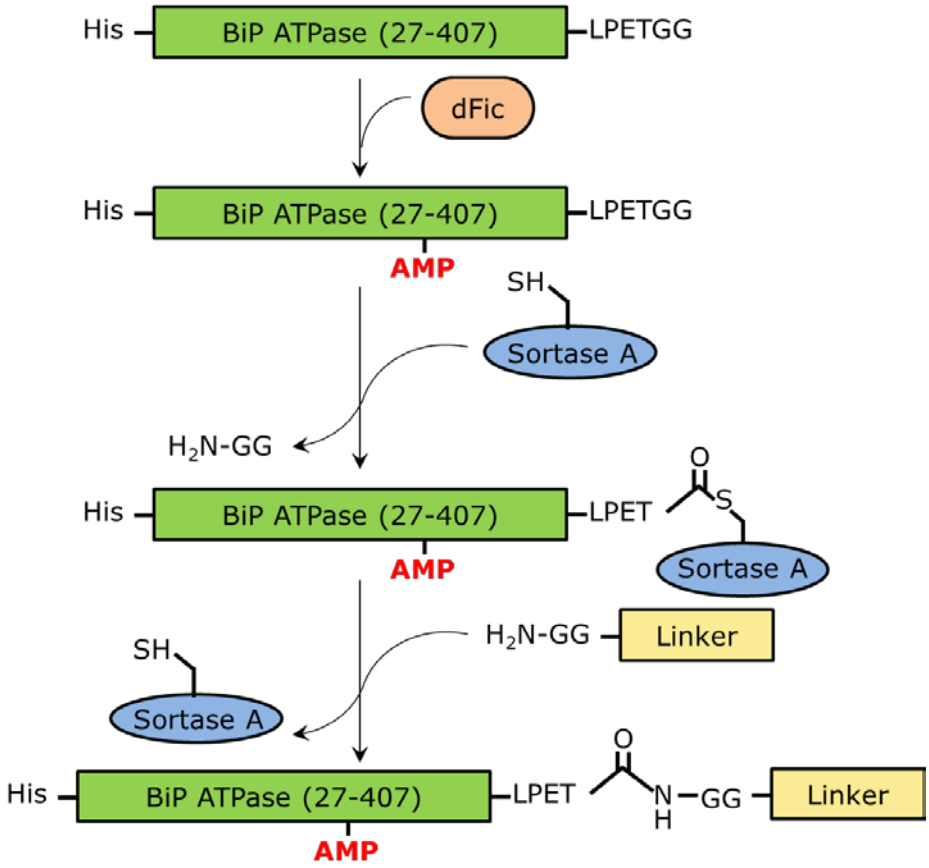

Figure 39. Strategy to measure the effect of AMPylation on ATPase activity of BiP. His-BiP ATPase (27-407) containing Sortase A recognition sequence LPETG will be AMPylated by dFic to the optimal level. Then Sortase A and 10-amino acid interdomain linker containing oligoglycine will be added to the reaction so that the AMPylated BiP ATPase (27-407) will be ligated with the linker and thereby become an active ATPase.

Another possible effect of AMPylation is to inhibit the allosteric coupling of the two domains of BiP. BiP undergoes conformational changes depending on the nucleotide binding mode of the NBD. When NBD is bound to ADP, the two domains are separated and held loosely by the aforementioned interdomain linker. When NBD is bound to ATP, SBD and the linker come in close contact with NBD forming a compact structure. These different conformational states could be examined by limited proteolysis **(Figure 40)**. When the His-BiPΔ26 was incubated with ATP, it was more resistant to proteinase K as the two domains were tightly bound. However, when upon ADP binding or without any nucleotides bound, His-BiPΔ26 was effectively cleaved by proteinase K as the two domains were dissociated. Therefore, we can assess how AMPylation affects such conformational changes by performing limited proteolysis on BiP purified from unstressed and stressed S2 cells. We found that BiP from resting cells, which is highly AMPylated, is sensitive to proteinase K whereas deAMPylated BiP from stressed cells is resistant **(Figure 41)**. This suggests that AMPylation of BiP may render the two domains to be dissociated and uncouple their allosteric cycle. However, to further confirm that this is specifically due to AMPylation and not by other modifications, T366A mutant BiP should be used for the same experiment which is predicted to show a similar pattern as wild-type BiP from cells undergoing ER stress.

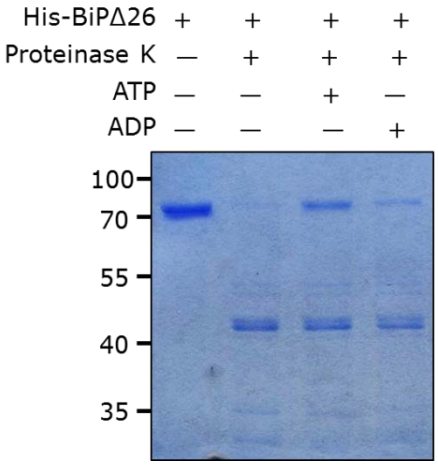

Figure 40. Different conformational states of BiP dependent on the bound nucleotide substrate. His-BiPΔ26 was either left alone or preincubated with ATP or ADP. Then the proteins were treated with proteinase K for limited proteolysis and analyzed by SDS-PAGE with coommassie staining.

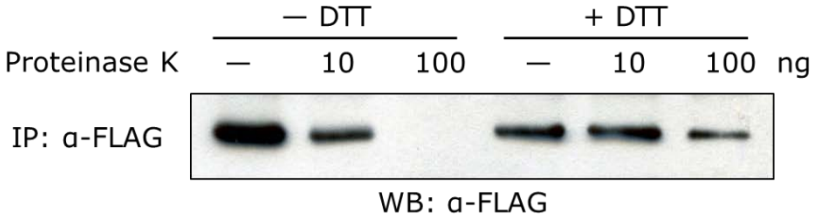

Figure 41. Limited proteolysis on BiP with different AMPylated status. FLAG-tagged BiP was transfected to S2 cells and affinity-purified by anti-FLAG beads. Then the indicated amount of proteinase K was added to the beads. The cells were either untreated or treated with DTT so that the AMPylated and deAMPylated BiP would be obtained, respectively.

AMPylation of BiP may also possibly affect its interaction with the binding partners via steric hindrance, as observed with the GTPases that are AMPylated by bacterial effectors. Hsp70 proteins including BiP have been shown to interact with Hsp40 cochaperones that collectively contain J domains (144). Specifically, ER Hsp40 chaperone ERdj3 binds to BiP and stimulates its ATPase activity which increases its affinity to substrate proteins (142,143). In addition, BiP interacts with ER lumenal nucleotide exchange factor BAP (BiP associated protein) that facilitates the exchange of ADP with ATP in the ATPase domain (145). Therefore, it will be worthwhile to examine the interaction between BiP and these cofactors upon different AMPylation status.

Additional AMPylated substrates

It is possible that dFic may have more than one substrate and therefore target other proteins in addition to BiP. We did observe more than one band from the S2 cell lyate using anti-AMP-Thr antibody. Moreover, *in vitro* AMPylation with different subcellular fractions revealed a number of bands labeled by dFic enzyme **(Figure 42)**. Interestingly, majority of these bands were found in a P3 fraction enriched with plasma membrane instead of the ER. Therefore, we can speculate that either the substrates are secreted to the cell surface after AMPylation, or they get AMPylated on the cell surface. The latter actually supports the observation that dFic is enriched in the plasma membrane in *Drosophila* glial cells.

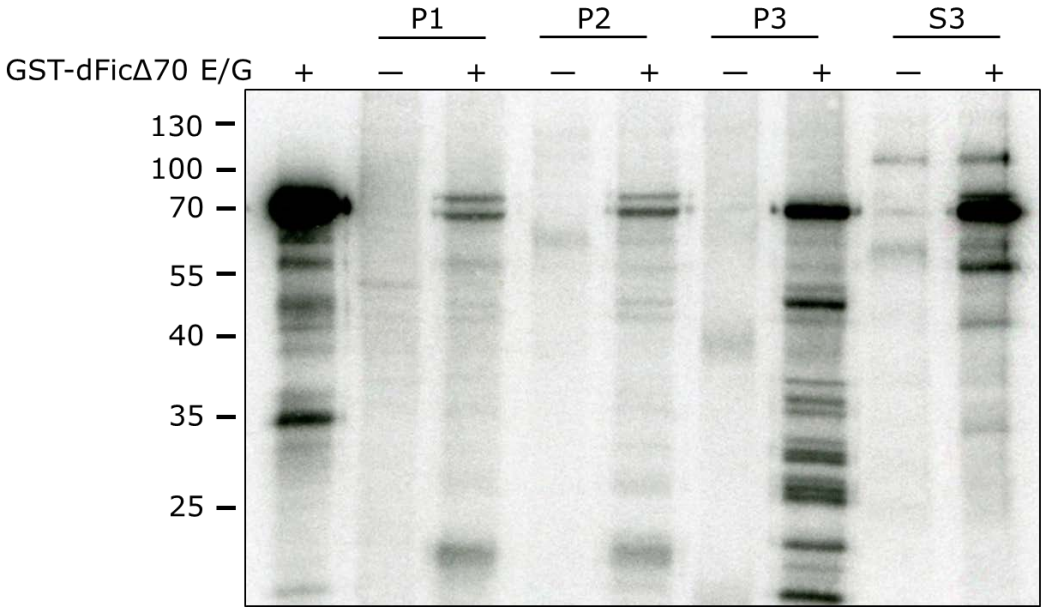

Figure 42. Potential substrates of dFic in the membrane fraction (P3) of S2 cells. Subcellular fractions of S2 cells separated by differential centrifugation were used as substrates for GST-dFicΔ70 E247G in an *in vitro* AMPylation assay. In addition to ~72kDa band found in P1 and P2 fraction, which is predicted to be BiP, many additional bands were observed in the P3 fraction.

We also observed a strong band at ~100kDa recognized by anti-AMP-Tyr antibody from S2 cell P2 fraction which is enriched with ER membranes **(Figure 43)**. The band was absent in the blot with preimmune serum, confirming the specificity of the antibody. The identity of these bands remains to be determined. As a way to identify these putative substrates, we have introduced chemical reporters using click chemistry. An alkyne-derivatized ATP analog can be used as a substrate to AMPylate unknown target proteins, and these proteins can be tagged with either flourophore or biotin through Cu(I)-catalyzed azide-alkyne cycloaddition reaction (151). Indeed, we observed many potential AMPylated substrates with S2 cell subcellular fractions using click chemistry, the profile of which was similar to what we observed using the radiolabeled ATP **(Figure 44)**. We will incorporate the biotin reporter to this assay, enrich the modified proteins with streptavidin beads, and identify them through MS analysis.

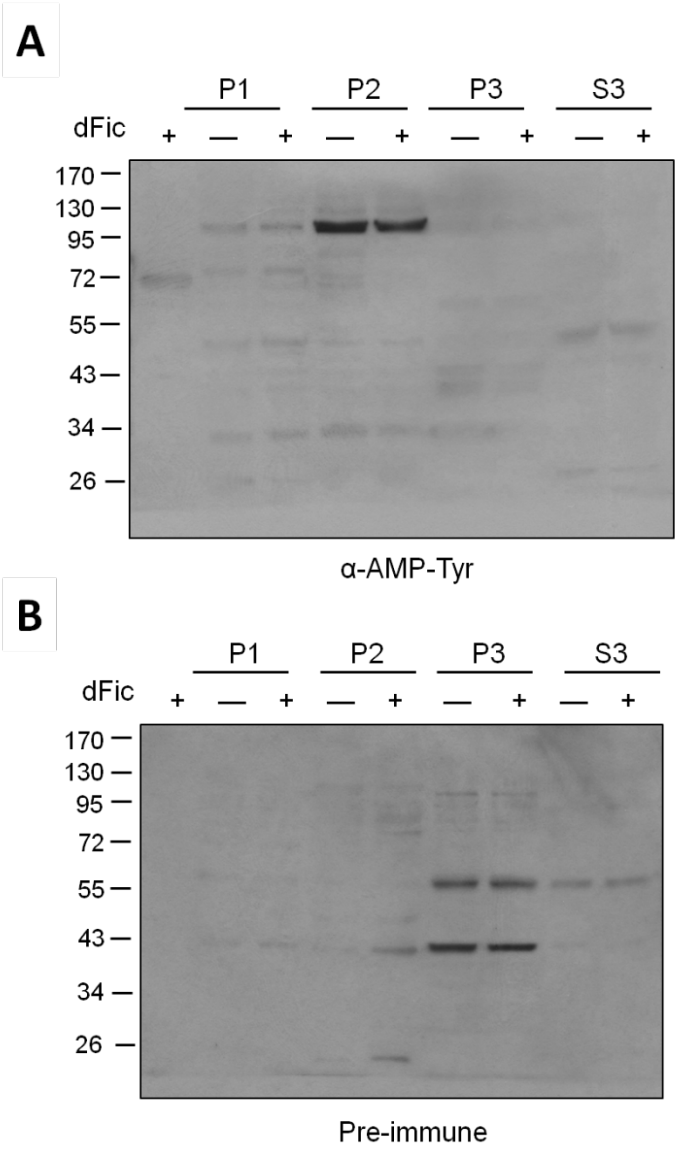

Figure 43. Potential substrate of AMPylation modified on a tyrosine residue from S2 cells. Subcellular fractions of S2 cells separated by differential centrifugation were used as substrates for AMPylation assay using cold ATP and analyzed by anti-AMP-Tyr antibody. Wile-type dFic was used in this assay instead of active E247G mutant.

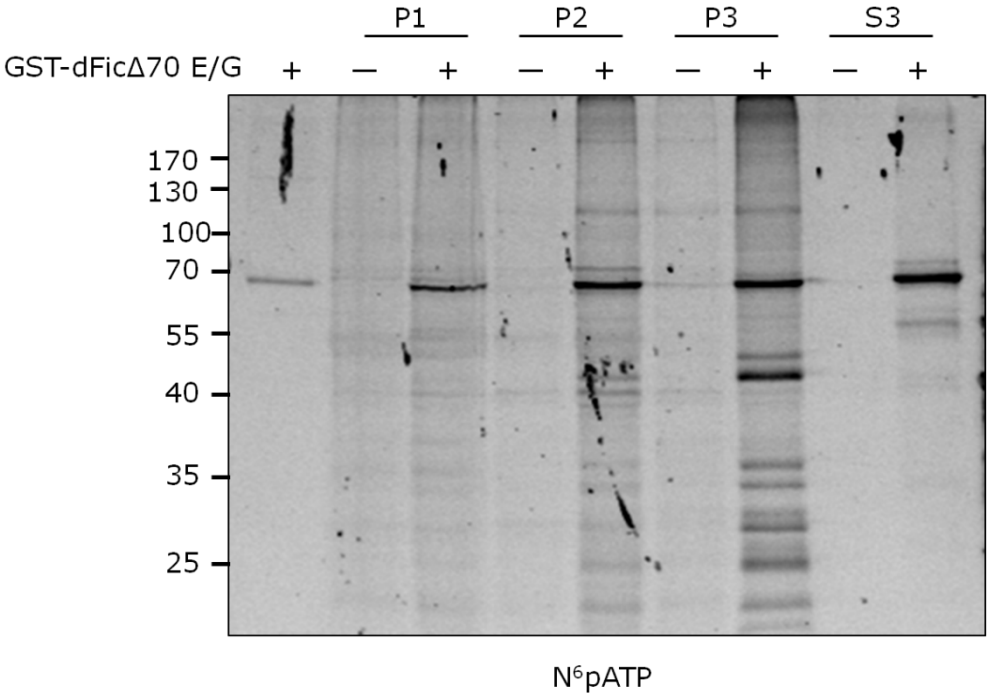

Figure 44. Potential substrates of dFic in the membrane fraction (P3) of S2 cells using click chemistry. Subcellular fractions of S2 cells separated by differential centrifugation were used as substrates for AMPylation assay using N^6ATP. The target proteins were then tagged with fluorophore using click chemistry and visualized by in-gel flurorescence.

In addition to S2 cells, we used fly extracts to search for the additional AMPylated substrates. When wild-type and *dfic* null mutant fly larval extracts were immunoblotted with anti-AMP-Thr antibody, we observed that a protein of ~105kDa was AMPylated only in the wild-type but not in the *dfic* mutant. This potential substrate of dFic was able to be enriched by concanavalin A beads **(Figure 45A)**. When the proteins bound to the beads were eluted and analyzed by silver stain, a single band was observed around 105kDa **(Figure 45B)**. MS analysis identified this protein to be CG14476, an uncharacterized protein which belongs to a glycosyl hydrolase family. It is predicted to have an alpha-glucosidase activity and function in the carbohydrate metabolic process. It needs to be validated whether this protein can be AMPylated and therefore is a legitimate substrate of dFic. Then the molecular function of AMPylation on this protein will be investigated.

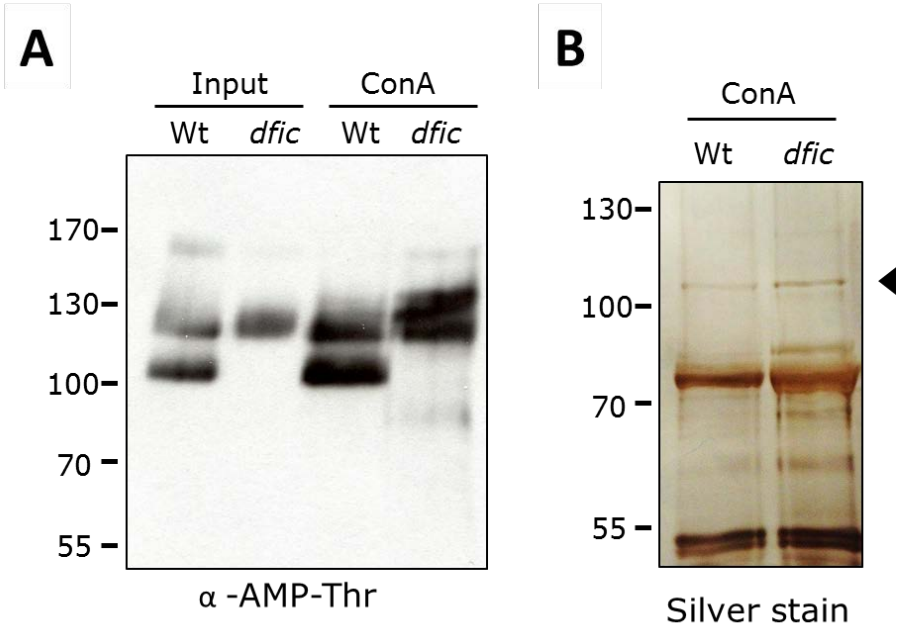

Figure 45. Potential substrate of AMPylation by dFic in flies. (A) Wild-type and *dfic* null mutant fly larva extracts were pulled down with concanavalin A (ConA) beads and blotted with anti-AMP-Thr antibody. (B) The proteins bound to concanavalin A beads were eluted and analyzed by SDS-PAGE silver stain. Arrowhead marks the potential substrate of dFic.

Regulatory mechanism of dFic

How dFic is regulated during ER homeostasis to AMPylate BiP is another avenue worthwhile to explore. We showed that dFic is upregulated during ER stress when BiP rapidly undergoes deAMPylation. Threfore, there is likely to be a regulatory mechanism that keeps the increased level of dFic inactive during ER stress. Once UPR is resolved, this suppression would be released so that dFic can promptly AMPylate and inactivate BiP. Otherwise, the increased amount of BiP staying active can prolong the maturation and secretion of the essential proteins. It is possible that dFic is regulated by other posttranslational modifications or gets translocated in and out of the ER during ER stress. Another interesting possibility is that the autoAMPylation we observe from dFic may play a role in its self-regulation. We have tried to identify the autoAMPylation sites of dFic and HYPE using LC-MS/MS and obtained a few threonine residues as potential hits **(Table 4)**. However, there was no significant decrease in the level of AMPylation when these threonines were mutated into alanines and used in the *in vitro* AMPylation assay **(Figure 46)**. We can try double or triple mutant with different combination of these threonines for the same assay, or express the single mutant proteins in the S2 cells and examine their AMPylation using anti-AMP-Thr antibody. Identifying the automodification sites may provide insight into the autoregulatory mechanism of dFic. Overall, determining the regulation of dFic during ER stress may further our understanding of the critical UPR pathway.

	T108	T181	T196	T357	T445
dFic hit	X		X	X	X
HYPE hit		X	X		
conserved	X	X	X		X

Table 4. Putative autoAMPylation sites of dFic and HYPE. Threonine residues modified in dFic and HYPE are shown, marked by X. The modification sites for HYPE are shown as the representative threonine residues of dFic that correspond to those of HYPE. Whether these threonine residues are conserved in both species is shown in the last row.

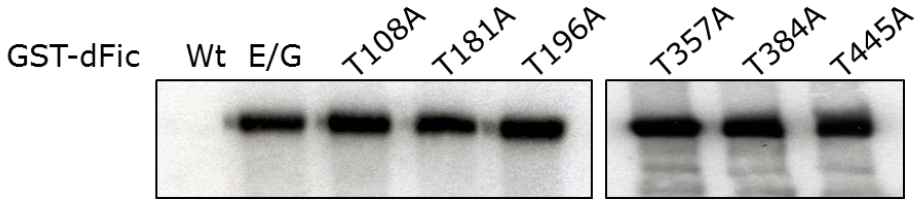

Figure 46. AutoAMPylation of the various dFic autoAMPylation site mutants. The putative modification sites of dFic were mutated into alanine and used in the *in vitro* AMPylation assay.

Cellular function of BiP AMPylation

We speculate that AMPylation may affect the activity of BiP at the molecular level, but what would be the functional outcome of this modification in the cells? Will AMPylated BiP dampen the UPR signaling pathway? To answer these questions, we can simply knockdown dFic and examine the changes in the UPR with or without ER stress. The possible readouts can be a splicing event of XBP1 mRNA or phosphorylation of eIF2α. However, the knockdown attempts in S2 cells have not been successful so far. Therefore, we are trying to analyze the differences in the UPR using wild-type and *dfic* null mutant flies by examining the XBP1 splicing. Another approach to explore the function of AMPylation is to create a knock-in T366A mutation in the BiP gene. We are currently in the process of generating flies in which wild-type BiP is replaced with the T366A mutant. Analyzing the phenotype of these flies will unravel the cellular function of AMPylation on BiP.

Identification of the deAMPylator

Identifying the enzyme that deAMPylates BiP during ER stress will be another exciting discovery. A thorough biochemical approach will be needed to accomplish this aim. We can induce ER stress to S2 cells, obtain the ER fraction, and further purify them by using a serious of different column chromatography. These fractions can then be added to the AMPylated BiP and assessed for their ability to reverse the modification.

Identifying the deAMPylator will not only complete the circuit of reversible AMPylation but also add valuable insight to the regulatory mechanism of BiP during ER homeostasis.

Study of HYPE, a human AMPylator

We showed that human Fic or HYPE also AMPylates human BiP and it is transcriptionally upregulated during ER stress. These data suggest the conservation of the cellular function of BiP AMPylation across species. To explore this hypothesis, we are currently working on the mammalian system to examine the AMPylation of BiP during ER stress. However, we have faced several challenges in the study of HYPE. First, the expression level of HYPE is very low in the widely-established human epithelial cell lines such as HeLa and HEK293T. Second, we currently do not have a reliable antibody for HYPE to detect or enrich it. Therefore, we are currently making cell lines containing genomic, epitope-tagged HYPE (wild-type and H363A mutant) using the CRISPR-Cas9 system. CRISPR-Cas9 system is an emerging genome editing technique which allows rapid and efficient modification of endogenous genes in a wide variety of cell types and organisms (152,153). It utilizes Cas9 endonuclease that is guided by short RNAs to virtually target any specific genome loci. By creating cell lines expressing epitope-tagged HYPE using this system, we can easily detect and enrich HYPE for our biochemical assays. Furthermore, creating cell lines expressing catalytically inactive HYPE (H363A) will allow us to examine the alteration of UPR in the AMPylation-defective cells. We are also creating cell lines that express wild-type and T366A mutant BiP fused to epitope tag.

This will enable the purification of endogenous BiP that are AMPylated or deAMPylated from cells. Importantly, analyzing cells expressing BiP T366A will allow us to assess the effect of AMPylation of BiP on the UPR.

AMPylation of BiP and its implication in cancer

BiP plays an essential role in tumor cell proliferation, survival, angiogenesis, metastasis, and resistance to therapy (99,103-105). Many cancer cells display elevated level of BiP and highly activated UPR that correlate with malignancy and progression of tumor. Hence, BiP is emerging as a biomarker and a potential target in cancer therapy and understanding its regulation will add tremendous insight to such therapeutic strategies. To this end, we are aiming to analyze Fic-mediated AMPylation in cancer cells. We can assess the expression profile of HYPE in a various cancer cell lines. We can also use CRISPR to known cancer cell lines that overexpress BiP, and introduce AMPylation-defective mutations to either HYPE (H363A) or BiP (T366A). This will allow us to examine the effect of BiP AMPylation in cancer cell proliferation, survival, and chemoresistance. Furthermore, identifying the deAMPylator may present another potential target for cancer therapy.

CHAPTER 6
Conclusion

Characterization of dFic AMPylator

Fic domain which mediates AMPylation is widely conserved in different organisms. For our study, we focused on *Drosophila* Fic protein (dFic) to assess its physiological function and identify the relevant substrates. We first analyzed the biochemical function and subcellular localization of the protein in order to optimize the assays we use to search for the substrates. We show that dFic has an AMPylation activity *in vitro* which is dependent on the catalytic motif. The enzymatic activity can be significantly increased upon mutation of the conserved glutamate located in the autoinhibitory motif (E247G). Using different nucleotide substrates in the *in vitro* labeling assay shows that ATP is a preferential substrate of dFic and that AMPylation is likely to be its primary catalytic mechanism.

We also examined the subcellular localization of dFic to narrow down the pool of potential substrates. dFic was shown to localize in the ER from subcellular fractionation and immunohistochemistry. dFic also undergoes N-linked glycosylation which is a common modification found in majority of the ER proteins, and this modification was sensitive to endoglycosidase H. Protease protection assay further confirmed that dFic is a type II transmembrane protein with N-linked glycosylation site and the Fic domain located in the ER lumen. Altogether, these data suggest that the substrate of dFic is also likely to be localized in the ER.

Genetic analysis of dFic using *Drosophila*

One way to explore a function of a protein is to genetically manipulate its expression in a model organism. To investigate the role of dFic, we generated flies with either overexpression or knockout of functional dFic. The transgenic flies with high-level expression of dFic were lethal, which was dependent on a catalytic activity of dFic. This suggests that AMPylation may regulate important cellular processes. Interestingly, *dfic* null mutant flies exhibited blind phenotype with a lack of phototactic behavior. ERG recording of the mutant flies revealed that the synaptic transmission in their eyes were impaired. Among different cell types present in flies eyes, dFic enzymatic activity is required in glial cells for the normal visual neurotransmission. One important role of glia cells in the *Drosophila* lamina is the recycling of histamine, the neurotransmitter released by photoreceptors. The mutant flies showed a significantly reduced level of histamine in the epithelial glia, and their mutant phenotype could be restored by histamine supplement. This indicates that histamine metabolism is one of the physiological processes regulated by the enzymatic activity of dFic in glia cells. dFic was enriched in the surface of glial cells specifically at the capitate projection that epithelial glia cells insert into synaptic endings of photoreceptors. Notably, capitate projections have been speculated to be the site of neurotransmitter recycling into photoreceptor cells. This further suggests the role of AMPylation in regulating histamine metabolism/recycling in the glial cells. Altogether, our genetic studies reveal the physiological function of dFic in

flies and establish a previously unknown regulatory mechanism in visual neurotransmission.

Identification of the AMPylated substrate

The genetic analysis of dFic using flies proposes that the molecular target of dFic could be a component of a visual signaling pathway, possibly a transporter of histamine neurotransmitter. However, as dFic is localized to the ER in the other tissues (fat bodies, eye discs, and salivary glands) in flies and in S2 cells, we postulated that there might be more common and ubiquitous substrates for dFic. Therefore we used S2 cells to identify substrates using biochemical assays. To enrich the substrates that are likely to be localized in the ER, we used ConA that binds to glycoproteins as majority of ER proteins undergo glycosylation. From the whole cell lysate, we found a strong labeling of a ~72kDa protein by dFic enzyme, which was only visible under assay condition with a high concentration of cations that are required for required for ConA binding. This putative substrate for dFic-mediated AMPylation in a pulled-down with ConA appeared as single band on a silver-stained gel. MS analysis revealed that this protein is heat shock protein 70 cognate 3, also known as BiP/GRP78.

In vitro AMPylation assay using recombinant BiP protein and dFic enzyme showed that BiP is AMPylated by dFic on its ATPase domain. PTM analysis by LC-MS/MS and the mutational analysis mapped the *in vivo* AMPylation site to Thr366. The available structure of BiP ATPase domain showed that this Thr366 is located in

proximity to the ATP binding pocket, suggesting that AMPylation of this residue could potentially affect the ATP hydrolysis.

AMPylation of BiP during ER homeostasis

We observed that the level of AMPylated BiP from S2 cells decreases upon ER stress induction and increases upon cycloheximide treatment. When cells undergo ER stress and therefore accumulates misfolded proteins in the ER, BiP needs to be acutely activated in order to trigger the UPR. In contrast, cycloheximide inhibits protein synthesis and reduces the unfolded protein load in the ER, the condition of which BiP needs to be inactivated. Hence, the AMPylation status of BiP inversely correlates with its active state during ER homeostasis, raising the possibility of inhibitory mechanism by AMPylation. We also show that the ATPase domain construct of BiP that represents the inactive state (27-407) is efficiently AMPylated by dFic *in vitro* whereas the active ATPase domain (27-417, containing interdomain linker) is poorly AMPylated. This correlates to our observation in cells that the level of AMPylation was high in normal cells and low upon the increased load of unfolded proteins.

BiP is a stable protein with a long half-life, and the high level of BiP is deleterious to cells as it can delay the maturation and secretion of essential proteins. Therefore, cells require a regulatory mechanism to rapidly control the activity of BiP and maintain ER homeostasis. AMPylation is likely to serve such a regulatory role on BiP depending on the state of newly synthesized/misfolded protein loads in the ER.

This study presents the first substrate of AMPylation by a eukaryotic Fic protein and proposes a new mode of posttranslational regulation of BiP, which is likely to serve a crucial role in maintaining ER protein homeostasis. Our study not only uncovers a novel role of AMPylation in the eukaryotic signaling system, but also provides a potential target for regulating the UPR, an emerging avenue for cancer therapy.

BIBLIOGRAPHY

1. Woolery, A. R., Luong, P., Broberg, C. A., and Orth, K. (2010) AMPylation: Something Old is New Again. *Front Microbiol* **1**, 113
2. Yarbrough, M. L., and Orth, K. (2009) AMPylation is a new post-translational modiFICation. *Nat Chem Biol* **5**, 378-379
3. Shapiro, B. M., Kingdon, H. S., and Stadtman, E. R. (1967) Regulation of glutamine synthetase. VII. Adenylyl glutamine synthetase: a new form of the enzyme with altered regulatory and kinetic properties. *Proc Natl Acad Sci U S A* **58**, 642-649
4. Kingdon, H. S., Shapiro, B. M., and Stadtman, E. R. (1967) Regulation of glutamine synthetase. 8. ATP: glutamine synthetase adenylyltransferase, an enzyme that catalyzes alterations in the regulatory properties of glutamine synthetase. *Proc Natl Acad Sci U S A* **58**, 1703-1710
5. Yarbrough, M. L., Li, Y., Kinch, L. N., Grishin, N. V., Ball, H. L., and Orth, K. (2009) AMPylation of Rho GTPases by Vibrio VopS disrupts effector binding and downstream signaling. *Science* **323**, 269-272
6. Woolery, A. R., Yu, X., LaBaer, J., and Orth, K. (2014) AMPylation of Rho GTPases subverts multiple host signaling processes. *J Biol Chem*
7. Worby, C. A., Mattoo, S., Kruger, R. P., Corbeil, L. B., Koller, A., Mendez, J. C., Zekarias, B., Lazar, C., and Dixon, J. E. (2009) The fic domain: regulation of cell signaling by adenylylation. *Mol Cell* **34**, 93-103
8. Muller, M. P., Peters, H., Blumer, J., Blankenfeldt, W., Goody, R. S., and Itzen, A. (2010) The Legionella effector protein DrrA AMPylates the membrane traffic regulator Rab1b. *Science* **329**, 946-949
9. Jaggi, R., van Heeswijk, W. C., Westerhoff, H. V., Ollis, D. L., and Vasudevan, S. G. (1997) The two opposing activities of adenylyl transferase reside in distinct homologous domains, with intramolecular signal transduction. *EMBO J* **16**, 5562-5571
10. Xu, Y., Carr, P. D., Vasudevan, S. G., and Ollis, D. L. (2010) Structure of the adenylylation domain of E. coli glutamine synthetase adenylyl transferase: evidence for gene duplication and evolution of a new active site. *J Mol Biol* **396**, 773-784
11. Tan, Y., and Luo, Z. Q. (2011) Legionella pneumophila SidD is a deAMPylase that modifies Rab1. *Nature* **475**, 506-509
12. Chen, Y., Tascon, I., Neunuebel, M. R., Pallara, C., Brady, J., Kinch, L. N., Fernandez-Recio, J., Rojas, A. L., Machner, M. P., and Hierro, A. (2013) Structural basis for Rab1 de-AMPylation by the Legionella pneumophila effector SidD. *PLoS Pathog* **9**, e1003382
13. Das, D., Krishna, S. S., McMullan, D., Miller, M. D., Xu, Q., Abdubek, P., Acosta, C., Astakhova, T., Axelrod, H. L., Burra, P., Carlton, D., Chiu, H. J., Clayton, T., Deller, M. C., Duan, L., Elias, Y., Elsliger, M. A., Ernst, D., Feuerhelm, J., Grzechnik, A., Grzechnik, S. K., Hale, J., Han, G. W., Jaroszewski, L., Jin, K. K., Klock, H. E., Knuth, M. W., Kozbial, P., Kumar, A., Marciano, D.,

Morse, A. T., Murphy, K. D., Nigoghossian, E., Okach, L., Oommachen, S., Paulsen, J., Reyes, R., Rife, C. L., Sefcovic, N., Tien, H., Trame, C. B., Trout, C. V., van den Bedem, H., Weekes, D., White, A., Hodgson, K. O., Wooley, J., Deacon, A. M., Godzik, A., Lesley, S. A., and Wilson, I. A. (2009) Crystal structure of the Fic (Filamentation induced by cAMP) family protein SO4266 (gi|24375750) from Shewanella oneidensis MR-1 at 1.6 A resolution. *Proteins* **75**, 264-271

14. Luong, P., Kinch, L. N., Brautigam, C. A., Grishin, N. V., Tomchick, D. R., and Orth, K. (2010) Kinetic and structural insights into the mechanism of AMPylation by VopS Fic domain. *J Biol Chem* **285**, 20155-20163
15. Xiao, J., Worby, C. A., Mattoo, S., Sankaran, B., and Dixon, J. E. (2010) Structural basis of Fic-mediated adenylylation. *Nat Struct Mol Biol* **17**, 1004-1010
16. Palanivelu, D. V., Goepfert, A., Meury, M., Guye, P., Dehio, C., and Schirmer, T. (2011) Fic domain-catalyzed adenylylation: insight provided by the structural analysis of the type IV secretion system effector BepA. *Protein Sci* **20**, 492-499
17. Kinch, L. N., Yarbrough, M. L., Orth, K., and Grishin, N. V. (2009) Fido, a novel AMPylation domain common to fic, doc, and AvrB. *PLoS One* **4**, e5818
18. Bunney, T. D., Cole, A. R., Broncel, M., Esposito, D., Tate, E. W., and Katan, M. (2014) Crystal Structure of the Human, FIC-Domain Containing Protein HYPE and Implications for Its Functions. *Structure*
19. Engel, P., Goepfert, A., Stanger, F. V., Harms, A., Schmidt, A., Schirmer, T., and Dehio, C. (2012) Adenylylation control by intra- or intermolecular active-site obstruction in Fic proteins. *Nature* **482**, 107-110
20. Mukherjee, S., Liu, X., Arasaki, K., McDonough, J., Galan, J. E., and Roy, C. R. (2011) Modulation of Rab GTPase function by a protein phosphocholine transferase. *Nature* **477**, 103-106
21. Campanacci, V., Mukherjee, S., Roy, C. R., and Cherfils, J. (2013) Structure of the Legionella effector AnkX reveals the mechanism of phosphocholine transfer by the FIC domain. *EMBO J* **32**, 1469-1477
22. Feng, F., Yang, F., Rong, W., Wu, X., Zhang, J., Chen, S., He, C., and Zhou, J. M. (2012) A Xanthomonas uridine 5'-monophosphate transferase inhibits plant immune kinases. *Nature* **485**, 114-118
23. Mukherjee, S., Keitany, G., Li, Y., Wang, Y., Ball, H. L., Goldsmith, E. J., and Orth, K. (2006) Yersinia YopJ acetylates and inhibits kinase activation by blocking phosphorylation. *Science* **312**, 1211-1214
24. Wang, X., and Wood, T. K. (2011) Toxin-antitoxin systems influence biofilm and persister cell formation and the general stress response. *Appl Environ Microbiol* **77**, 5577-5583
25. Castro-Roa, D., Garcia-Pino, A., De Gieter, S., van Nuland, N. A., Loris, R., and Zenkin, N. (2013) The Fic protein Doc uses an inverted substrate to phosphorylate and inactivate EF-Tu. *Nat Chem Biol* **9**, 811-817
26. Cruz, J. W., Rothenbacher, F. P., Maehigashi, T., Lane, W. S., Dunham, C. M., and Woychik, N. A. (2014) Doc toxin is a kinase that inactivates elongation factor Tu. *J Biol Chem* **289**, 7788-7798

27. Garcia-Pino, A., Zenkin, N., and Loris, R. (2014) The many faces of Fic: structural and functional aspects of Fic enzymes. *Trends Biochem Sci* **39**, 121-129
28. Chevet, E., Cameron, P. H., Pelletier, M. F., Thomas, D. Y., and Bergeron, J. J. (2001) The endoplasmic reticulum: integration of protein folding, quality control, signaling and degradation. *Curr Opin Struct Biol* **11**, 120-124
29. Kleizen, B., and Braakman, I. (2004) Protein folding and quality control in the endoplasmic reticulum. *Curr Opin Cell Biol* **16**, 343-349
30. Brodsky, J. L., and Skach, W. R. (2011) Protein folding and quality control in the endoplasmic reticulum: Recent lessons from yeast and mammalian cell systems. *Curr Opin Cell Biol* **23**, 464-475
31. Brodsky, J. L., and McCracken, A. A. (1997) ER-associated and proteasomemediated protein degradation: how two topologically restricted events came together. *Trends Cell Biol* **7**, 151-156
32. Vembar, S. S., and Brodsky, J. L. (2008) One step at a time: endoplasmic reticulum-associated degradation. *Nat Rev Mol Cell Biol* **9**, 944-957
33. Ruggiano, A., Foresti, O., and Carvalho, P. (2014) Quality control: ER-associated degradation: protein quality control and beyond. *J Cell Biol* **204**, 869-879
34. Olzmann, J. A., Kopito, R. R., and Christianson, J. C. (2013) The mammalian endoplasmic reticulum-associated degradation system. *Cold Spring Harb Perspect Biol* **5**
35. Hiller, M. M., Finger, A., Schweiger, M., and Wolf, D. H. (1996) ER degradation of a misfolded luminal protein by the cytosolic ubiquitin-proteasome pathway. *Science* **273**, 1725-1728
36. Smith, M. H., Ploegh, H. L., and Weissman, J. S. (2011) Road to ruin: targeting proteins for degradation in the endoplasmic reticulum. *Science* **334**, 1086-1090
37. Haas, I. G. (1994) BiP (GRP78), an essential hsp70 resident protein in the endoplasmic reticulum. *Experientia* **50**, 1012-1020
38. Gething, M. J. (1999) Role and regulation of the ER chaperone BiP. *Semin Cell Dev Biol* **10**, 465-472
39. Hamman, B. D., Hendershot, L. M., and Johnson, A. E. (1998) BiP maintains the permeability barrier of the ER membrane by sealing the lumenal end of the translocon pore before and early in translocation. *Cell* **92**, 747-758
40. Corsi, A. K., and Schekman, R. (1997) The lumenal domain of Sec63p stimulates the ATPase activity of BiP and mediates BiP recruitment to the translocon in Saccharomyces cerevisiae. *J Cell Biol* **137**, 1483-1493
41. McClellan, A. J., Endres, J. B., Vogel, J. P., Palazzi, D., Rose, M. D., and Brodsky, J. L. (1998) Specific molecular chaperone interactions and an ATP-dependent conformational change are required during posttranslational protein translocation into the yeast ER. *Mol Biol Cell* **9**, 3533-3545
42. Brodsky, J. L., Werner, E. D., Dubas, M. E., Goeckeler, J. L., Kruse, K. B., and McCracken, A. A. (1999) The requirement for molecular chaperones during endoplasmic reticulum-associated protein degradation demonstrates that protein export and import are mechanistically distinct. *J Biol Chem* **274**, 3453-3460

43. Plemper, R. K., Bohmler, S., Bordallo, J., Sommer, T., and Wolf, D. H. (1997) Mutant analysis links the translocon and BiP to retrograde protein transport for ER degradation. *Nature* **388**, 891-895
44. McCracken, A. A., and Brodsky, J. L. (2003) Evolving questions and paradigm shifts in endoplasmic-reticulum-associated degradation (ERAD). *Bioessays* **25**, 868-877
45. Tsai, B., Ye, Y., and Rapoport, T. A. (2002) Retro-translocation of proteins from the endoplasmic reticulum into the cytosol. *Nat Rev Mol Cell Biol* **3**, 246-255
46. Gardner, B. M., Pincus, D., Gotthardt, K., Gallagher, C. M., and Walter, P. (2013) Endoplasmic reticulum stress sensing in the unfolded protein response. *Cold Spring Harb Perspect Biol* **5**, a013169
47. Mori, K. (2009) Signalling pathways in the unfolded protein response: development from yeast to mammals. *J Biochem* **146**, 743-750
48. Bukau, B., and Horwich, A. L. (1998) The Hsp70 and Hsp60 chaperone machines. *Cell* **92**, 351-366
49. Zuiderweg, E. R., Bertelsen, E. B., Rousaki, A., Mayer, M. P., Gestwicki, J. E., and Ahmad, A. (2013) Allostery in the Hsp70 chaperone proteins. *Top Curr Chem* **328**, 99-153
50. Kim, Y. E., Hipp, M. S., Bracher, A., Hayer-Hartl, M., and Hartl, F. U. (2013) Molecular chaperone functions in protein folding and proteostasis. *Annu Rev Biochem* **82**, 323-355
51. Bertelsen, E. B., Chang, L., Gestwicki, J. E., and Zuiderweg, E. R. (2009) Solution conformation of wild-type E. coli Hsp70 (DnaK) chaperone complexed with ADP and substrate. *Proc Natl Acad Sci U S A* **106**, 8471-8476
52. Mapa, K., Sikor, M., Kudryavtsev, V., Waegemann, K., Kalinin, S., Seidel, C. A., Neupert, W., Lamb, D. C., and Mokranjac, D. (2010) The conformational dynamics of the mitochondrial Hsp70 chaperone. *Mol Cell* **38**, 89-100
53. Schweizer, R. S., Aponte, R. A., Zimmermann, S., Weber, A., and Reinstein, J. (2011) Fine tuning of a biological machine: DnaK gains improved chaperone activity by altered allosteric communication and substrate binding. *Chembiochem* **12**, 1559-1573
54. Swain, J. F., Dinler, G., Sivendran, R., Montgomery, D. L., Stotz, M., and Gierasch, L. M. (2007) Hsp70 chaperone ligands control domain association via an allosteric mechanism mediated by the interdomain linker. *Mol Cell* **26**, 27-39
55. Smock, R. G., Rivoire, O., Russ, W. P., Swain, J. F., Leibler, S., Ranganathan, R., and Gierasch, L. M. (2010) An interdomain sector mediating allostery in Hsp70 molecular chaperones. *Mol Syst Biol* **6**, 414
56. Zhuravleva, A., and Gierasch, L. M. (2011) Allosteric signal transmission in the nucleotide-binding domain of 70-kDa heat shock protein (Hsp70) molecular chaperones. *Proc Natl Acad Sci U S A* **108**, 6987-6992
57. Zhuravleva, A., Clerico, E. M., and Gierasch, L. M. (2012) An interdomain energetic tug-of-war creates the allosterically active state in Hsp70 molecular chaperones. *Cell* **151**, 1296-1307

58. Walter, P., and Ron, D. (2011) The unfolded protein response: from stress pathway to homeostatic regulation. *Science* **334**, 1081-1086
59. Harding, H. P., Zhang, Y., and Ron, D. (1999) Protein translation and folding are coupled by an endoplasmic-reticulum-resident kinase. *Nature* **397**, 271-274
60. Jackson, R. J., Hellen, C. U., and Pestova, T. V. (2010) The mechanism of eukaryotic translation initiation and principles of its regulation. *Nat Rev Mol Cell Biol* **11**, 113-127
61. Harding, H. P., Novoa, I., Zhang, Y., Zeng, H., Wek, R., Schapira, M., and Ron, D. (2000) Regulated translation initiation controls stress-induced gene expression in mammalian cells. *Mol Cell* **6**, 1099-1108
62. Scheuner, D., Song, B., McEwen, E., Liu, C., Laybutt, R., Gillespie, P., Saunders, T., Bonner-Weir, S., and Kaufman, R. J. (2001) Translational control is required for the unfolded protein response and in vivo glucose homeostasis. *Mol Cell* **7**, 1165-1176
63. Novoa, I., Zeng, H., Harding, H. P., and Ron, D. (2001) Feedback inhibition of the unfolded protein response by GADD34-mediated dephosphorylation of eIF2alpha. *J Cell Biol* **153**, 1011-1022
64. Wang, X. Z., Kuroda, M., Sok, J., Batchvarova, N., Kimmel, R., Chung, P., Zinszner, H., and Ron, D. (1998) Identification of novel stress-induced genes downstream of chop. *EMBO J* **17**, 3619-3630
65. Zinszner, H., Kuroda, M., Wang, X., Batchvarova, N., Lightfoot, R. T., Remotti, H., Stevens, J. L., and Ron, D. (1998) CHOP is implicated in programmed cell death in response to impaired function of the endoplasmic reticulum. *Genes Dev* **12**, 982-995
66. Haze, K., Yoshida, H., Yanagi, H., Yura, T., and Mori, K. (1999) Mammalian transcription factor ATF6 is synthesized as a transmembrane protein and activated by proteolysis in response to endoplasmic reticulum stress. *Mol Biol Cell* **10**, 3787-3799
67. Adachi, Y., Yamamoto, K., Okada, T., Yoshida, H., Harada, A., and Mori, K. (2008) ATF6 is a transcription factor specializing in the regulation of quality control proteins in the endoplasmic reticulum. *Cell Struct Funct* **33**, 75-89
68. Bommiasamy, H., Back, S. H., Fagone, P., Lee, K., Meshinchi, S., Vink, E., Sriburi, R., Frank, M., Jackowski, S., Kaufman, R. J., and Brewer, J. W. (2009) ATF6alpha induces XBP1-independent expansion of the endoplasmic reticulum. *J Cell Sci* **122**, 1626-1636
69. Zhang, K., and Kaufman, R. J. (2008) From endoplasmic-reticulum stress to the inflammatory response. *Nature* **454**, 455-462
70. Leustek, T., Toledo, H., Brot, N., and Weissbach, H. (1991) Calcium-dependent autophosphorylation of the glucose-regulated protein, Grp78. *Arch Biochem Biophys* **289**, 256-261
71. Hendershot, L. M., Ting, J., and Lee, A. S. (1988) Identity of the immunoglobulin heavy-chain-binding protein with the 78,000-dalton glucose-regulated protein and the role of posttranslational modifications in its binding function. *Mol Cell Biol* **8**, 4250-4256

72. Gaut, J. R., and Hendershot, L. M. (1993) The immunoglobulin-binding protein in vitro autophosphorylation site maps to a threonine within the ATP binding cleft but is not a detectable site of in vivo phosphorylation. *J Biol Chem* **268**, 12691-12698
73. Gaut, J. R. (1997) In vivo threonine phosphorylation of immunoglobulin binding protein (BiP) maps to its protein binding domain. *Cell Stress Chaperones* **2**, 252-262
74. Carlsson, L., and Lazarides, E. (1983) ADP-ribosylation of the Mr 83,000 stress-inducible and glucose-regulated protein in avian and mammalian cells: modulation by heat shock and glucose starvation. *Proc Natl Acad Sci U S A* **80**, 4664-4668
75. Leno, G. H., and Ledford, B. E. (1990) Reversible ADP-ribosylation of the 78 kDa glucose-regulated protein. *FEBS Lett* **276**, 29-33
76. Ledford, B. E., and Leno, G. H. (1994) ADP-ribosylation of the molecular chaperone GRP78/BiP. *Mol Cell Biochem* **138**, 141-148
77. Chambers, J. E., Petrova, K., Tomba, G., Vendruscolo, M., and Ron, D. (2012) ADP ribosylation adapts an ER chaperone response to short-term fluctuations in unfolded protein load. *J Cell Biol* **198**, 371-385
78. Pfaffenbach, K. T., and Lee, A. S. (2011) The critical role of GRP78 in physiologic and pathologic stress. *Curr Opin Cell Biol* **23**, 150-156
79. Wang, M., Wey, S., Zhang, Y., Ye, R., and Lee, A. S. (2009) Role of the unfolded protein response regulator GRP78/BiP in development, cancer, and neurological disorders. *Antioxid Redox Signal* **11**, 2307-2316
80. Mei, Y., Thompson, M. D., Cohen, R. A., and Tong, X. (2013) Endoplasmic Reticulum Stress and Related Pathological Processes. *J Pharmacol Biomed Anal* **1**, 1000107
81. Kim, S. K., Kim, Y. K., and Lee, A. S. (1990) Expression of the glucose-regulated proteins (GRP94 and GRP78) in differentiated and undifferentiated mouse embryonic cells and the use of the GRP78 promoter as an expression system in embryonic cells. *Differentiation* **42**, 153-159
82. Barnes, J. A., and Smoak, I. W. (2000) Glucose-regulated protein 78 (GRP78) is elevated in embryonic mouse heart and induced following hypoglycemic stress. *Anat Embryol (Berl)* **202**, 67-74
83. Luo, S., Mao, C., Lee, B., and Lee, A. S. (2006) GRP78/BiP is required for cell proliferation and protecting the inner cell mass from apoptosis during early mouse embryonic development. *Mol Cell Biol* **26**, 5688-5697
84. Zhang, X., Szabo, E., Michalak, M., and Opas, M. (2007) Endoplasmic reticulum stress during the embryonic development of the central nervous system in the mouse. *Int J Dev Neurosci* **25**, 455-463
85. Henis-Korenblit, S., Zhang, P., Hansen, M., McCormick, M., Lee, S. J., Cary, M., and Kenyon, C. (2010) Insulin/IGF-1 signaling mutants reprogram ER stress response regulators to promote longevity. *Proc Natl Acad Sci U S A* **107**, 9730-9735

86. Paz Gavilan, M., Vela, J., Castano, A., Ramos, B., del Rio, J. C., Vitorica, J., and Ruano, D. (2006) Cellular environment facilitates protein accumulation in aged rat hippocampus. *Neurobiol Aging* **27**, 973-982
87. Naidoo, N., Ferber, M., Master, M., Zhu, Y., and Pack, A. I. (2008) Aging impairs the unfolded protein response to sleep deprivation and leads to proapoptotic signaling. *J Neurosci* **28**, 6539-6548
88. Rabek, J. P., Boylston, W. H., 3rd, and Papaconstantinou, J. (2003) Carbonylation of ER chaperone proteins in aged mouse liver. *Biochem Biophys Res Commun* **305**, 566-572
89. Nuss, J. E., Choksi, K. B., DeFord, J. H., and Papaconstantinou, J. (2008) Decreased enzyme activities of chaperones PDI and BiP in aged mouse livers. *Biochem Biophys Res Commun* **365**, 355-361
90. Erickson, R. R., Dunning, L. M., and Holtzman, J. L. (2006) The effect of aging on the chaperone concentrations in the hepatic, endoplasmic reticulum of male rats: the possible role of protein misfolding due to the loss of chaperones in the decline in physiological function seen with age. *J Gerontol A Biol Sci Med Sci* **61**, 435-443
91. Rao, R. V., and Bredesen, D. E. (2004) Misfolded proteins, endoplasmic reticulum stress and neurodegeneration. *Curr Opin Cell Biol* **16**, 653-662
92. Paschen, W., and Mengesdorf, T. (2005) Endoplasmic reticulum stress response and neurodegeneration. *Cell Calcium* **38**, 409-415
93. Lindholm, D., Wootz, H., and Korhonen, L. (2006) ER stress and neurodegenerative diseases. *Cell Death Differ* **13**, 385-392
94. Scheper, W., and Hoozemans, J. J. (2009) Endoplasmic reticulum protein quality control in neurodegenerative disease: the good, the bad and the therapy. *Curr Med Chem* **16**, 615-626
95. Weng, W. C., Lee, W. T., Hsu, W. M., Chang, B. E., and Lee, H. (2011) Role of glucose-regulated Protein 78 in embryonic development and neurological disorders. *J Formos Med Assoc* **110**, 428-437
96. Wang, M., Ye, R., Barron, E., Baumeister, P., Mao, C., Luo, S., Fu, Y., Luo, B., Dubeau, L., Hinton, D. R., and Lee, A. S. (2010) Essential role of the unfolded protein response regulator GRP78/BiP in protection from neuronal apoptosis. *Cell Death Differ* **17**, 488-498
97. Anttonen, A. K., Mahjneh, I., Hamalainen, R. H., Lagier-Tourenne, C., Kopra, O., Waris, L., Anttonen, M., Joensuu, T., Kalimo, H., Paetau, A., Tranebjaerg, L., Chaigne, D., Koenig, M., Eeg-Olofsson, O., Udd, B., Somer, M., Somer, H., and Lehesjoki, A. E. (2005) The gene disrupted in Marinesco-Sjogren syndrome encodes SIL1, an HSPA5 cochaperone. *Nat Genet* **37**, 1309-1311
98. Senderek, J., Krieger, M., Stendel, C., Bergmann, C., Moser, M., Breitbach-Faller, N., Rudnik-Schoneborn, S., Blaschek, A., Wolf, N. I., Harting, I., North, K., Smith, J., Muntoni, F., Brockington, M., Quijano-Roy, S., Renault, F., Herrmann, R., Hendershot, L. M., Schroder, J. M., Lochmuller, H., Topaloglu, H., Voit, T., Weis, J., Ebinger, F., and Zerres, K. (2005) Mutations in SIL1 cause

Marinesco-Sjogren syndrome, a cerebellar ataxia with cataract and myopathy. *Nat Genet* **37**, 1312-1314

99. Zhang, L. H., and Zhang, X. (2010) Roles of GRP78 in physiology and cancer. *J Cell Biochem* **110**, 1299-1305
100. Lee, E., Nichols, P., Spicer, D., Groshen, S., Yu, M. C., and Lee, A. S. (2006) GRP78 as a novel predictor of responsiveness to chemotherapy in breast cancer. *Cancer Res* **66**, 7849-7853
101. Zheng, H. C., Takahashi, H., Li, X. H., Hara, T., Masuda, S., Guan, Y. F., and Takano, Y. (2008) Overexpression of GRP78 and GRP94 are markers for aggressive behavior and poor prognosis in gastric carcinomas. *Hum Pathol* **39**, 1042-1049
102. Su, R., Li, Z., Li, H., Song, H., Bao, C., Wei, J., and Cheng, L. (2010) Grp78 promotes the invasion of hepatocellular carcinoma. *BMC Cancer* **10**, 20
103. Li, Z., and Li, Z. (2012) Glucose regulated protein 78: a critical link between tumor microenvironment and cancer hallmarks. *Biochim Biophys Acta* **1826**, 13-22
104. Virrey, J. J., Dong, D., Stiles, C., Patterson, J. B., Pen, L., Ni, M., Schonthal, A. H., Chen, T. C., Hofman, F. M., and Lee, A. S. (2008) Stress chaperone GRP78/BiP confers chemoresistance to tumor-associated endothelial cells. *Mol Cancer Res* **6**, 1268-1275
105. Roller, C., and Maddalo, D. (2013) The Molecular Chaperone GRP78/BiP in the Development of Chemoresistance: Mechanism and Possible Treatment. *Front Pharmacol* **4**, 10
106. Arap, M. A., Lahdenranta, J., Mintz, P. J., Hajitou, A., Sarkis, A. S., Arap, W., and Pasqualini, R. (2004) Cell surface expression of the stress response chaperone GRP78 enables tumor targeting by circulating ligands. *Cancer Cell* **6**, 275-284
107. Zhang, Y., Liu, R., Ni, M., Gill, P., and Lee, A. S. (2010) Cell surface relocalization of the endoplasmic reticulum chaperone and unfolded protein response regulator GRP78/BiP. *J Biol Chem* **285**, 15065-15075
108. Misra, U. K., Deedwania, R., and Pizzo, S. V. (2006) Activation and cross-talk between Akt, NF-kappaB, and unfolded protein response signaling in 1-LN prostate cancer cells consequent to ligation of cell surface-associated GRP78. *J Biol Chem* **281**, 13694-13707
109. Burikhanov, R., Zhao, Y., Goswami, A., Qiu, S., Schwarze, S. R., and Rangnekar, V. M. (2009) The tumor suppressor Par-4 activates an extrinsic pathway for apoptosis. *Cell* **138**, 377-388
110. Shani, G., Fischer, W. H., Justice, N. J., Kelber, J. A., Vale, W., and Gray, P. C. (2008) GRP78 and Cripto form a complex at the cell surface and collaborate to inhibit transforming growth factor beta signaling and enhance cell growth. *Mol Cell Biol* **28**, 666-677
111. Misra, U. K., and Pizzo, S. V. (2010) Modulation of the unfolded protein response in prostate cancer cells by antibody-directed against the carboxyl-terminal domain of GRP78. *Apoptosis* **15**, 173-182

112. Ceriani, M. F. (2007) Basic protocols for Drosophila S2 cell line: maintenance and transfection. *Methods Mol Biol* **362**, 415-422
113. Hao, Y. H., Chuang, T., Ball, H. L., Luong, P., Li, Y., Flores-Saaib, R. D., and Orth, K. (2011) Characterization of a rabbit polyclonal antibody against threonine-AMPylation. *J Biotechnol* **151**, 251-254
114. Williamson, W. R., Wang, D., Haberman, A. S., and Hiesinger, P. R. (2010) A dual function of V0-ATPase a1 provides an endolysosomal degradation mechanism in Drosophila melanogaster photoreceptors. *J Cell Biol* **189**, 885-899
115. Sharma, A., Mariappan, M., Appathurai, S., and Hegde, R. S. (2010) In vitro dissection of protein translocation into the mammalian endoplasmic reticulum. *Methods Mol Biol* **619**, 339-363
116. Sunio, A., Metcalf, A. B., and Kramer, H. (1999) Genetic dissection of endocytic trafficking in Drosophila using a horseradish peroxidase-bride of sevenless chimera: hook is required for normal maturation of multivesicular endosomes. *Mol Biol Cell* **10**, 847-859
117. Fabian-Fine, R., Verstreken, P., Hiesinger, P. R., Horne, J. A., Kostyleva, R., Zhou, Y., Bellen, H. J., and Meinertzhagen, I. A. (2003) Endophilin promotes a late step in endocytosis at glial invaginations in Drosophila photoreceptor terminals. *J Neurosci* **23**, 10732-10744
118. Benzer, S. (1967) BEHAVIORAL MUTANTS OF Drosophila ISOLATED BY COUNTERCURRENT DISTRIBUTION. *Proc Natl Acad Sci U S A* **58**, 1112-1119
119. Melzig, J., Buchner, S., Wiebel, F., Wolf, R., Burg, M., Pak, W. L., and Buchner, E. (1996) Genetic depletion of histamine from the nervous system of Drosophila eliminates specific visual and mechanosensory behavior. *J Comp Physiol A* **179**, 763-773
120. Alawi, A. A., and Pak, W. L. (1971) On-transient of insect electroretinogram: its cellular origin. *Science* **172**, 1055-1057
121. Heisenberg, M. (1971) Separation of receptor and lamina potentials in the electroretinogram of normal and mutant Drosophila. *J Exp Biol* **55**, 85-100
122. Zhu, Y., Nern, A., Zipursky, S. L., and Frye, M. A. (2009) Peripheral visual circuits functionally segregate motion and phototaxis behaviors in the fly. *Curr Biol* **19**, 613-619
123. Gavin, B. A., Arruda, S. E., and Dolph, P. J. (2007) The role of carcinine in signaling at the Drosophila photoreceptor synapse. *PLoS Genet* **3**, e206
124. Melzig, J., Burg, M., Gruhn, M., Pak, W. L., and Buchner, E. (1998) Selective histamine uptake rescues photo- and mechanoreceptor function of histidine decarboxylase-deficient Drosophila mutant. *J Neurosci* **18**, 7160-7166
125. Wagner, S., Heseding, C., Szlachta, K., True, J. R., Prinz, H., and Hovemann, B. T. (2007) Drosophila photoreceptors express cysteine peptidase tan. *J Comp Neurol* **500**, 601-611
126. Burg, M. G., Sarthy, P. V., Koliantz, G., and Pak, W. L. (1993) Genetic and molecular identification of a Drosophila histidine decarboxylase gene required in photoreceptor transmitter synthesis. *EMBO J* **12**, 911-919

127. Borycz, J. A., Borycz, J., Kubow, A., Kostyleva, R., and Meinertzhagen, I. A. (2005) Histamine compartments of the Drosophila brain with an estimate of the quantum content at the photoreceptor synapse. *J Neurophysiol* **93**, 1611-1619
128. Richardt, A., Rybak, J., Stortkuhl, K. F., Meinertzhagen, I. A., and Hovemann, B. T. (2002) Ebony protein in the Drosophila nervous system: optic neuropile expression in glial cells. *J Comp Neurol* **452**, 93-102
129. Richardt, A., Kemme, T., Wagner, S., Schwarzer, D., Marahiel, M. A., and Hovemann, B. T. (2003) Ebony, a novel nonribosomal peptide synthetase for beta-alanine conjugation with biogenic amines in Drosophila. *J Biol Chem* **278**, 41160-41166
130. Romero-Calderon, R., Uhlenbrock, G., Borycz, J., Simon, A. F., Grygoruk, A., Yee, S. K., Shyer, A., Ackerson, L. C., Maidment, N. T., Meinertzhagen, I. A., Hovemann, B. T., and Krantz, D. E. (2008) A glial variant of the vesicular monoamine transporter is required to store histamine in the Drosophila visual system. *PLoS Genet* **4**, e1000245
131. Edwards, T. N., and Meinertzhagen, I. A. (2010) The functional organisation of glia in the adult brain of Drosophila and other insects. *Prog Neurobiol* **90**, 471-497
132. Borycz, J., Borycz, J. A., Loubani, M., and Meinertzhagen, I. A. (2002) tan and ebony genes regulate a novel pathway for transmitter metabolism at fly photoreceptor terminals. *J Neurosci* **22**, 10549-10557
133. Stark, W. S., and Carlson, S. D. (1986) Ultrastructure of capitate projections in the optic neuropil of Diptera. *Cell Tissue Res* **246**, 481-486
134. Rahman, M., Ham, H., Liu, X., Sugiura, Y., Orth, K., and Kramer, H. (2012) Visual neurotransmission in Drosophila requires expression of Fic in glial capitate projections. *Nat Neurosci* **15**, 871-875
135. Munro, S., and Pelham, H. R. (1986) An Hsp70-like protein in the ER: identity with the 78 kd glucose-regulated protein and immunoglobulin heavy chain binding protein. *Cell* **46**, 291-300
136. Bukau, B., Weissman, J., and Horwich, A. (2006) Molecular chaperones and protein quality control. *Cell* **125**, 443-451
137. Li, J., and Lee, A. S. (2006) Stress induction of GRP78/BiP and its role in cancer. *Curr Mol Med* **6**, 45-54
138. Koch, G. L. (1990) The endoplasmic reticulum and calcium storage. *Bioessays* **12**, 527-531
139. Sriram, M., Osipiuk, J., Freeman, B., Morimoto, R., and Joachimiak, A. (1997) Human Hsp70 molecular chaperone binds two calcium ions within the ATPase domain. *Structure* **5**, 403-414
140. Dorner, A. J., Wasley, L. C., and Kaufman, R. J. (1992) Overexpression of GRP78 mitigates stress induction of glucose regulated proteins and blocks secretion of selective proteins in Chinese hamster ovary cells. *EMBO J* **11**, 1563-1571

141. Feder, J. H., Rossi, J. M., Solomon, J., Solomon, N., and Lindquist, S. (1992) The consequences of expressing hsp70 in Drosophila cells at normal temperatures. *Genes Dev* **6**, 1402-1413
142. Chevalier, M., Rhee, H., Elguindi, E. C., and Blond, S. Y. (2000) Interaction of murine BiP/GRP78 with the DnaJ homologue MTJ1. *J Biol Chem* **275**, 19620-19627
143. Shen, Y., Meunier, L., and Hendershot, L. M. (2002) Identification and characterization of a novel endoplasmic reticulum (ER) DnaJ homologue, which stimulates ATPase activity of BiP in vitro and is induced by ER stress. *J Biol Chem* **277**, 15947-15956
144. Qiu, X. B., Shao, Y. M., Miao, S., and Wang, L. (2006) The diversity of the DnaJ/Hsp40 family, the crucial partners for Hsp70 chaperones. *Cell Mol Life Sci* **63**, 2560-2570
145. Chung, K. T., Shen, Y., and Hendershot, L. M. (2002) BAP, a mammalian BiP-associated protein, is a nucleotide exchange factor that regulates the ATPase activity of BiP. *J Biol Chem* **277**, 47557-47563
146. Dragovic, Z., Broadley, S. A., Shomura, Y., Bracher, A., and Hartl, F. U. (2006) Molecular chaperones of the Hsp110 family act as nucleotide exchange factors of Hsp70s. *EMBO J* **25**, 2519-2528
147. Andreasson, C., Rampelt, H., Fiaux, J., Druffel-Augustin, S., and Bukau, B. (2010) The endoplasmic reticulum Grp170 acts as a nucleotide exchange factor of Hsp70 via a mechanism similar to that of the cytosolic Hsp110. *J Biol Chem* **285**, 12445-12453
148. Hipp, M. S., Park, S. H., and Hartl, F. U. (2014) Proteostasis impairment in protein-misfolding and -aggregation diseases. *Trends Cell Biol* **24**, 506-514
149. Vandewynckel, Y. P., Laukens, D., Geerts, A., Bogaerts, E., Paridaens, A., Verhelst, X., Janssens, S., Heindryckx, F., and Van Vlierberghe, H. (2013) The paradox of the unfolded protein response in cancer. *Anticancer Res* **33**, 4683-4694
150. Popp, M. W., Antos, J. M., and Ploegh, H. L. (2009) Site-specific protein labeling via sortase-mediated transpeptidation. *Curr Protoc Protein Sci* **Chapter 15**, Unit 15 13
151. Grammel, M., Luong, P., Orth, K., and Hang, H. C. (2011) A chemical reporter for protein AMPylation. *J Am Chem Soc* **133**, 17103-17105
152. Cong, L., Ran, F. A., Cox, D., Lin, S., Barretto, R., Habib, N., Hsu, P. D., Wu, X., Jiang, W., Marraffini, L. A., and Zhang, F. (2013) Multiplex genome engineering using CRISPR/Cas systems. *Science* **339**, 819-823
153. Mali, P., Yang, L., Esvelt, K. M., Aach, J., Guell, M., DiCarlo, J. E., Norville, J. E., and Church, G. M. (2013) RNA-guided human genome engineering via Cas9. *Science* **339**, 823-826